

DECOLORIZATION OF SYNTHETIC DYE SOLUTIONS BY USING  
BASALTIC TEPHRA AND CLINOPTILOLITE

A THESIS SUBMITTED TO  
THE GRADUATE SCHOOL OF NATURAL AND APPLIED SCIENCES  
OF  
MIDDLE EAST TECHNICAL UNIVERSITY

BY

YUSUF BAHADIR DUYGULU

IN PARTIAL FULFILLMENT OF THE REQUIREMENTS FOR  
THE DEGREE OF MASTER OF SCIENCE  
IN  
ENVIRONMENTAL ENGINEERING

JULY 2004

Approval of the Graduate School of Natural and Applied Sciences

\_\_\_\_\_  
Prof. Dr. Canan Özgen  
Director

I certify that this thesis satisfies all the requirements as a thesis for the degree of Master of Science.

\_\_\_\_\_  
Prof. Dr. Filiz B. Dilek  
Head of Department

This is to certify that we have read this thesis and that in our opinion it is fully adequate, in scope and quality, as a thesis for the degree of Master of Science.

\_\_\_\_\_  
Prof. Dr. Aysel Atımtay  
Supervisor

Examining Committee Members

Prof. Dr. Filiz B. Dilek (METU, ENVE) \_\_\_\_\_

Prof. Dr. Aysel Atımtay (METU, ENVE) \_\_\_\_\_

Prof. Dr. Hayrettin Yücel (METU, CHE) \_\_\_\_\_

Assoc. Prof. Dr. Dilek Sanin (METU, ENVE) \_\_\_\_\_

Assist. Prof. Dr. İpek İmamoğlu (METU, ENVE) \_\_\_\_\_

I hereby declare that all information in this document has been obtained and presented in accordance with academic rules and ethical conduct. I also declare that, as required by these rules and conduct, I have fully cited and referenced all material and results that are not original to this work.

Name, Last name : Yusuf Bahadır DUYGULU

Signature :

## **ABSTRACT**

### **DECOLORIZATION OF SYNTHETIC DYE SOLUTIONS BY USING BASALTIC TEPHRA AND CLINOPTILOLITE**

Duygulu, Yusuf Bahadır

M. Sc. Department of Environmental Engineering

Supervisor: Prof. Dr. Aysel Atımtay

July 2004, 110 pages

Discharge of colored effluents without decoloration originated from textile industries may cause serious problems in the receiving environments.

In this study, natural materials that are basaltic tephra and clinoptilolite were used to remove various dyestuffs used in the textile industry. Those materials are cheap and available in large quantities in Turkey. The investigation of adsorption of basic, acidic and reactive dyes on these materials is the objective of this study.

During preliminary experiments it was seen that adsorption equilibrium was reached in about 2 days. In adsorption experiments, in order to obtain adsorption isotherms, a fixed amount of adsorbent and 100 mL dye solutions of different concentrations were placed in glass bottles which were shaken at 200 rpm and  $25\pm 2^{\circ}\text{C}$  for 2 days. Then, samples were filtered and the equilibrium concentrations of dyestuffs in the solutions were determined by using spectrophotometer at appropriate wavelength corresponding to the maximum absorbency. After equilibrium concentrations of the solutions were obtained, Langmuir and Freundlich adsorption isotherm constants were calculated for the adsorbents used in this study.

The removal efficiencies for cationic basic dyes are higher than those for anionic acidic and reactive dyes with the natural materials. Therefore, modification of surface properties of natural materials with a cationic surfactant was considered to increase the removal efficiencies of those for anionic dyes. After modification of the surface properties, adsorption capacities of adsorbents for anionic dyes were higher than those of natural materials.

Finally, the adsorption capacity of activated carbon for the same dyes was determined to compare with that of natural and modified materials.

The results showed that the adsorption of dyes on adsorbents used in this study fitted nicely the Langmuir Isotherm Equations.

Keywords: Adsorption, Basaltic Tephra, Clinoptilolite, Freundlich Isotherm, Langmuir Isotherm.

## ÖZ

### SENTETİK BOYA ÇÖZELTİLERİNDEN BAZALT TÜFÜ VE KLİNOPTİLOLİT KULLANARAK RENK GİDERİMİ

Duygulu, Yusuf Bahadır

Yüksek Lisans, Çevre Mühendisliği Bölümü

Tez Yöneticisi: Prof. Dr. Aysel Atımtay

Temmuz 2004, 110 sayfa

Tekstil endüstrisinden kaynaklanan boyalı atıksulardan boyar maddelerin uzaklaştırılmadan alıcı ortamlara bırakılması önemli problemlere neden olabilir.

Bu çalışmada, tekstil kuruluşlarında boyama işlemi esnasında kullanılan çeşitli boyar maddelerin atıksulardan uzaklaştırılması amacıyla ülkemizde bol miktarlarda rezervleri bulunan bazalt tüfleri ve klinoptilolit gibi ucuz iki doğal mineral kullanılmıştır. Bu çalışmanın amacı, tekstil endüstrisinde kullanılan bazik, asidik ve reaktif boyaların bazalt tüfleri ve klinoptilolit üzerine adsorpsiyon özelliklerinin araştırılmasıdır.

Adsorpsiyon deneylerine başlamadan önce yapılan ön deneyler sırasında adsorpsiyon dengesine yaklaşık 2 gün içerisinde ulaşıldığı gözlenmiştir. Adsorpsiyon deneyleri sırasında 0.1 g adsorban / 100 mL boya çözeltisi oranı kullanılarak değişik konsantrasyonlarda hazırlanan çözeltiler 200 rpm karıştırma hızında ve  $25\pm 2^{\circ}\text{C}$  sıcaklıkta karıştırılmıştır. Daha sonra alınan numuneler filtre sisteminde süzildükten sonra spektrofotometrede boyaların maksimum absorbanşı sağladığı dalga boylarında çözeltilerin dengede verdikleri adsorpsiyon değerleri belirlenmiş ve önceden çizilen kalibrasyon eğrilerinden çözeltilerin denge konsantrasyonları elde edilmiştir. Daha sonra denge konsantrasyonlarının Langmuir ve Freundlich adsorpsiyon izotermine uygunluğu incelenmiştir.

Katyonik bazik boyaların doğal malzemeler üzerine adsorpsiyonu anyonik özellikteki asidik ve reaktif boyaların verdiği sonuçlardan daha iyi sonuçlar vermiştir. Bazalt tüfleri ve klinoptilolit anyonik boyar maddeleri adsorplama kapasitelerinin artırılması amacıyla bir çeşit katyonik yüzey aktif maddesi ile doğal malzemeler yüzey modifikasyonu işlemine tabi tutulmuşlardır. Modifikasyon işlemi sonucunda bazalt tüfü ve klinoptilolit anyonik boyaları giderme kapasitelerinin belirli miktarlarda arttığı görülmüştür.

Ayrıca, bu çalışmada aynı boyaların aktif karbon üzerine adsorpsiyon kapasitesi belirlenmiş ve elde edilen sonuçlar karşılaştırılmıştır.

Kullanılan boyaların adsorpsiyon özelliklerinin Langmuir İzotermine uygun olduğu görülmüştür.

Anahtar Kelimeler: Adsorpsiyon, Bazalt Tüfü, Klinoptilolit, Freundlich İzotermi, Langmuir İzotermi.

To My Family



## **ACKNOWLEDGEMENTS**

I wish to express my deepest gratitude to my supervisor Prof. Dr. Aysel Atımtay for her guidances, advices, criticisms and encouragements and insights throughout the research.

I would like to express my special appreciation to my parents for their belief in me and their valuable support during this study.

I also wish to thank to my dear friends Erkan Şahinkaya, Nimet Uzal, Recep Kaya Göktaş, Baran Görmez, İrem Önoğlu, Ebru Harmancı and Hakan Moral for their helps and friendships throughout my study.

I am grateful to my brother Burak Duygulu, and my dear friend Uğur Benli for their endless moral support.

The technical assistances of Kemal Demirtaş, Aynur Yıldırım, and Ramazan Demir from Environmental Engineering Department and of Cengiz Tan from Metallurgical and Materials Engineering Department for taking SEM photographs are gratefully acknowledged.

Finally, I am very thankful to Zühre Bosnalı for her love and encouragement throughout my study.

## TABLE OF CONTENT

PLAGIARISM.....	iii
ABSTRACT.....	iv
ÖZ.....	vi
ACKNOWLEDGEMENT.....	ix
TABLE OF CONTENT.....	x
LIST OF TABLES.....	xii
LIST OF FIGURES.....	xiv
LIST OF SYMBOLS.....	xviii
CHAPTER	
1. INTRODUCTION .....	1
2. LITERATURE SURVEY .....	7
3. THEORY .....	21
3.1. Adsorption .....	21
3.2. The Relation Between Surface Tension and Adsorption .....	21
3.3. Causes and Types of Adsorption.....	23
3.4. Adsorption Equilibria and the Adsorption Isotherm .....	25
3.5. Sorption Kinetics in Batch Reactors .....	28
3.6. Factors Influencing Adsorption.....	30
4. MATERIALS AND METHOD.....	33
4.1. Adsorbents.....	33
4.2. Dyestuffs .....	34
4.3. Physical and Chemical Properties of Adsorbents.....	35
4.4. Experimental Setup .....	41
4.5. Calibration Curves.....	42
4.6. Experimental Procedure .....	42
4.7. Modification of Surface Properties .....	44

5. RESULTS AND DISCUSSION .....	46
5.1. Selection of Solid Concentration.....	46
5.2. Effect of Mixing Time.....	46
5.3. Effect of Filter in Removal of Dyes During Filtration.....	46
5.4. Effect of Modification .....	47
5.5. Adsorption of Dyestuffs onto Basaltic Tephra.....	53
5.5.1. Effect of Particle Size on Adsorption .....	53
5.5.2. Adsorption of Basic Dyestuffs onto Basaltic Tephra .....	54
5.5.3. Adsorption of Acid Dyestuffs onto Basaltic Tephra .....	58
5.5.4. Adsorption of Reactive Dyestuffs onto Basaltic Tephra .....	61
5.6. Adsorption of Dyestuffs onto Clinoptilolite.....	65
5.6.1. Effect of Particle Size on Adsorption .....	65
5.6.2. Adsorption of Basic Dyestuffs onto Clinoptilolite .....	66
5.6.3. Adsorption of Acid Dyestuffs onto Clinoptilolite .....	70
5.6.4. Adsorption of Reactive Dyestuffs onto Clinoptilolite.....	73
5.7. Adsorption of Dyestuffs onto Powdered Activated Carbon.....	76
5.7.1. Adsorption of Basic Dyestuffs onto PAC.....	76
5.7.2. Adsorption of Acid Dyestuffs onto PAC.....	79
5.7.3. Adsorption of Reactive Dyestuffs onto PAC .....	82
5.8. Comparison of the Adsorption Capacities of the Adsorbents .....	85
6. CONCLUSION.....	89
REFERENCES.....	91
APPENDICES	
A. CALIBRATION CURVES .....	96
B. RATE CURVES.....	102
C. EFFECT OF FILTER PAPER IN DYE REMOVAL .....	108

## LIST OF TABLES

Table 1.1 Yarn, textile and carpet production in 2002 in Turkey .....	2
Table 2.1 Summary of the studies performed between 1976-2003.....	17
Table 4.1 Dyestuffs used in the experiments.....	34
Table 4.2 Chemical composition of basaltic tephra .....	35
Table 4.3 Classification of tephra .....	36
Table 4.4 Particle sizes of basaltic tephra and clinoptilolite used in experiments.	36
Table 4.5 Surface areas of the adsorbents .....	37
Table 4.6 Average pore diameters and total pore volumes of the adsorbents .....	37
Table 4.7 Zeta potentials of the adsorbents at pH=7 .....	40
Table 4.8 Wavelengths corresponding to maximum absorbance .....	42
Table 5.1 Surface areas of the adsorbents before and after surface modification..	49
Table 5.2 Average pore diameter and total pore volumes of the natural and modified adsorbents.....	52
Table 5.3 Langmuir isotherm constants for natural and modified basaltic tephra	56
Table 5.4 Freundlich isotherm constants for natural and modified basaltic tephra .....	57
Table 5.5 Langmuir isotherm constants for modified basaltic tephra .....	59
Table 5.6 Freundlich isotherm constants for modified basaltic tephra .....	61
Table 5.7 Langmuir isotherm constants for modified basaltic tephra .....	63
Table 5.8 Freundlich isotherm constants for modified basaltic tephra .....	64
Table 5.9 Langmuir isotherm constants for natural and modified clinoptilolite ....	68
Table 5.10 Freundlich isotherm constants for natural and modified clinoptilolite .....	69
Table 5.11 Langmuir isotherm constants for natural and modified clinoptilolite..	71
Table 5.12 Freundlich isotherm constants for modified clinoptilolite .....	73
Table 5.13 Langmuir isotherm constants for modified clinoptilolite .....	75
Table 5.14 Freundlich isotherm constants for modified clinoptilolite .....	75

Table 5.15	Langmuir isotherm constants for PAC .....	78
Table 5.16	Freundlich isotherm constants for PAC .....	78
Table 5.17	Langmuir isotherm constants for PAC .....	80
Table 5.18	Freundlich isotherm constants for PAC .....	82
Table 5.19	Langmuir isotherm constants for PAC .....	84
Table 5.20	Freundlich isotherm constants for PAC .....	84
Table 5.21	Adsorption capacities of the adsorbents used in this study .....	85
Table 5.22	Summary of some studies from literature .....	88
Table A.1	Data for calibration curve of basic blue dye (BB) .....	96
Table A.2	Data for calibration curve of basic yellow dye (BY) .....	97
Table A.3	Data for calibration curve of acid yellow (AY) .....	98
Table A.4	Data for calibration curve of acid red dye (AR) .....	99
Table A.5	Data for calibration curve of reactive yellow (RY) .....	100
Table A.6	Data for calibration curve of reactive red (RR) .....	101

## LIST OF FIGURES

Figure 4.1 SEM photograph of basaltic tephra for $d_p < 0.60$ mm (x 4,500) .....	38
Figure 4.2 SEM photograph of basaltic tephra for $2.85 < d_p < 3.35$ mm (x 22 ) .....	39
Figure 4.3 SEM photograph of clinoptilolite for $d_p < 0.25$ mm (x 10,000) .....	39
Figure 4.4 SEM photograph of clinoptilolite for $d_p < 0.25$ mm (x 500) .....	40
Figure 4.5 Schematic diagram of the experimental setup .....	41
Figure 4.6 Flowsheet for preparing modified adsorbents .....	45
Figure 5.1 Zeta potential versus pH profiles of natural and modified basaltic tephra .....	48
Figure 5.2 Zeta potential versus pH profiles of natural and modified clinoptilolite .....	48
Figure 5.3 Incremental pore area versus pore diameter plot for basaltic tephra ....	49
Figure 5.4 Incremental pore area versus pore diameter plot for clinoptilolite .....	50
Figure 5.5 Incremental pore area versus pore diameter plot for PAC .....	50
Figure 5.6 Incremental pore volume versus pore diameter plot for basaltic tephra .....	51
Figure 5.7 Incremental pore volume versus pore diameter plot for clinoptilolite..	51
Figure 5.8 Incremental pore volume versus pore diameter plot for PAC .....	52
Figure 5.9 Adsorption isotherms for basic blue on two sizes of basaltic tephra ...	53
Figure 5.10 Adsorption isotherms for basic blue on natural and modified basaltic tephra.....	54
Figure 5.11 Langmuir plots for the adsorption of basic blue on natural and modified basaltic tephra.....	56
Figure 5.12 Freundlich plots for the adsorption of basic blue on natural and modified basaltic tephra.....	57
Figure 5.13 Adsorption isotherms for acid dyes on natural and modified basaltic tephra.....	58

Figure 5.14 Langmuir plots for the adsorption of acid dyes on modified basaltic tephra .....	60
Figure 5.15 Freundlich plots for the adsorption of acid dyes on modified basaltic tephra .....	60
Figure 5.16 Adsorption isotherms for reactive dyes on natural and modified basaltic tephra .....	62
Figure 5.17 Langmuir plots for adsorption of reactive dyes on modified basaltic tephra .....	63
Figure 5.18 Freundlich plots for the adsorption of reactive dyes on modified basaltic tephra .....	64
Figure 5.19 Adsorption of basic blue dyestuff onto natural clinoptilolite .....	65
Figure 5.20 Adsorption isotherms for basic dyestuffs on natural and modified clinoptilolite .....	66
Figure 5.21 Langmuir plots for the adsorption of basic dyestuffs on natural and modified clinoptilolite .....	68
Figure 5.22 Freundlich plots for the adsorption of basic dyestuffs on natural and modified clinoptilolite .....	69
Figure 5.23 Adsorption isotherms for acid dyes on natural and modified clinoptilolite .....	70
Figure 5.24 Langmuir plots for the adsorption of acid dyes on natural and modified clinoptilolite .....	72
Figure 5.25 Freundlich plots for the adsorption of acid dyes on modified clinoptilolite .....	72
Figure 5.26 Adsorption isotherms for reactive dyes on natural and modified clinoptilolite.....	74
Figure 5.27 Langmuir plots for the adsorption of reactive dyes on modified clinoptilolite .....	75
Figure 5.28 Freundlich plots for the adsorption of reactive dyes on modified clinoptilolite .....	76
Figure 5.29 Adsorption isotherms for basic dyestuffs on PAC .....	77

Figure 5.30 Langmuir plots for the adsorption of basic dyestuffs on PAC .....	78
Figure 5.31 Freundlich plots for the adsorption of basic dyestuffs on PAC .....	79
Figure 5.32 Adsorption isotherms for acid dyes on PAC .....	80
Figure 5.33 Langmuir plots for the adsorption of acid dyes on PAC .....	81
Figure 5.34 Freundlich plots for the adsorption of acid dyes on PAC .....	81
Figure 5.35 Adsorption isotherms for reactive dyes on PAC .....	83
Figure 5.36 Langmuir plots for the adsorption of reactive dyes on PAC .....	83
Figure 5.37 Freundlich plots for the adsorption of reactive dyes on PAC .....	84
Figure A.1 Calibration curve for basic blue dye .....	96
Figure A.2 Calibration curve for basic yellow dye .....	97
Figure A.3 Calibration curve for acid yellow dye .....	98
Figure A.4 Calibration curve for acid red dye .....	99
Figure A.5 Calibration curve for reactive yellow dye .....	100
Figure A.6 Calibration curve for reactive red dye .....	101
Figure B.1 Rate curve of basaltic tephra for basic blue .....	102
Figure B.2 Rate curve of basaltic tephra for basic yellow .....	102
Figure B.3 Rate curve of basaltic tephra for acid yellow .....	103
Figure B.4 Rate curve of basaltic tephra for acid red .....	103
Figure B.5 Rate curve of basaltic tephra for reactive yellow .....	104
Figure B.6 Rate curve of basaltic tephra for reactive red .....	104
Figure B.7 Rate curve of clinoptilolite for basic blue .....	105
Figure B.8 Rate curve of clinoptilolite for basic yellow .....	105
Figure B.9 Rate curve of clinoptilolite for acid yellow .....	106
Figure B.10 Rate curve of clinoptilolite for acid red .....	106
Figure B.11 Rate curve of clinoptilolite for reactive yellow .....	107
Figure B.12 Rate curve of clinoptilolite for reactive red .....	107
Figure C.1 Amount of acid red dyestuff adsorbed by the filter paper .....	108
Figure C.2 Amount of basic yellow dyestuff adsorbed by the filter paper .....	108
Figure C.3 Amount of reactive red dyestuff adsorbed by the filter paper .....	109
Figure C.4 Amount of basic blue dyestuff adsorbed by the filter paper .....	109



Figure C.5 Amount of acid yellow dyestuff adsorbed by the filter paper .....	110
Figure C.6 Amount of reactive yellow dyestuff adsorbed by the filter paper .....	110

## LIST OF SYMBOLS

$b_F$	: Freundlich exponent
$C_o$	: Initial dye concentration in solution (mg/L) .
$C_e$	: Equilibrium liquid phase dye concentration (mg/L)
$d_p$	: Particle diameter
$K_F$	: Constant in Freundlich Isotherm
$K_L$	: Langmuir equilibrium constant (L/g)
$q_e$	: The amount of dye adsorbed per unit mass of adsorbent (mg/g)
$q_{mon}$	: The amount of dye adsorbed corresponding to monolayer coverage (mg/g)
$R_L,$	: Dimensionless separation factor defined by Equation 3.3.
$R^2$	: Correlation coefficient

# CHAPTER 1

## INTRODUCTION

Textile industry is one of the most important industries in Turkey. The water consumption in textile industry, especially in dyeing and washing processes, is too high. Therefore, large amount of wastewater is produced and discharged to the receiving environment during textile production process. According to a study performed in Germany 30–120 L of water is used in preparing 1 kg of cotton textile for dyeing process. Also, 50–120 L of water is consumed for each kg of cotton textile for dyeing. Therefore, totally 80–240 L of water is required for dyeing 1 kg of cotton textile. Marzinkowski (1998) has reported that for 1 kg of textile consisting of 55 % polyester and 45 % of cotton, 9–14 L of water is consumed for washing and 75–96 L of water is consumed for dyeing process (Marzinkowski, 1998).

The amount of water used in stoning of 1 kg of textile during various processes in Germany is given by Marzinkowski (1998) as follows:

• Pre washing	: 5.0 L
• Stoning	: 7.5 L
• Rinsing 1	: 6.87 L
• Washing	: 10.0 L
• Rinsing 2	: 13.75 L
• Rinsing 3	: 13.75 L
• Finishing	: 21.25 L
<b>Total</b>	<b>: 78.12 L</b>

As one can see from these water consumption data given in the literature, the amount of water consumed per unit amount of textile produced is quite high. Besides, wastewater from textile industry contains various colorants due to printing or dyeing process.

Amount of yarn, textile and carpet production in Turkey for the year 2002 is given in Table 1.1.

**Table 1.1.** Yarn, textile and carpet production in 2002 in Turkey (SIS, 2003)

<b>Production type</b>	<b>Amount*</b>
<i>Yarn (tons)</i>	
Cotton	644,785
Wool	34,127
<i>Textiles (meters) (*1000)</i>	
Cotton	663,164
Woolen	46,369
<i>Carpets (m<sup>2</sup>)</i>	13,853,709

\* Sum of production by private and public firms

Assuming very roughly that 100 L of water is used on the average in Turkey for 1 kg of cotton textile produced, the amount of water necessary will be about 65 million tons for 644,785 tons/year of cotton yarn. When we look at textile production values given in Table 1.1, we can have an idea about how much water is consumed in textile industry in Turkey per year. We know that much of the water used in various processes in Turkish textile industry is discharged to a receiving environment without treatment. Therefore, there is a large burden on the receiving water bodies.

In textile industry the use of organic dyes has increased dramatically. In the world, the amount of various dyestuff consumption is more than 700,000 tons for an annual production of 30 million tons of textile (Armagan et al., 2003a). About 90% of this dyestuff ends up on fabrics. Therefore, approximately 70,000 tons of dyestuffs are discharged into waste streams each year. Dyestuff producers and users are interested in stability and fastness of dyes on the fabric and they are continually producing dyestuffs which are more difficult to degrade after use (Choy et al., 1999). Therefore, this also poses a problem on the degradation of dyestuffs in the environment by natural processes.

Although, many of dyes are not normally toxic, discharge of colored effluents to environment without removing the color may cause several problems in water. They can be listed as follows:

1. Depending on the exposure time and dye concentration, dyes may have acute and/or chronic effects on exposed organisms.
2. Dyes may absorb and reflect sunlight entering the water so the growth of bacteria, to levels sufficient to degrade impurities in the water and to start the food chain, may be interfered.
3. Abnormal coloration of surface waters captures the attention of both the public and the authorities (Slokar and Marechal, 1998).

The removal of dyestuffs from effluents is of great importance for many countries in the world, both from environmental and economical aspects. Because water consumption in the textile industry is too high and water is very costly in many developed countries, such as Germany, advanced treatment methods are considered for re-use of wastewaters generated from textile industries. For example, in Germany cost of 1 m<sup>3</sup> fresh water is about 1 Euro and cost of 1 m<sup>3</sup> wastewater is about 2.5 Euro. The total cost of 1 m<sup>3</sup> water used in the textile industry is 3.5 Euro (Marzinkowski, 1998).

Cost of water in Turkey is not as high as in Germany. For example, cost of 1 m<sup>3</sup> fresh water supplied by ASKI to work places in Ankara is about 2,661,827 TL, and cost of 1m<sup>3</sup> wastewater generated is about 1,330,913 TL. Therefore, the total cost of 1 m<sup>3</sup> water used is about 3,992,740 TL (approximately 2.5 Euro). However, use of water resources inconsiderately may cause water shortage in the future. Increasing population and increasing industrialization demand more and more of our limited water resources.

The treatment of colored wastewaters (mostly resulting from finishing plants) should not be restricted to the reduction of ecological parameters only, such as chemical oxygen demand (COD), biological oxygen demand (BOD), total organic carbon (TOC), adsorbable organic halide (AOX), temperature and pH, but also reduction of dye concentrations in the wastewaters should be considered (Slokar and Marechal, 1998). In Turkey, the control of related parameters in textile effluents required in the Water Pollution Control Regulation (1988) is almost achieved. However, there is no limit in Turkey in the regulations for the control of “color” in effluents originated from textile industry. This limit has to be defined in the nearest future in order to protect the water receiving bodies from discharge of colored wastewaters.

In the past, municipal wastewater treatment systems were used for the treatment of textile dye effluent, but because of the xenobiotic and recalcitrant nature of many dyes, those systems were found to be ineffective. In addition, when dyes are released into aquatic systems anaerobic bacteria in the sediment are unable to mineralize dyes completely. Therefore, the result is the formation of toxic amines (Robinson et al., 2002a). It is therefore necessary for dye-containing effluents to be treated in an effective manner before being discharged into natural waterways (Robinson et al., 2002a). Many physical and chemical processes for color removal have been applied including coagulation and flocculation, biosorption, photo-decomposition, and ultrafiltration (Annadurai et al., 2001). Due to relatively high

operation costs and low removal efficiencies in using the above-mentioned processes, textile, tannery, pulp, and paper industries seldom apply these processes to treat their effluents (Annadurai et al., 2001).

Among those methods, adsorption techniques have gained favour in recent years because of their proven efficiency in the removal of pollutants from effluents too stable for conventional treatment methods (Choy et al., 1999). The removal of dyes and organics in an economic way remains as an important problem although a number of systems have been developed with adsorption techniques. Adsorption has been found to be superior to other techniques for water re-use in terms of initial cost, simplicity of design, ease of operation and insensitivity to toxic substances (Meshko et al., 2001).

Activated carbon is the most widely used adsorbent for adsorption method because it has a high capacity for the adsorption of organics, but its use is limited due to its high cost. This has led to a search for cheaper and more effective substitutions, such as coal, fly ash, wood, silica gel, bentonite clay, bagasse pith, maize cob, coconut shell, rice husk, and cotton waste have been tried with varying success for color removal (Juang, 1997a).

In Turkey, adsorptive capacities of several materials for color removal were investigated. Especially, natural zeolite, sepiolite and bentonite and their modified forms were used for the removal of some dyestuffs (Armagan et al., 2003, Turabik and Kumbur, 2003, Turabik, 2003 ). Modification processes were applied whether to increase their surface area or to change their surface properties in order to improve their color removal capacities.

## **Objective of the study**

Turkey is very rich in various kinds of porous natural materials. They are very cheap and available in vast quantities. One of them is “basaltic tephra” which is present in the southern part of Turkey in very large quantities. The other mineral is “natural zeolite”, like clinoptilolite. The objective of this study is to use basaltic tephra and clinoptilolite to remove basic, acidic and reactive types of dyes from textile wastewater. The determination of dye removing capacities and adsorption isotherms of these adsorbents are among the objectives of this study.

The second objective is to modify the surface properties of these adsorbents by using a surfactant chemical and then determine their equilibrium sorbent capacities again with basic, acidic and reactive dyes.

The last objective is to compare the capacities of these natural sorbents with that of powdered activated carbon.



## CHAPTER 2

### LITERATURE SURVEY

The use of adsorption process to remove dyestuffs from textile industry wastewaters has been popular in recent years. Some of the studies about the adsorption of dyestuffs are summarized below.

Armagan et al. (2003b) studied the adsorption mechanism of three reactive azo dyes (Everzol Black B, Everzol Red 3BS, Everzol Yellow 3RS H/C) by two natural minerals. They carried out a series of batch adsorption tests as a function of pH, solids concentration, mixing time and dye concentration using sepiolite and zeolite. They selected solids concentration as 0.05 g/mL (5 %) for sepiolite and zeolite. It is stated that most of the adsorption was found to take place within the first 2 h of mixing. Taking into account the extreme changes like pH and concentration, the mixing period was selected as 4 h for further testing. They found adsorption capacity of sepiolite as 0.5–1 mg/g and negative adsorption of zeolite on reactive dyestuffs was observed (Armagan et al., 2003b).

In another study, Armagan et al. (2003c) investigated the adsorption mechanism of the same dyes on modified sepiolite and zeolite. The adsorption results given above indicated that sepiolite and zeolite have a limited adsorption capacity for reactive dyes but is substantially improved upon modifying its surface charges with quaternary amines. It is reported that the adsorption data obtained in the experiments were fitted to the Langmuir Isotherm, and adsorption capacities of modified sepiolite were stated as 169, 120, 108 mg/g for Yellow, Black, and Red, that of modified zeolite were reported as 111, 89, and 61 mg/g for Red, Yellow and Black, respectively (Armagan et al., 2003 c).

Turabik (2003) investigated the removal of Basic Blue 3 from a synthetic wastewater by adsorption onto bentonite. The effects of contact time, initial dye concentrations, mass of adsorbent, agitation speed, pH and temperature on adsorption were examined in this study. Turabik stated that the adsorption capacity of bentonite increases with a decrease of particle size and initial dye concentration. Langmuir Isotherm was applied and adsorption capacity of bentonite was obtained as 75.18 mg/g. Turabik found that the effects of agitation speed and temperature on adsorption were not important. Also, different pH values gave similar adsorption capacities except for pH at 12 at which a slightly lower adsorption capacity was achieved (Turabik, 2003).

Turabik and Kumbur (2003) studied the removal of some basic dyes (Basic Red 46 and Basic Blue 41) with adsorption onto natural and activated bentonite. In this study, bentonite was activated with 25% sulfuric acid at different mass ratios of 10%, 20%, 30%, 40%, 50%, 60%. After activation, surface area of natural bentonite that had been 72.5 m<sup>2</sup>/g was increased to 75.5, 125.7, 156.6, 172.0, 149.8, 140.9 m<sup>2</sup>/g, respectively. During activation process, while acid ratio was increased, Al<sup>+3</sup>, Fe<sup>+3</sup>, Ca<sup>+2</sup>, Mg<sup>+2</sup>, Na<sup>+</sup>, K<sup>+</sup> ions in the bentonite were removed and those spaces formed were turned to meso and micro pores. When mass ratio of acid and bentonite was increased over 40%, surface area of activated bentonite started to decrease due to formation of macro pores as a result of the collapse of the walls between micro and meso pores.

Cation exchange capacity of natural bentonite was 99.19 meq/100 g bentonite and while acid ratio is increasing this value is decreasing to 84.24, 78.81, 72.82, 62.5, 55.71, 51.63 meq/100 g bentonite, respectively, due to removal of Al<sup>+3</sup>, Fe<sup>+3</sup>, Ca<sup>+2</sup>, Mg<sup>+2</sup>, Na<sup>+</sup>, K<sup>+</sup> ions from bentonite. In addition, equilibrium time is reached in 60 minutes in this study.

However, Turabik and Kumbur stated that maximum adsorption capacity of natural bentonite was calculated as 312.12 and 476.45 mg/g for BR46 and BB41, respectively. After acid activation, adsorption capacity of bentonite was obtained lower than that of natural bentonite. For the highest acid ratio, the lowest adsorption capacity was obtained (Turabik and Kumbur, 2003).

Atun et al. (2003) investigated the adsorption behavior of methylene blue (MB) on four fuller's earth (FE) samples of varying compositions. They stated that MB could be strongly adsorbed on the surface of FE samples. Therefore, FE samples can be used as economic adsorbents for cationic dyestuffs (Atun et al., 2003).

Allen et al. (2003) assessed the adsorption capacity of "kudzu" which is a vine native to Eastern Asia as an adsorbent medium for the removal of two basic dyes, Basic Yellow 21, and Basic Red 22 from aqueous solutions. Results of adsorption experiments were analyzed using Langmuir, Freundlich, Redlich-Peterson, Temkin, and Toth isotherm equations. 21-day equilibrium time was used in that study. The performance of the "kudzu" was compared with an activated carbon. Monolayer saturation capacities were found as 720, 860 mg/g for activated carbon and 210, 160 mg/g for "kudzu" for Basic Red 21 and Basic Yellow 21, respectively. "Kudzu" was considered as an effective adsorbent for basic dye color removal, though its capacity for color removal was not as high as activated carbon, the potential appeared to exist to use it as an alternative to activated carbon where carbon cost was prohibitive. Also, the highest  $R^2$  regression coefficient was provided for the Redlich-Peterson isotherm.

Robinson et al. in 2002 studied the adsorption of five reactive dyes onto barley husk in static-batch mode and in a continuous flow, packed-bed, reactor (CFPBR). They investigated effective adsorption, thermodynamics and various initial concentrations of dye solutions for static batch conditions. In addition, the effects of initial dye concentrations and retention time, by varying height and weight of

packing, along with the kinetics of dye adsorption in CFPBR were examined. They stated that the Langmuir Isotherm was used to predict adsorption capacity that was obtained as approximately 8.5 mg/g in static batch condition after 24 hours. Also, barley husks were found to remove 8 mg/g of dyes at initial concentration of 100 mg/L in CFPBR with a residence of 11 minutes with 90% adsorption being achieved (Robinson et al., 2002a).

In another study, Robinson et al. (2002) investigated effect of pretreatment of three agricultural residues, wheat straw, corncob, and barley husk, on adsorption process. In order to delignify or to increase the surface area of untreated sorbents, steam, alkali, ammonia steeping and milling were applied as pretreatment processes. Robinson et al. (2002) stated that a higher percentage of dye removal was achieved at a faster rate by the milled samples proving milling to be a better and more cost effective treatment, except for barley husk which had a higher percentage removal for the control (Robinson et al., 2002b).

Annadurai et al. (2001) applied one gram of activated carbon to shake for 48 hours with the aqueous solutions containing dye concentration, Rhomadine 6G (Basic Red 1), about 5-45 mg/L and examined the effects of pH (7-9), temperature (30-60°C) and particle sizes (0.5, 0.7, 1.0 mm) on the adsorption capacity of the activated carbon. They reported that adsorption capacity of the adsorbent will increase if the particle size decreases, and temperature increases and also pH at neutral range gives the maximum adsorption capacity. In that study, maximum adsorption capacity of the activated carbon was obtained as 44.7 mg/g at T: 60°C, pH: 7.0, particle size: 0.5 mm. In addition, Annadurai et al. (2001) investigated the kinetic data for dye adsorption at the same conditions and indicated the validity of first-order rate expression (Annadurai et al., 2001).

Meshko et al. (2001) compared the adsorption capacities of natural zeolite and granular activated carbon on some basic dyes from aqueous solutions. In this

study, influence of agitation, initial dye concentration and adsorbent mass on adsorptive behavior of adsorbents was investigated and Langmuir and Freundlich adsorption isotherm parameters were determined. Activated carbon was used after washing with deionized water to remove any leachable impurities and adherent powder and drying to constant weight at 110°C for 24 hours. Also, natural zeolite was dried at 300°C for 48 hours in order to remove any traces of moisture or other contaminants prior to adsorption experiments. In accordance with the Lambert–Beer law, the absorbance was found to vary linearly with concentration and dilutions were undertaken when absorbance exceeded 0.6 during the determination of the absorbencies of the samples in this study. At the end of the study, the adsorption capacities of activated carbon that were 159 and 309.2 mg/g for various dyes were obtained higher than those of natural zeolite that were 14.91, 55.86 mg/g for the same dyes, respectively. They stated that the rate of dye removal was not significantly influenced by the degree of agitation (Meshko et al., 2001).

Wu et al. (2001) studied kinetics and mechanism of adsorption of one basic dye (BB 69) and one direct dye (DR 227) onto activated clay in the temperature range 15-75°C. Activation of clay was made by treatment with 1 molar sulfuric acid at 80°C for 2 hours. Pseudo first and second-order kinetic models were tested. It was shown that the adsorption process of the dyes was well defined by the pseudo second-order equation. The related rate constants and apparent activation energies were evaluated. It was reported that adsorption capacity of BB 69 on activated clay increases with increasing temperature, but that of DR 227 decreases probably due to different adsorption nature; that is, the adsorption of BB 69 was extremely favorable and that of DR 227 was classified as reversible adsorption. In that study, it was concluded that the reaction mechanism might be partly as a result of the complexation or ion exchange between the charged groups in dye molecules and the SiO<sub>2</sub> or Al<sub>2</sub>O<sub>3</sub> groups on the adsorbent surface. Also, relatively large pore size of the adsorbent (20-50 nm) was considered as a possible reason of adsorption.

The apparent activation energy for adsorption of BB 69 and DR 227 was found as 8.03 and 17.5 kJ/mol, respectively (Wu et al., 2001).

Öztürk et al. (2000) studied adsorption of a dyestuff, Rifazol Black B (Reactive Dye) from aqueous solution on different adsorbents that are activated carbon, natural sepiolite, activated sepiolite and slag which is generated from combustion of Soma coal in a Textile Factory. Effects of pH, temperature and particle size on adsorption were investigated. Activation of sepiolite was done by using 0.75 M HCl and HNO<sub>3</sub>. Maximum adsorption capacities of the adsorbents are given as follows; activated carbon > slag > activated sepiolite > natural sepiolite (Öztürk et al., 2000).

Al-Degs et al. (2000) studied the removal of three reactive dyes, namely Remazol Reactive Yellow, Remazol Reactive Black and Remazol Reactive Red, by using activated carbon. Experiments were performed at a constant temperature of 18°C and a constant agitation speed of 150 rpm. Adsorbent/solute ratio was used as 0.1%, and the dye concentrations ranged from 50 to 1000 mg/L for each isotherm experiment. A good removal of dyes from aqueous solutions observed at the end of the study was attributed to the net positive surface charge of the adsorbent. Also, surface acidity, surface basicity, H<sup>+</sup> and OH<sup>-</sup> adsorption capacities and pH<sub>ZPC</sub> for the adsorbent were estimated. Al-Degs et al. (2000) determined that at a particle size range of 300-500 µm the values of saturation capacities were 1111, 434 and 400 mg/g for reactive yellow, reactive black and reactive red, respectively (Al-Degs et al., 2000).

Lin and Liu (2000) investigated the adsorption of basic yellow dye on activated carbon from aqueous solutions under a centrifugal field. It is stated that the adsorption process, based on the assumption of a pseudo-first-order mechanism, was developed to estimate the rate constant with the effect of centrifugal force, initial dye concentration. In addition, the rate parameter based on the intraparticle

diffusion model was presented. It is concluded that the centrifugal force could enhance the rate constant, the rate parameter, and the diffusion coefficient. Therefore, better mass transfer could be provided with centrifugal force (Lin and Liu, 2000).

Choy et al. (1999) performed an investigation to determine the adsorption capacity of activated carbon on some acid dyes, namely, Acid Red 114, Polar Yellow and Polar Blue RAWL, from effluents. Ratio of adsorbent mass to solution volume was used as 0.05 g /50 mL, and initial dye concentration of solutions were varied between 10 and 250 mg/L, temperature and agitation speed was maintained at  $20\pm 2^{\circ}\text{C}$  and 400 rpm, respectively, and equilibrium was reached after 21 days in this study. Choy et al. (1999) stated that analysis of data was carried out in two stages: 1) In single component analysis, the experimental isotherm data were analysed using Langmuir, Freundlich, Redlich-Peterson, Temkin and Dubinin-Radushkevich equations for each individual dye. The monolayer adsorption capacities were found as 101.0 mg Acid Red per g carbon, 100.9 mg Acid Blue per g carbon and 128.8 mg Acid Yellow per g carbon. 2) In multicomponent analysis, one binary system was analysed using an extended form of the Langmuir equation. The correlation between theoretical data and experimental data only had limited success due to competitive and interactive effects between the dyes and dye-surface interactions. For example, in a binary, Yellow plus Blue system, the total capacity was 117 mg/g, a value between the adsorption capacities of the two individual dyes (Choy et al., 1999).

Morais et al. (1999) used eucalyptus bark that is a very abundant, inexpensive, forest residue in their country, Portugal, as an adsorbent to remove Remazol BB which is a reactive dyestuff from aqueous solutions. They examined the effects of different variables that were temperature, initial pH, sodium chloride concentration and initial dye concentration/bark concentration ratio on adsorption of the dye. For the variables given above they carried out experiments in two stages. Morais et

al. (1999) found the maximum adsorption capacity about 90 mg of dye/g of dry bark at pH 2.50 for a sodium chloride concentration of 50 g/L, an initial dye concentration equal to 500 ppm, a bark concentration equal to 2 g/L and at 18°C. Also, they performed experiments under the same conditions with an activated carbon and reported that adsorption capacity of eucalyptus bark obtained as about one half of the activated carbon (Morais et al., 1999).

Dai (1998) investigated adsorption mechanism of two cationic and three anionic dyes on activated carbon. It is stated that saturated adsorption capacity of the dyes on activated carbon is correlated with electrostatic forces between charges on the carbon surface and ionic dyes. According to experimental results, there are three distinct states regarding the effect of zeta potential on carbon surface. In the neutral potential state, i.e. zeta potential is nearly zero, the electrostatic interactions between carbon surface and the dyes are negligible and the adsorption forces are mainly dispersion forces. Therefore, pH has no effect on saturated adsorption amount. In the positive or negative potential states, there exist the electrostatic attractive or repulsive forces between the adsorbent and adsorbate. Therefore, the adsorption forces are the sum or difference of dispersion and electrostatic forces (Dai, 1998).

Juang et al. (1997a) studied the adsorption of six dyes; two basic, one acidic, one disperse, one direct dye and one reactive, from aqueous solutions onto activated clay. Activation of clay was done with 1 M H<sub>2</sub>SO<sub>4</sub>. In adsorption experiments, a fixed amount of activated clay (0.1-1 g) and 100 mL of an aqueous solution were placed in a 250 mL glass-stoppered flask, which was shaken at 130 rpm for 5 days using a thermostated shaker bath. The equilibrium data were analysed by using Langmuir equation over the entire range of concentration (50-500 mg/L). The adsorption capacity of activated clay was reported as 394, 406.3, 256.1, 49.64, 37.88, and 36.63 for Basic Blue, Basic Red, Acidic Blue, Disperse Blue, Direct Red and Reactive Red, respectively (Juang et al., 1997a).



In another study, Juang et al. (1997b) examined the removal of some reactive dyes, Reactive Red 222, Reactive Yellow 145, and Reactive Blue 222, from aqueous solutions by adsorption on “chitosan”. Effects of dye concentration, the amount and particle size of “chitosan” were investigated during experiments. Maximum adsorption capacity of “chitosan” was obtained as 380, 179, and 87 g/kg for RR222, RY145, and RB 222, respectively. Among the most frequently used isotherm equations, Langmuir, Freundlich and Redlich-Peterson Equations, the equilibrium data could be best fitted by the Redlich-Peterson equation over entire concentration range. In addition, the smaller the “chitosan” particles, the greater the capacity of dye (Juang et al., 1997b).

Wu et al. (1997) studied the adsorption of several anionic dyes, D&C Red 6, Acid Yellow 1, Acid Blue 25, Guinea Green B, on nanosize alumina-modified silica particles of different compositions and modal sizes. They stated that the negatively charged dyes were electrostatically attracted positively charged cores and chemisorbed by forming a surface Al lake. The advantage of the adsorbent was its small size (<20 nm) and the ability of the dyes to form chemical bonds with surface  $\equiv \text{AlOH}$  groups of the core particles. In that study adsorption capacities of the adsorbent for different dyestuffs were obtained at some values that were between 0.12-0.70 g dye/ g adsorbent (Wu et al., 1997).

Nassar and Magdy (1997) investigated the adsorption of three basic dyes, namely, Basic Yellow, Basic Red and Basic Blue, from an aqueous solution on palm-fruit particles. Nassar and Magdy stated that the maximum adsorption capacities of the palm-fruit particles were found to be 327 mg yellow dye per gram of adsorbent, 180 mg red dye per gram of adsorbent and 92 mg blue dye per gram of adsorbent. In addition, a comparative cost study, based on the adsorption capacity alone, showed that the costs of the adsorbent required were 1.9%, 4.4%, 7.1%, respectively, compared with the case of commercial activated carbon granules (Nassar and Magdy, 1997).

Sun and Xu (1997) performed a study to determine adsorption capacity of sunflower stalks for two basic dyes, Methylene Blue and Basic Red 9, and two direct dyes, Congo Red and Direct Blue 71. The maximum adsorption capacity of the adsorbent was much higher for basic dyes, i.e. 205 and 317 mg/g for Methylene Blue and Basic Red 9, respectively, than that for direct dyes. Sun and Wu stated that the components of sunflower stalk have different adsorption capacities. The pith, the soft and porous material in the center of stalks, has twice the adsorptive capacity of the skin. For example, maximum adsorption capacity of total stalks for basic red 9 dye was 317 mg/g, that of pith was 510 mg/g and that of skin was 185 mg/g. Adsorption capacity of the adsorbent and its components for anionic dyes was obtained in the range 15 –76 mg/g that are much lower than that of cationic dyes (Sun and Wu, 1997).

Arbeola et al. (1997) studied the adsorption of Rhodamine 6G (R6G) on sepiolite of which surface area and cation exchange capacity (CEC) were reported as 310 m<sup>2</sup>/g and 15 mequiv/100 g, respectively. It is stated that the adsorption of R6G molecules on sepiolite particles was initially performed on the external surface of the clay for samples with low loadings (in the 0-4 % CEC range), the dye being adsorbed in its monomeric form. For intermediate relative dye/clay concentration (2-12 % CEC) samples and long stirring time, the association of clay particles (favored by the presence of dye molecules on the external surface of the clay) gave rise to the preflocculation of the samples. For high loading (>20 %CEC) samples the clay aggregation lead to the flocculation of the sepiolite particles (Arbeola et al., 1997).

Summary of the studies performed between 2003 and 1976 is given in Table 2.1.

**Table 2.1.** Summary of the studies performed between 1976-2003

Reference	Adsorbent	Adsorbent Form	Dye used		q <sub>mon</sub> , mg/g
			Type	Name	
Armağan et al. (2003)	Sepiolite	Natural	Reactive	Black 5  Red 239  Yellow 176	0.5-1
	Zeolite				Neg. values
	Sepiolite	Modified with HTAB			120 108 169
	Zeolite				111 61 89
Turabik and Kumbur (2003)	Bentonite	Natural	Basic	Red 46	312 476
		Acid activated		Blue 41	263 270
Turabik (2003)	Bentonite	Natural	Basic	Blue 3	75
Allen et al. (2003)	Kudzu	Natural	Basic	Yellow 21 Red 22	160 210
Annadurai et al. (2001)	Granular Activated Carbon	Natural	Basic	Rhodamine 6G	44
Meshko et al. (2001)	Granular Activated Carbon	Natural Natural	Basic	Maxilon Schwarz FBL-01 Maxilon Goldgelb GL EC	309 159
	Zeolite				55 14
Al-Degs et al. (2000)	Granular Activated Carbon	Natural	Reactive	Remazol Yellow Remazol Black Remazol Red	1111 434 400
Choy et al. (1999)	Granular Activated Carbon	Natural	Acid	Red 114 Polar Yellow Polar Blue	101 129 101
Morais et al. (1999)	Eucalyptus Bark	Natural	Reactive	Remazol BB	90

**Table 2.1.** Summary of the studies performed between 1976-2003 (cont'd)

Dai (1998)	Powdered Activated Carbon	Natural	Cationic	Methyl Green Methyl Violet	943 694
			Anionic	Phenol Red Carmine Titan Yellow	172 457 1538
Juang et al. (1997)	Chitosan	Natural	Reactive	Red 222 Yellow 145 Blue 222	379 179 87
Juang et al. (1997)	Clay	Acid activated	Basic	Blue 69 Red 62	394 406
			Acid	Blue 25	256
			Direct	Blue 183 Red 227	49 37
			Reactive	Red 123	36
Nassar and Magdy (1997)	Palm Fruit Bunch Particles	Natural	Basic	Yellow 21 Red 22 Blue 3	327 180 92
Sun and Xu (1997)	Sunflower Stalks	Natural	Basic	Methylene Blue Red 9	428 510
			Direct	Congo Red Blue 71	37 75
Wu et al. (1997)	Silica Particles	Alunima Modified	Acid	D&C Red 6 Yellow 1 Blue 25 Guinea Green B	300 190 700 600
Nassar and El-Geundi (1991)	Activated Carbon	Natural	Basic	Maxilon Red ANL Astrazon Blue FRR	790 648
			Acid	Telon Blue ANL	120
	Clay	Natural	Basic	Maxilon Red ANL Astrazon Blue FRR	326 378
			Acid	Telon Blue ANL	39
	Maize Cob	Natural	Basic	Maxilon Red ANL Astrazon Blue FRR	94 167
			Acid	Telon Blue ANL	41
	Bagasse Pith	Natural	Basic	Maxilon Red ANL Astrazon Blue FRR	76 160
			Acid	Telon Blue ANL	23

**Table 2.1.** Summary of the studies performed between 1976-2003 (cont'd)

McKay et al. (1987)	Bagasse Pith	Natural	Basic	Blue 69 Red 22	158 77
			Acid	Red 114 Blue 25	23 22
Asfour et al. (1985)	Hardwood Sawdust	Natural	Basic	Astrazon Blue FRR 69	80
McKay (1985)	Rice Husk	Natural	Basic	Safranine Methylene Blue	76 28
			Acid	Sandolan Rhodine Sandolan Blue	0 0
			Direct	Congo Red Solar Blue	0 0
			Disperse	Foron Brill Red Foron Blue	0 0
	Teakwood Bark		Basic	Safranine Methylene Blue	>100 84
			Acid	Sandolan Rhodine Sandolan Blue	0 15
			Direct	Congo Red Solar Blue	0 0
			Disperse	Foron Brill Red Foron Blue	12 0
	Cotton Waste		Basic	Safranine Methylene Blue	73 24
			Acid	Sandolan Rhodine Sandolan Blue	0 0
			Direct	Congo Red Solar Blue	45 0
			Disperse	Foron Brill Red Foron Blue	0 0
	Hair		Basic	Safranine Methylene Blue	18 12
			Acid	Sandolan Rhodine Sandolan Blue	0 0
			Direct	Congo Red Solar Blue	0 0
			Disperse	Foron Brill Red Foron Blue	0 0

**Table 2.1.** Summary of the studies performed between 1976-2003 (cont'd)

McKay (1985)	Coal	Natural	Basic	Safranine Methylene Blue	10 23
			Acid	Sandolan Rhodine Sandolan Blue	0 0
			Direct	Congo Red Solar Blue	0 0
			Disperse	Foron Brill Red Foron Blue	7 0
	Bentonite		Basic	Safranine Methylene Blue	>100 >100
			Acid	Sandolan Rhodine Sandolan Blue	0 20
			Direct	Congo Red Solar Blue	49 0
			Disperse	Foron Brill Red Foron Blue	26 41
Poots et al. (1976)	Wood	Natural	Acid	Blue 25	16

## CHAPTER 3

### THEORY

#### 3.1. Adsorption

Adsorption involves the interphase accumulation or concentration of substances at a surface or interface. The process can occur at an interface between any two phases, such as, liquid-liquid, gas-solid, gas-liquid, or liquid-solid interfaces. The material being concentrated or adsorbed is the *adsorbate*, and the adsorbing phase is termed the *adsorbent* (Weber, 1972).

Absorption, conversely, is a process in which the molecules or atoms of one phase interpenetrate nearly uniformly among those of another phase to form a “solution” with the second phase. The term *sorption*, which includes both adsorption and absorption, is a general expression for a process in which a component moves from one phase to be accumulated in another, particularly for cases in which the second phase is solid (Weber, 1972).

#### 3.2. The Relation Between Surface Tension and Adsorption

Surface reaction in adsorption process must occur at least partly as a result of –and must likewise influence and alter- the forces active within the phase boundaries, or surface boundaries; these forces result in characteristic boundary energies. Classical chemistry defines the properties of a system by the properties of its mass; for surface phenomena, however, the significant properties are those of the surface or boundary (Weber, 1972).

A pure liquid always tends to reduce its free surface energy through the action of surface tension, which is quantitatively equal to the amount of work that would be necessary to compensate the natural reduction in free surface energy. From a molecular point of view, enlarging a surface requires the breaking of bonds between molecules making up the liquid phase, and the forming of bonds between molecules of different phases. Hence, to increase the surface of liquid requires an input of work in excess of that necessary to merely compensate the tension at the surface. To induce frothing at a liquid-gas interface, for example, the surface tension must be overcompensated (Weber, 1972).

It is well known that a large number of soluble materials can effectively alter the surface tension of a liquid. Detergents, for example, lower surface tension dramatically, and can thus act to cause spreading of the water drop on the flat plate, resulting in a wetting of the plate. Detergent-like substances are thus termed “wetting” agents or “surface-active” agents. If a material which tends to be active at the surface is present in a liquid system, a decrease in the tension at the surface will occur upon movement of the solute to the surface. Migration of the substance to the surface or boundary results in a net reduction of the work required to enlarge the surface area, the reduction being proportional to the concentration of adsorbate at the surface. Hence the energy balance of the system favors the adsorptive concentration of such surface-active substances at the phase interface. Stated in a manner more appropriate for the objectives of the present discussion, a solute that decreases surface tension must be concentrated at the surface because the solvent molecules have a smaller attractive force for the molecules of the solute than for each other. The phenomenon of increased concentration of the soluble material in a boundary or surface is adsorption, and any solute which lowers the surface tension of a liquid in which it is dissolved will adsorb at the boundary of the liquid phase. Conversely, any solute which increases the surface tension is “negatively adsorbed” at the boundary of the liquid phase, that is, the solute migrates away from the surface toward the center of the liquid phase (Weber, 1972).



### 3.3. Causes and Types of Adsorption

The primary driving force for adsorption may be a consequence of *lyophobic* (solvent-disliking) character of the solute relative to the particular solvent, or of a high affinity of the solute for the solid. For the majority of systems encountered in water and wastewater treatment practice, adsorption results from the combination of the two forces (Weber, 1972).

The degree of solubility of a dissolved substance is by far the most significant factor in determining the intensity of *lyophobic* character of the solute (Weber, 1972).

The more a substance likes the solvent systems –the more *hydrophilic* in the case of an aqueous solution- the less likely it is to move toward an interface to be adsorbed. Conversely, a *hydrophobic* –water disliking- substance will more likely be adsorbed from aqueous solution. A large number of organic contaminants, such as sulfonated alkylbenzenes, have a molecular structure comprised of both hydrophilic and hydrophobic groups. In this case, the hydrophobic part of the molecule tends to be active at the surface and undergo adsorption, whereas the hydrophilic part tends to stay in the solution phase is at all possible (Weber, 1972).

The “solubility-amphoteric” character of the substance results in an orientation of the molecule at the interface; the hydrophobic part adsorbed at the surface, and the hydrophilic part directed toward the solvent phase (Weber, 1972).

The second primary driving force for adsorption results from a specific affinity of the solute for the solid. In this context, it is desirable to distinguish between three principal types of adsorption. According to the most plausible of present concepts of adsorption, this surface phenomenon may be predominantly one of the electrical attractions of the solute to the adsorbent, of van der Waals attraction, or of a chemical nature (Weber, 1972).

Adsorption of the first type falls within the realm of ion-exchange and is often referred to as *exchange* adsorption. Exchange adsorption is, as the term implies, a process in which ions of one substance concentrate at a surface as a result of electrostatic attraction to charged sites at the surface (Weber, 1972).

For two potential ionic adsorbates in like concentrations and in the absence of other specific sorption effects, the charge on the ions is the determining factor for exchange adsorption. In a system containing a monovalent ion and a trivalent ion under the stated conditions, the influence of kinetic energy to remain in solution phase is the same for each, but the trivalent ion is attracted much more strongly toward a site of opposite charge on the surface of the adsorbent. For ions of equal charge, molecular size (hydrated radius) determines order of preference for adsorption, the smaller ion being able to accomplish closer approach to the adsorption site and thus being favored.

Adsorption occurring as a result of van der Waals forces is generally termed “physical” adsorption, a term which has come to represent cases in which the adsorbed molecule is not affixed to a specific site at the surface but is, rather, free to undergo translational movement within the interface. Adsorption of this type is sometimes referred to also as “ideal” adsorption (Weber, 1972).

If the adsorbate undergoes chemical interaction with the adsorbent, the phenomenon is referred to as “chemical” adsorption, “activated” adsorption, or “chemisorption”. “Chemically adsorbed” molecules are considered not to be free to move on the surface, or within the interface (Weber, 1972).

Physical adsorption is usually predominant at low temperature, and is characterized by a relatively low energy of adsorption, that is, the adsorbate is not held as strongly to the adsorbent as for chemical adsorption. Chemical adsorption processes exhibit high energies of adsorption, because the adsorbate forms strong

localized bonds at active centers on the adsorbent. Chemical interaction between the adsorbent and the adsorbate is favored by higher temperature, because chemical reactions proceed more rapidly at elevated temperatures than at lower temperatures (Weber, 1972).

Most adsorption phenomena are combinations of the three forms of adsorption; that is, the several forces which influence the different types of adsorption often interact to cause concentration of a particular solute at an interface. Thus it is generally not easy to distinguish between physical and chemical adsorption (Weber, 1972).

Many adsorption processes involving organic molecules result from specific interactions between identifiable structural elements of the sorbate and the sorbent. These interactions may be designated as “specific adsorptions” as opposed to adsorption which occurs as a result of simple coulombic interactions. It is possible for specific adsorption interactions to exhibit a large range of binding energies, from values commonly associated with so called “physical” adsorption on the lower end of the spectrum to higher energies involved in so called “chemisorption”. The adsorptive interactions of aromatic hydroxyl and nitro-substituted compounds with active carbon, for example, may be considered to be specific adsorption processes resulting from the formation of donor-acceptor complexes of the organic molecule with surface carbonyl oxygen groups, with adsorption continuing after these sites are exhausted by complexation with the rings of the basal planes of the carbon microcrystallite (Weber, 1972).

### **3.4. Adsorption Equilibria and the Adsorption Isotherm**

Positive adsorption in a solid-liquid system results in the removal of solutes from solution and their concentration at the surface of the solid, to such time as the concentration of the solute remaining in solution is in a dynamic equilibrium with

that at the surface. At this position of equilibrium, there is a defined distribution of solute between the liquid and solid phases. The distribution ratio is a measure of the position of equilibrium in the adsorption process; it may be a function of the concentration of the solute, the concentration and nature of competing solutes, the nature of the solution, and so on. The preferred form for depicting this distribution is to express the quantity  $q_e$  as a function of  $C$  at fixed temperature, the quantity  $q_e$  being the amount of solute adsorbed per unit weight of solid adsorbent, and  $C$  the concentration of solute remaining in solution at equilibrium. An expression of this type is termed an *adsorption isotherm*. The adsorption isotherm is a functional expression for the variation of adsorption with concentration of adsorbate in bulk solution at constant temperature (Weber, 1972).

In general, the adsorption isotherm describes how adsorbates will interact with adsorbents and so is critical in optimizing the use of adsorbents (Juang, 1997).

Langmuir and Freundlich adsorption expressions are frequently used in the adsorption experiments.

***The Langmuir isotherm*** assumes a monolayer coverage of adsorbate over a homogenous adsorbent surface. Graphically, a plateau characterizes the Langmuir isotherm. Therefore, at equilibrium, a saturation point is reached where no further adsorption can occur. Sorption is assumed to take place at specific homogenous sites within the adsorbent. Once a dye molecule occupies a site, no further adsorption can take place at that site (Allen et al., 2003).

Langmuir Equation is given in Equation (1) (Juang, 1997a),

$$\frac{q_e}{q_{mon}} = \frac{K_L C_e}{1 + K_L C_e} \quad (1)$$

Rearranging Equation (1), we have:

$$\frac{C_e}{q_e} = \frac{1}{K_L q_{mon}} + \frac{1}{q_{mon}} C_e \quad (2)$$

Therefore, by plotting  $C_e/q_e$  against  $C_e$  it is possible to obtain the value of  $q_{mon}$  from the slope, which is  $(1/q_{mon})$  and the value of  $K_L$  from the intercept which is  $(1/K_L q_{mon})$ .

The Langmuir Equation is applicable to homogenous sorption where the sorption of each molecule has equal sorption activation energy (Allen et al., 2003). The equation is thermodynamically consistent and follows Henry's Law at concentrations approaching zero (Juang, 1997a).

The essential characteristics of the Langmuir Equation can be expressed in terms of a dimensionless factor,  $R_L$ , which is given below;

$$R_L = \frac{1}{1 + K_L C_o} \quad (3)$$

The value of the isotherm to be either;

- unfavorable ( $R_L > 1$ ),
- linear ( $R_L = 1$ ),
- favorable ( $0 < R_L < 1$ ),
- irreversible ( $R_L = 0$ ) (Juang, 1997a).

**The Freundlich Expression** given in Equation (4) is an exponential equation and therefore, assumes that as the adsorbate concentration increases so does the concentration of adsorbate on the adsorbent surface. Theoretically, using this expression, an infinite amount of adsorption can occur.

$$q_e = K_F C_e^{b_F} \quad (4)$$

This expression is characterized by the heterogeneity factor,  $b_F$ , and so the Freundlich isotherm may be used to describe heterogeneous systems (Allen et al., 2003). For favorable adsorption, value of  $b_F$  must be between 0 and 1 (Atun et al., 2003).

The Freundlich equation agrees well with the Langmuir over moderate concentration ranges but, unlike the Langmuir expression, it does not reduce to the linear isotherm (Henry's Law) at low surface coverage. Both these theories suffer from the disadvantage that equilibrium data over a wide concentration range cannot be fitted with a single set of constants (Allen et al., 2003).

To determine the constants  $K_F$  and  $b_F$ , the linear form of the Equation (4) shown below may be used to produce a graph of  $\ln(q_e)$  against  $\ln(C_e)$ .

$$\ln q_e = \ln K_F + b_F \ln C_e \quad (5)$$

### **3.5. Sorption Kinetics in Batch Reactors**

Molecular diffusion is one of several phenomena contributing to establishment of rates of transfer of adsorbed materials from the exterior sites of a porous adsorbent to surfaces bounding inner pore spaces. For many applications of adsorption and ion exchange, the rate of intraparticle transport in turn governs the overall rate of removal of solute from solution. For example, although it is certain that adsorptive forces govern positions of equilibrium attained for adsorption of phenol and sulfonated alkylbenzene compounds on porous granular carbon, results of the studies of adsorption of these substances from a dilute solution indicate that in rapidly stirred, batch-type systems the rate of uptake is controlled primarily by rate at which adsorbate is transported from the exterior to the interior sites of the adsorbent particles. There is much further experimental evidence to support the

theory that “diffusion” in the pores of solid adsorbents or resins is the rate-controlling step in many adsorption and ion-exchange processes (Weber, 1972).

Pore diffusion kinetics deriving from intraparticle transport process are particularly pertinent in batch reactors operated at levels of mixing or agitation sufficient to render resistance to film transport less than that for pore transport (Weber, 1972).

Intraparticle transport phenomena may derive from the net action of several molecular forces. For most systems of interest in water and waste treatment applications these may be enumerated as follows: adsorption, two-dimensional micelle formation, three-dimensional micelle formation, electrokinetic interactions, and molecular diffusion (Weber, 1972).

Adsorption, resulting from attractive forces between adsorbate and surfaces of capillary walls and repulsive forces between adsorbate and the aqueous solvent, serves to withdraw adsorbate temporarily from solution. Withdrawal by adsorption retards the transfer of an individual molecule or ion of adsorbate and, at the same time, reduces the effective cross section of the capillary to inhibit diffusion of other molecules. An individual molecular species continually undergoes an exchange process at the surface, alternately, adsorbing at the wall and returning to the solution within the pore space to continue net movement in the direction of decreasing concentration. The detention time at the surface may be increased substantially by the formation of two-dimensional micelles in the adsorbed film, thus further inhibiting free diffusion (Weber, 1972).

The total pore volume of the adsorbent is small relative to the volume of solution being treated. The overall concentration of adsorbate contained in the pore volume may therefore approach the critical micelle concentration for certain organic compounds soon after initial contact of the adsorbent with the solution. As three-dimensional micelles form in the pore spaces of the adsorbent, the micelles, rather than individual molecular species, must be transferred through the capillaries. The

micelles, or agglomerations of molecules, naturally are transported more slowly than single molecules (Weber, 1972).

Elektrokinetic interaction between adsorbate and adsorbent or between adsorbate and other solutes in a given system may be an important factor in intraparticle transport phenomena, particularly in ion-exchange processes. Carbon surface are generally considered to bear net negative charges; some interference with the movement of ions through the pores of activated carbon may therefore be anticipated (Weber, 1972).

Molecular diffusion may be considered most representative of the overall transport process, for the other physicochemical phenomena cited generally tend to interfere with the gradient-oriented movement of migrating species (Weber, 1972).

### **3.6. Factors Influencing Adsorption**

*Surface Area:* Adsorption is a surface phenomenon; as such, the extent of adsorption is proportional to specific surface area. Specific surface area can be defined as that portion of the total surface area that is available for adsorption. Thus the amount of adsorption accomplished per unit weight of a solid adsorbent is greater the more finely divided and the more porous the solid (Weber, 1972).

*Nature of the Adsorbate:* In any consideration of adsorption from solution one fact is immediately evident; the solubility of the solute is, to a large extent, a controlling factor for adsorption equilibria (Weber, 1972).

In general, an inverse relationship can be anticipated between the extent of adsorption of a solute and its solubility in the solvent from which adsorption occurs. The effects noted relative to solubility-adsorption relationships can be interpreted by postulating the necessity of breaking some form of solute-solvent



bond before adsorption can occur. The greater the solubility, the stronger the solute-solvent bond and the smaller the extent of adsorption (Weber, 1972).

Molecular size is of significance also as it relates to rate of uptake of organic solutes by porous adsorbent if the rate is controlled by intraparticle transport, in which case the reaction generally will proceed more rapidly the smaller the adsorbate molecule (Weber, 1972).

The bulk of the observations relative to ionization effects on adsorption seem to point to the generalization that as long as the compounds are structurally simple, adsorption is at a minimum for the charged species and at a maximum for the neutral species. As compounds become more complex, the effect of ionization becomes of decreasing importance (Weber, 1972).

There are also amphoteric compounds which have the capacity to be both an acid and a base. Studies on this type of compound indicate an adsorption maximum at the isoelectric point, or that pH at which both the acidic end and the basic end of the compound are ionized and the compound bears a net charge of zero. This is again accords with the observation that adsorption is at a maximum for neutral species (Weber, 1972).

A general rule for prediction of the effect of solute polarity on adsorption is that a polar solute will prefer the phase which is more polar. In other words, a polar solute will be strongly adsorbed from a nonpolar solvent by a polar adsorbent, but will much prefer a polar solvent to a nonpolar adsorbent. Polarity of organic compounds is a function of charge separation within the molecule. Almost any asymmetric compound will be found more or less polar, but several types of functional groups tend to produce fairly high polarities in compounds (Weber, 1972).

*pH:* The pH of a solution from which adsorption occurs may, for one or more of a number of reasons, influence the extent of adsorption. Because hydrogen and hydroxide ions are adsorbed quite strongly, the adsorption of other ions is influenced by the pH of the solution. Furthermore, to the extent to which the ionization of an acidic or basic compound affects its adsorption, pH affects adsorption in that it governs the degree of ionization (Weber, 1972).

*Temperature:* Adsorption reactions are normally exothermic; thus the extent of adsorption generally increases with decreasing temperature. The changes in enthalpy for adsorption are usually of the order of those for condensation or crystallization reactions. Thus small variations in the temperature tend not to alter the adsorption process to a significant extent (Weber, 1972).

*Adsorption of Mixed Solutes:* In the application of adsorption for purification of waters and wastewaters the material to be adsorbed commonly will be a mixture of many compounds rather than a single one. The compounds may mutually enhance adsorption, may act relatively independently, or may interfere with one another. Mutual inhibition of adsorption capacity can be predicted to occur provided: adsorption is confined to a single or a few molecular layers; the adsorption affinities of the solutes do not differ by several orders of magnitude; and there is not a specific interaction between solutes enhancing adsorption. Similarly, because the adsorption of one substance will tend to reduce the number of open sites, hence the “concentration” of adsorbent available as a driving force to produce adsorption of the other substance, mutually depressing effects on rates of adsorption may be predicted (Weber, 1972).

*Nature of the Adsorbent:* The physicochemical nature of the adsorbent can have profound effects on both rate and capacity for adsorption (Weber, 1972). It should not be forgotten that every solid is a potential adsorbent with its surface characteristics.

## CHAPTER 4

### MATERIALS AND METHOD

The use of natural materials as low cost adsorbents has found an important application for the adsorption of various dyestuffs from wastewater of textile industry. In this chapter, the adsorbents and dyestuffs used in the adsorption process, their physical and chemical properties are explained.

#### 4.1. Adsorbents

“Basaltic tephra” and “clinoptilolite” were used as adsorbents in this study. They are naturally occurring minerals. In addition to these minerals, “activated carbon” in powdered form (PAC) was also used to compare adsorption capacities of the adsorbents for the dyestuffs used in this study.

“Basaltic tephra” is a kind of volcanic stone that is containing large amount of gas space formed by dissociation of evolved gases due to rapid cooling of magma. Its apparent density is less than  $1.0 \text{ g/cm}^3$  and its hardness is about 5-6 according to mohs scale (TSI, 6918, 1989) (Kilavuz, 1994). Bayraktar (1984) studied about the characterization of “basaltic tephra” in the particle size of 0.5-30 mm and reported that the density and porosity of “basaltic tephra” is  $0.87 \text{ g/cm}^3$  and 40 %, respectively. It can adsorb water in the amount of 1/3 of its volume due to open pores in its structure (Bayraktar, 1984). “Basaltic tephra” used in this study was obtained from Osmaniye-Adana region.

“Clinoptilolite” is a natural zeolite mineral and is a natural Aluminum Silicate. The typical unit cell formula is given as  $\text{Na}_6[(\text{AlO}_2)_6(\text{SiO}_2)_{30}].24\text{H}_2\text{O}$ . “Clinoptilolite”,

like most of the zeolites, has a three-dimensional crystal structure and it contains two-dimensional channels in it. Therefore, some exchangeable cations like  $\text{Na}^+$ ,  $\text{K}^+$ ,  $\text{Ca}^{++}$  and  $\text{Mg}^{++}$  can be exchanged with organic and inorganic cations, like  $\text{NH}_4^+$ , metal ions (Armagan et al., 2003a). Some dye molecules can also be exchanged like cations. “Clinoptilolite” used in this study was obtained from Gördes-Manisa region.

## 4.2. Dyestuffs

The dyestuffs used in this study were obtained from Setas Chemistry Co. (Bursa). Name and color index numbers of the six different dyestuffs are presented in Table 4.1.

**Table 4.1.** Dyestuffs used in the experiments

Commercial name	Color index	Chemical class	Abbreviations
Setacryl Golden Yellow GL	Basic Yellow 28	Methine	BY
Setacryl Blue FGRL	Basic Blue Mix	Mix	BB
Nyloset Yellow SN6G	Acidic Yellow 95	Azo	AY
Nyloset Red EBL	Acidic Red 57	Monoazo	AR
Setazol Yellow 3RS	Reactive Yellow 145	Monoazo	RY
Setazol Red 3BS	Reactive Red 195	Monoazo	RR

### 4.3. Physical and Chemical Properties of Adsorbents

The **chemical composition** of the “tephra” is given in Table 4.2. As can be seen from this table  $\text{SiO}_2$  and  $\text{Al}_2\text{O}_3$  are the main constituents found in the structure of the “basaltic tephra”.

**Table 4.2.** Chemical composition of basaltic tephra

Constituent	Basaltic tephra, % by weight
$\text{SiO}_2$	47.35
$\text{Al}_2\text{O}_3$	19.99
$\text{CaO}$	9.23
$\text{Fe}_2\text{O}_3$	12.26
$\text{MgO}$	4.03
$\text{Na}_2\text{O}$	2.97
$\text{K}_2\text{O}$	2.56
$\text{TiO}_2$	1.61

$\text{SiO}_2$  and  $\text{Al}_2\text{O}_3$  are also the main constituents in the structure of “clinoptilolite”. The other oxides found in “basaltic tephra” are also present in “clinoptilolite” in various quantities. The amount of  $\text{SiO}_2$  in the clinoptilolite is approximately 70-76% and that of  $\text{Al}_2\text{O}_3$  is about 14-15% by weight.  $\text{SiO}_2/\text{Al}_2\text{O}_3$  ratio in the structure is about 5 (Armagan et al., 2003, Yasyerli et al., 2002).

Tephra is classified as acidic, neutral and basic according to its  $\text{SiO}_2$  content as presented in Table 4.3 (Ulasoglu, 1995).

**Table 4.3.** Classification of tephra

<b>SiO<sub>2</sub> content, % by weight</b>	<b>Type</b>
> 66	Acid (Granite)
66 - 52	Neutral (Andezit)
52 - 45	Basic (Basaltic)
< 45	Ultrabasic (Limburgit)

As seen from Table 4.3, tephra used in this study is “basaltic tephra” since the SiO<sub>2</sub> content is 47%.

**Particle sizes** of “basaltic tephra” and “clinoptilolite” used in this study are given in Table 4.4.

**Table 4.4.** Particle sizes of basaltic tephra and clinoptilolite used in the experiments

<b>Material</b>	<b>Particle size, mm</b>
Basaltic Tephra	$d_p < 0.60$
Basaltic Tephra	$0.60 < d_p < 1.00$
Clinoptilolite	$d_p < 0.50$
Clinoptilolite, Powdered Form	$d_p < 0.063$

The **surface areas** of the adsorbents used in the experiments was determined by the BET method. The analyses were done in the Department of Chemical Engineering at METU by using Micromeritics ASAP 2000. The results of the analysis are given in Table 4.5.

**Table 4.5.** Surface areas of the adsorbents

<b>Material</b>	<b>BET surface area, m<sup>2</sup>/g</b>
Basaltic Tephra, <0.60 mm	6.4
Basaltic Tephra, 0.60-1.00 mm	4.2
Clinoptilolite, <0.50 mm	28.4
Clinoptilolite, Powdered Form	36.7
Powdered Activated Carbon	598.4

As seen from Table 4.5, surface area of “basaltic tephra” is smaller than that of “clinoptilolite” for all particle sizes. Also, surface areas of the adsorbents increase if particle sizes decrease, i.e. the smallest particle size has the largest surface area. In addition “powdered activated carbon” has much higher BET surface area than other adsorbents.

**Average pore diameters** and **total pore volumes** of the adsorbents used in this study are given in Table 4.6. These parameters were measured in the Department of Chemical Engineering at METU by using Micromeritics ASAP 2000.

**Table 4.6.** Average pore diameters and total pore volumes of the adsorbents

<b>Material</b>	<b>Average pore diameter, Å<sup>o</sup></b>	<b>Total pore volume, mL/g</b>
Basaltic Tephra, 0-0.60 mm	92.6	0.0184
Basaltic Tephra, 0.60-1.00 mm	83.9	0.0087
Clinoptilolite, 0-0.50 mm	91.3	0.0647
Clinoptilolite, Powdered Form	96.5	0.0884
Powdered Activated Carbon	22.0	0.4498

The average pore diameters of “basaltic tephra” and “clinoptilolite” are very similar, approximately 85-95 Å. The total pore volume of “basaltic tephra” is about 3.5 times smaller than “clinoptilolite” for almost the same particle sizes. However, for “powdered activated carbon” which was taken as reference material in this study, the total pore volume is about 7 times larger than that of “clinoptilolite”, although the average pore diameter is about 4 times smaller.

The **Scanning Electron Microscope (SEM)** photographs of basaltic tephra were taken in the Department of Metallurgical and Materials Engineering at METU. The instrument is Jeol, JSM-6400 Scanning Microscope. As an example two SEM photographs of the basaltic tephra are given Figure 4.1 and Figure 4.2. Also the SEM photographs of clinoptilolite were obtained from the literature in order to give an idea about the crystal structure, and they are given in Figure 4.3 and Figure 4.4.

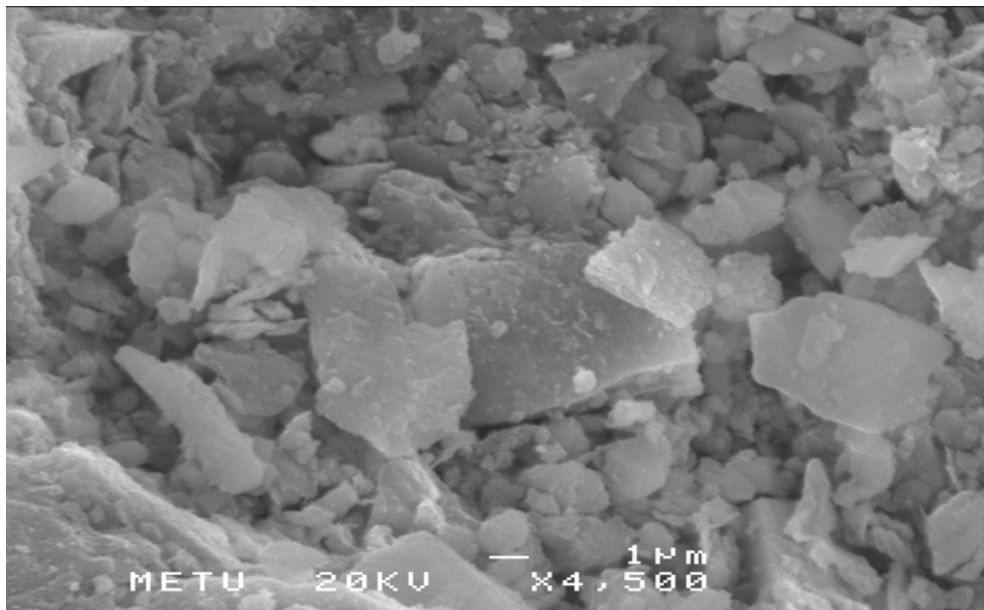


**Figure 4.1.** SEM photograph of basaltic tephra for  $d_p < 0.60$  mm (x 4,500)



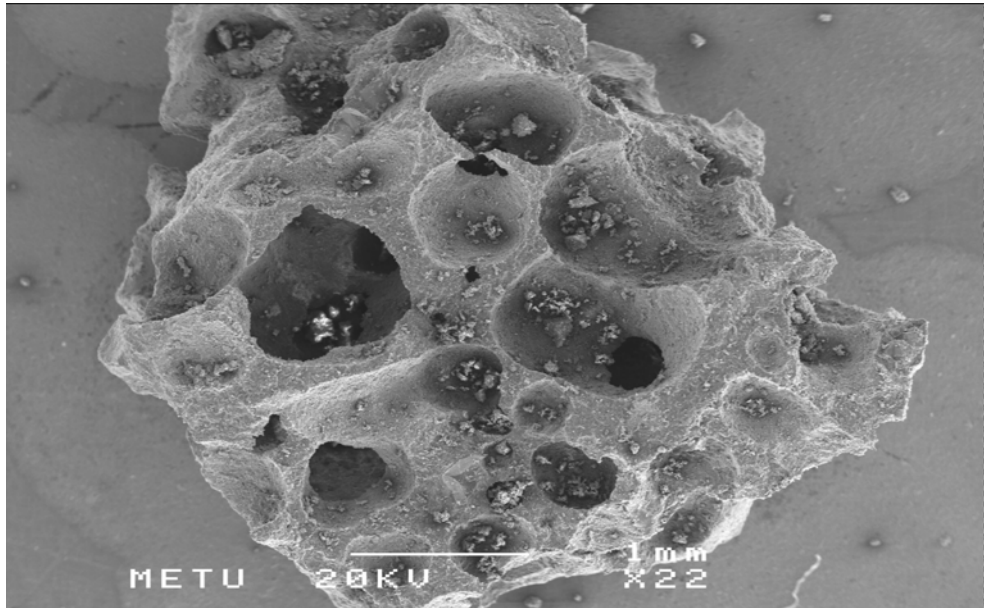


**Figure 4.2.** SEM photograph of basaltic tephra for  $2.85 < d_p < 3.35$  mm (x 22 )

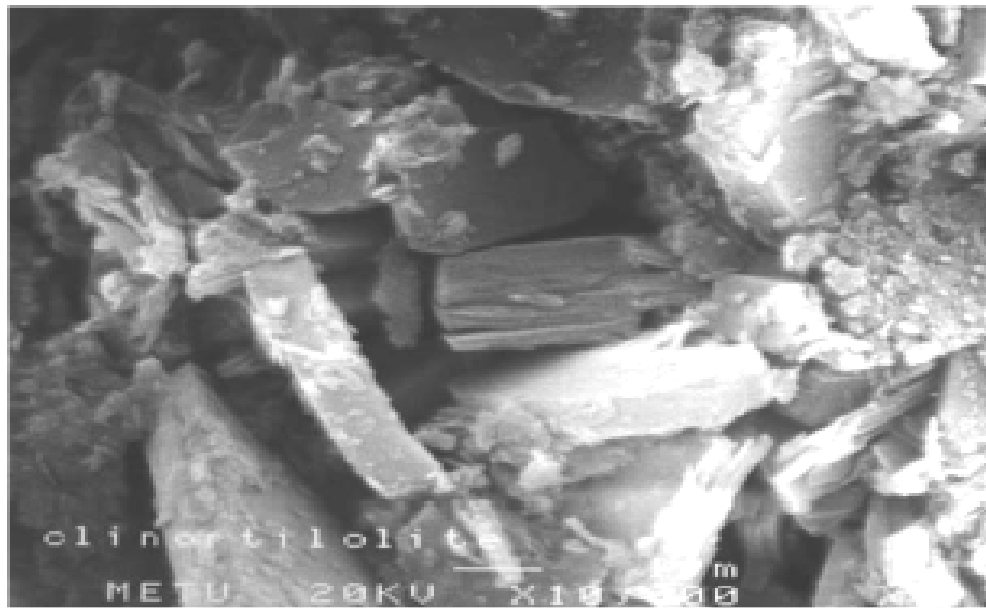


**Figure 4.3.** SEM photograph of clinoptilolite for  $d_p < 0.25$  mm (x 10,000)  
(Yasyerli et al., 2002)

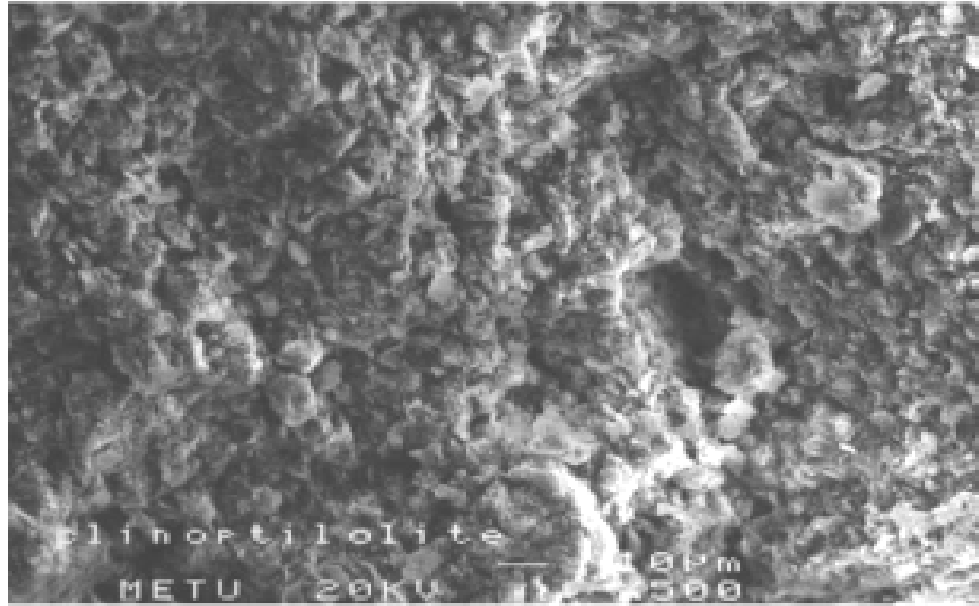


**Figure 4.4.** SEM photograph of clinoptilolite for  $d_p < 0.25$  mm (x 500)  
(Yasyerli et al., 2002)

The **electrokinetic properties** of “basaltic tephra” and “clinoptilolite” were determined by using Zeta Sizer (Nano-ZS90) in the Central Laboratory of METU. In the preparation of the samples to measure zeta potentials, 1 g of material was conditioned in 250 mL of distilled water for 10 min. The suspension was kept still for 5 min to allow the larger particles to settle. Each data point is an average of 30 measurements. As all adsorption experiments were conducted at neutral potential state, zeta potentials of “basaltic tephra” and “clinoptilolite” were determined at the pH of 7 and the results are given in Table 4.7.

**Table 4.7.** Zeta potentials of the adsorbents at pH=7

Material	Zeta potential, mV
Natural Basaltic Tephra	-20
Natural Clinoptilolite	-28

#### 4.4. Experimental Setup

A schematic diagram of the setup used in experiments is shown in Figure 4.5. The setup consists of a shaker, a filter system and a visible spectrophotometer. The shaker used in this study is Gallenkamp Orbital Incubator (Cat. No: 10x400.xx1.C, Serial No: S094/02/019). Samples were filtered through 0.45  $\mu\text{m}$  filter system. Absorbance of the samples were measured with a DR/2000 model Direct Reading Visible Spectrophotometer. The range of wavelength and absorbance for the spectrophotometer is 325-900 nm and  $-0.3$ - $3.0$ , respectively.

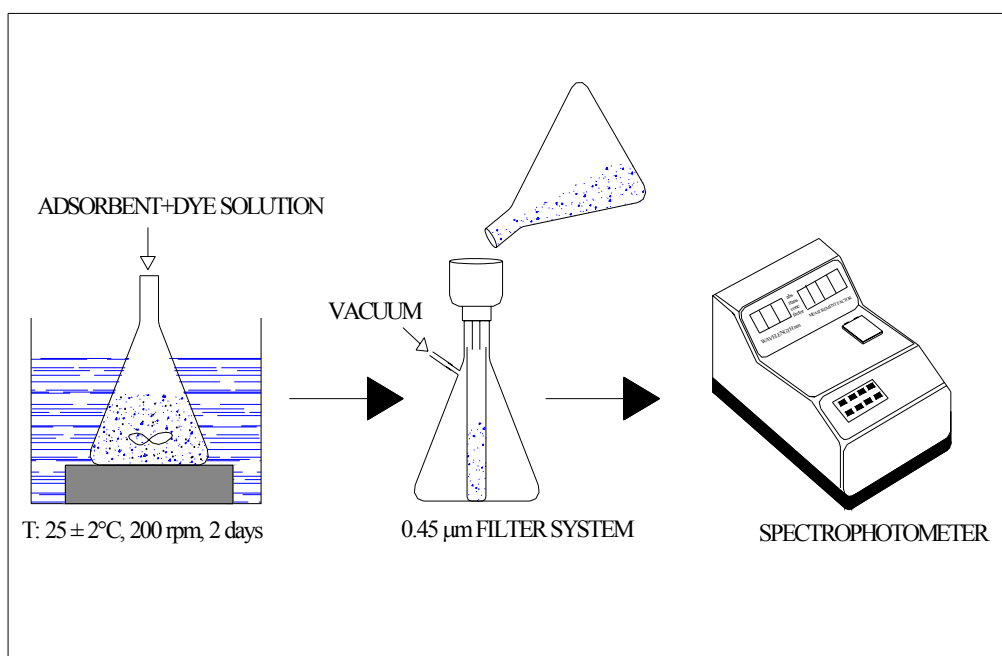


**Figure 4.5.** Schematic diagram of the experimental setup

#### 4.5. Calibration Curves

Calibration curves were prepared by plotting known concentrations of each dyestuff versus corresponding absorbance values. The concentrations of dyestuffs in the solutions were measured with the spectrophotometer at appropriate wavelengths corresponding to the maximum absorbency for each dye listed in Table 4.8. Absorbance versus concentration plots for all dyestuffs are given in Appendix A.

**Table 4.8.** Wavelengths corresponding to maximum absorbance

Dyestuffs	Wavelengths, nm
• Basic Blue	600
• Basic Yellow	445
• Acidic Yellow	420
• Acidic Red	515
• Reactive Yellow	420
• Reactive Red	540

#### 4.6. Experimental Procedure

First of all, duration of the experiments were determined because the determination of equilibrium time is very important and should be decided in order to define agitation period during adsorption experiments. Therefore, for each set of experiment 5-8 Erlenmeyer flasks of 500 mL volume were taken and 100 mL of dye solution with a concentration of 100 mg/L was placed into each flask. An adsorbent of 0.1 g/100 mL for *basic dyes*, and 0.5 g/100 mL for *acid* and *reactive dyes* was added to the solution. The top of the flasks was closed and they were placed in the shaker. The Erlenmeyer flasks were agitated in the shaker at 200 rpm

and at a temperature of  $25 \pm 2$  °C. After the start of the experiment, one flask was taken out of the shaker at a time in order to see how much of the dye in the solution was adsorbed by the adsorbent during the time elapsed between the start of the experiment and the time at which the flask was taken out, while the adsorption of dyes continued in the other flasks. From each flask about 20 mL of the solution was filtered through a 0.45  $\mu\text{m}$  filter system to avoid turbidity interference during color determination. Then, dye concentration of the filtered solution was measured by the spectrophotometer with a 1 cm path length and concentration of the dye solution was determined by using the calibration curves. Finally, percent removal versus time graphs, given in Appendix B, were plotted to determine the equilibrium time.

After the determination of the equilibrium time, adsorption experiments were conducted by mixing a fixed amount of dry adsorbent (0.1 g) with 100 mL dye solutions at 8 different concentrations, which were varied from 25 to 500 mg/L, in 500 mL Erlenmeyer flasks which were shaken at 200 rpm and  $25 \pm 2$ °C for 2 days. Then, at the end of the experiment approximately 20 mL of a sample from each flask was filtered through 0.45  $\mu\text{m}$  filter system and dye concentrations of the filtered solutions was measured by using the spectrophotometer with a 1 cm path length. If the absorbance value measured was higher than 0.6, dilution of the solution was applied. Finally, adsorption isotherms were plotted to see the relationship between adsorption capacity of the adsorbent and equilibrium concentration of the adsorbate.

It was noted during the filtration of solutions through 0.45  $\mu\text{m}$  filter system that filter paper adsorbs the dye to a small extent for various dyes. In order to determine the amount of adsorption by filter paper, solutions with various dyes used in this study at various concentrations were prepared, filtered through the paper and the concentration of the dye solutions before and after filtration were measured. The results of the measurements are given in Appendix C.

The concentration measurements for all the adsorption experiments were corrected accordingly based on the curves obtained in Appendix C.

#### **4.7. Modification of Surface Properties**

At the end of the adsorption experiments, adsorption capacities of the natural adsorbents were determined. *Basic dyes* were adsorbed better due to electrostatic interactions between the adsorbate and adsorbent. *Basic dyes* are cationic dyes and the surface charges of both “basaltic tephra” and “clinoptilolite” are negative. However, little or no adsorption for *acid dyes* and *reactive dyes* were obtained because they are anionic dyes. Therefore, modification of surface properties of the natural materials was considered. Surface modification of “basaltic tephra” and “clinoptilolite” was made by using a quaternary amine, hexadecyltrimethylammonium bromide (HTAB,  $C_{19}H_{42}BrN$ ) that is a cationic surfactant purchased from Sigma. The molecular weight of HTAB is 346.46 g. The procedure of modification is given in Figure 4.6 (Armagan et al., 2003a). The experiments were conducted again under the same conditions by using modified adsorbents. The results obtained are given in Chapter 5. It should be noted that 0.02 M of the HTAB is approximately 7.5 g and that amount was used to modify 50 g of the natural adsorbent. After agitation of natural adsorbents in HTAB solution, the solids were washed with distilled water twice until no HTAB is present. Therefore, it is safe to assume that no HTAB was released to dye solutions during adsorption experiments.

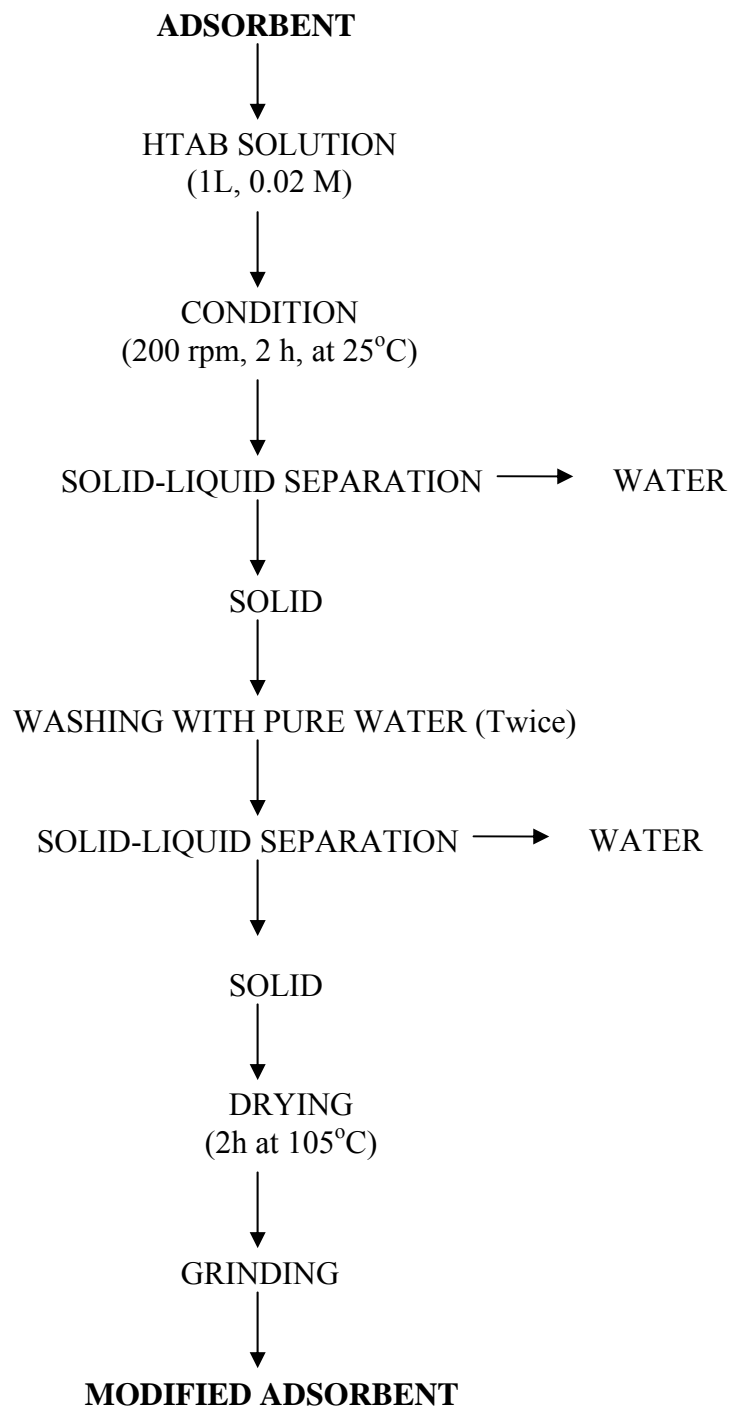


**Figure 4.6.** Flowsheet for preparing modified adsorbents

## **CHAPTER 5**

### **RESULTS AND DISCUSSION**

#### **5.1. Selection of Solid Concentration**

In this study, solid concentration used in the experiments was 0.1% (0.1 g adsorbent/100 mL of solution). This value was decided to be used at the end of the literature survey, i.e, similar values for solids concentrations were used in the similar studies. In the calculation of the adsorption capacities of the adsorbents, unit mass of adsorbent was used in this study.

#### **5.2. Effect of Mixing Time**

A series of experiments were conducted to determine the equilibrium time in the adsorption experiments. The procedure for the determination of equilibrium time is given in Part 4.6. Some of the rate curves are given in Appendix B.

It can be seen from Figures B.1-B.12 that, most of the adsorption process has taken place in a few hours. However, after that time adsorption continued slowly. In this study, a period of 2 days was decided to be used as the mixing time in order to find the maximum adsorption capacities of the adsorbents.

#### **5.3. Effect of Filter in Removal of Dyes During Filtration**

While filtering the dye solutions through 0.45  $\mu\text{m}$  filter system, some amount of dyes was removed by the filter. Therefore, the adsorption capacities of the



adsorbents were corrected by considering the amount held by filter. In order to see the effect of filter in the removal of the dyestuffs during filtration, the percentage removal by filter against dye concentrations in Figures C.1-C.6 were plotted. These plots are given in Appendix C.

As can be seen from Figures C.1 and C.2 very small amount of *acid yellow* and *reactive yellow* dyestuffs (less than 1%) was held by the filter. However, the filter adsorbed *basic yellow*, *acid red* and *reactive red* dyestuffs in higher amounts than *acid yellow* and *reactive yellow* dyestuffs. The highest amount of removal by the filter was observed for *basic blue* dyestuff as given in Figure C.6.

#### **5.4. Effect of Modification**

After modification of the surface properties of “basaltic tephra” and “clinoptilolite” by using HTAB, some changes in the properties of the adsorbents were observed. The most interesting change was observed in the electrokinetic properties of the adsorbents.

Zeta potentials for natural and modified “basaltic tephra” and “clinoptilolite” were measured at different pH values and zeta potential versus pH profiles are plotted as given in Figure 5.1 and Figure 5.2, respectively.

As can be seen from Figure 5.1, the zeta potential curve for the “modified basaltic tephra” lies above the curve for the “natural basaltic tephra”. The zeta potentials of “natural basaltic tephra” after the surface modification were increased for all pH range. This figure shows that HTAB has been effective in changing the surface charge of “basaltic tephra”. As seen from Figure 5.2, the surface charge of the “clinoptilolite” was changed from anionic state to cationic state with the modification. The effect of the modification process on “basaltic tephra” and

“clinoptilolite” was different from each other probably due to different surface structures of the materials.

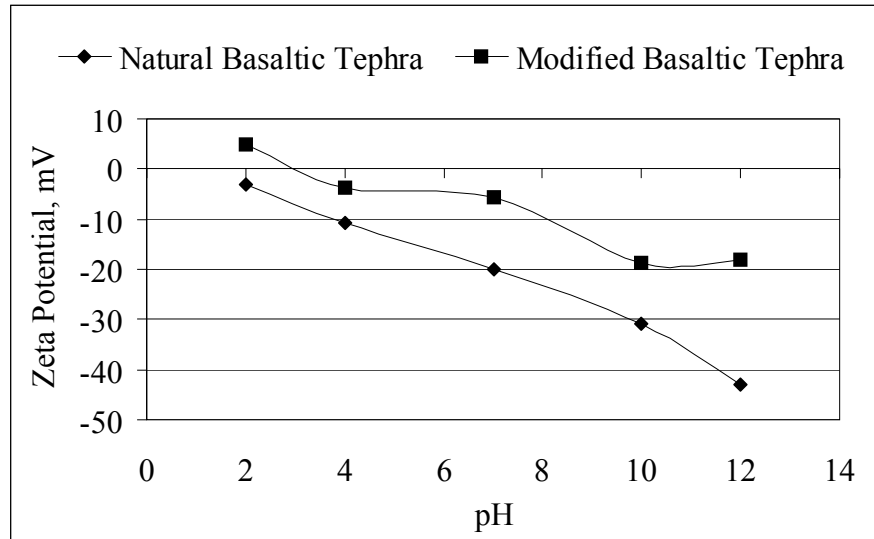


**Figure 5.1.** Zeta potential versus pH profiles of natural and modified basaltic tephra

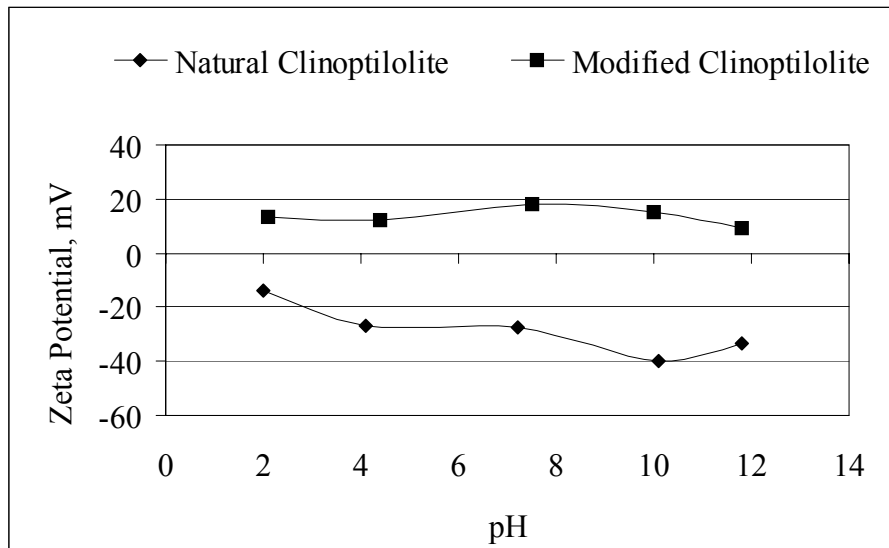


**Figure 5.2.** Zeta potential versus pH profiles of natural and modified clinoptilolite

Surface areas of “basaltic tephra” and “clinoptilolite” were determined after the modification. The results have shown that surface areas of the “basaltic tephra” and “clinoptilolite” were changed after surface modification with HTAB. The results are given in Table 5.1.

**Table 5.1.** Surface areas of the adsorbents before and after surface modification

Material	BET surface area, m <sup>2</sup> /g
Basaltic Tephra, <0.60 mm	6.44
Modified Tephra	2.73
Clinoptilolite, <0.063 mm	36.65
Modified Clinoptilolite	19.14

As can be seen from Table 5.1, surface areas of natural materials were decreased after modification most probably due to the closure of the pores with bigger HTAB molecules. Incremental pore area distribution versus pore diameter plots for natural and modified adsorbents are given in Figures 5.3-5.5.

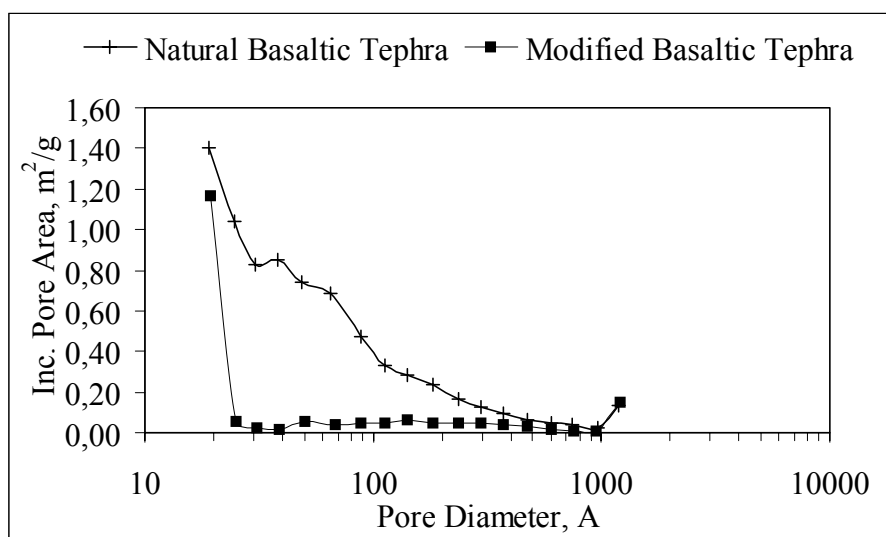


**Figure 5.3.** Incremental pore area versus pore diameter plot for basaltic tephra

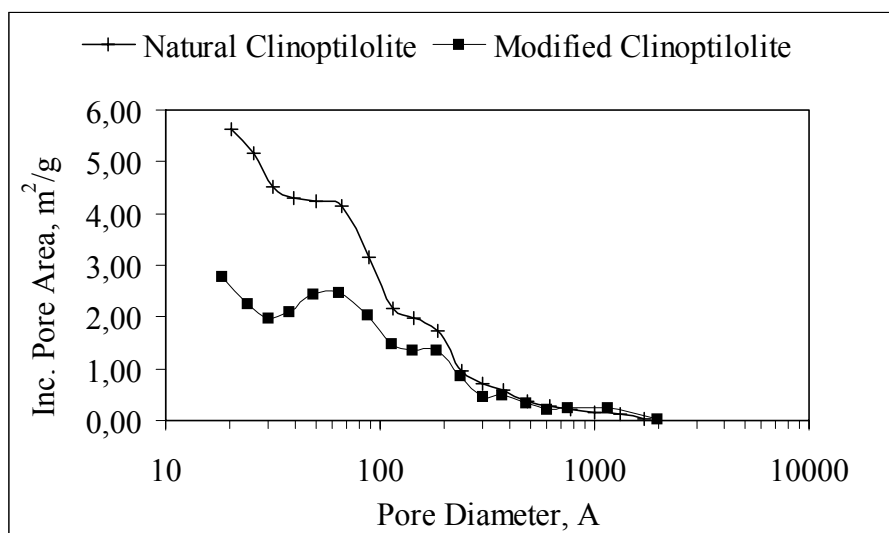


**Figure 5.4.** Incremental pore area versus pore diameter plot for clinoptilolite

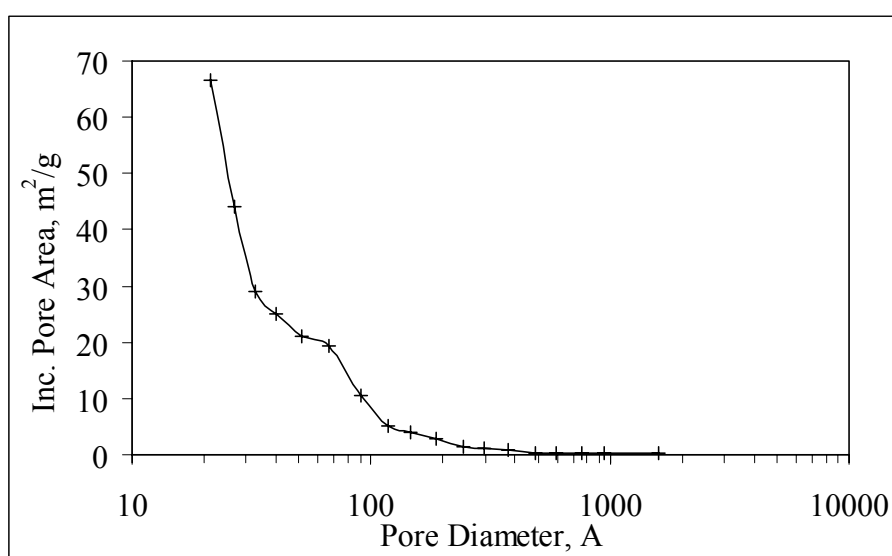


**Figure 5.5.** Incremental pore area versus pore diameter plot for PAC

From these figures it can be seen that surface areas of the natural adsorbents, especially for smaller pore diameters were decreased about 50% after modification with HTAB. “Powdered activated carbon” has the highest pore area among all adsorbents.

Incremental pore volume distribution versus pore diameter plots for natural and modified adsorbents are given in Figures 5.6-5.8.

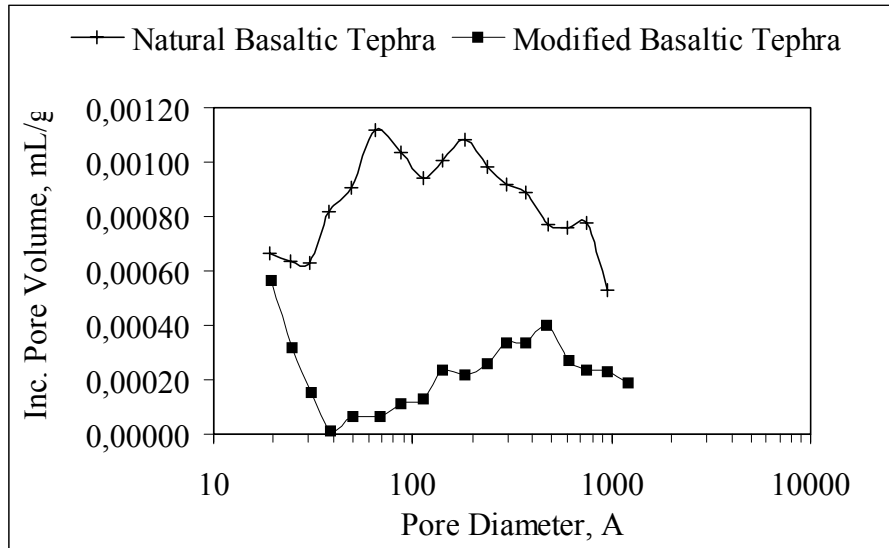


**Figure 5.6.** Incremental pore volume versus pore diameter plot for basaltic tephra

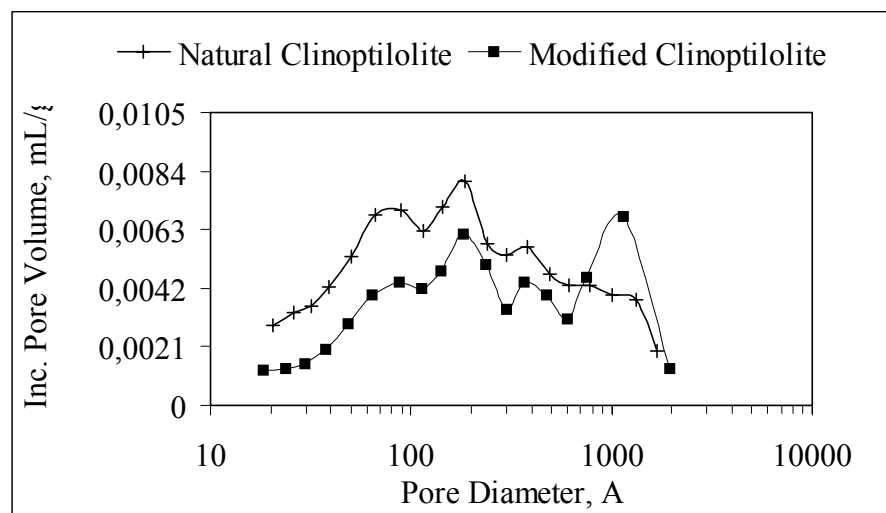


**Figure 5.7.** Incremental pore volume versus pore diameter plot for clinoptilolite

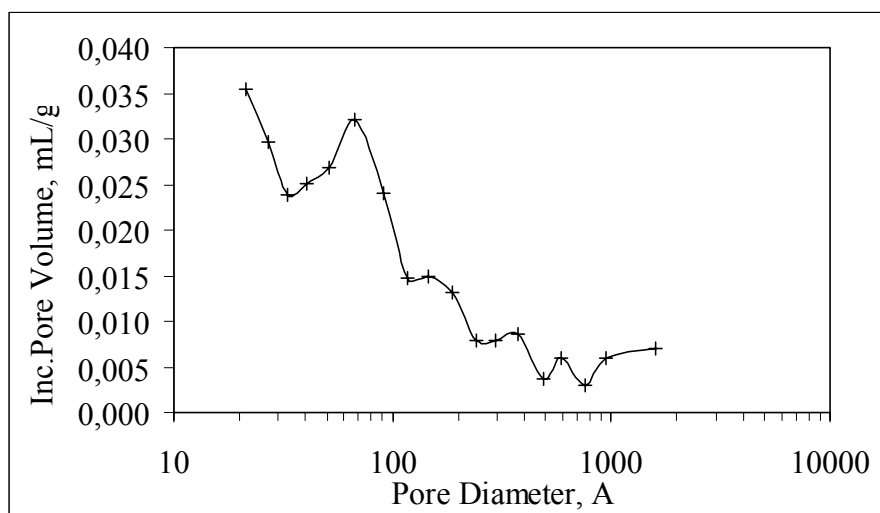


**Figure 5.8.** Incremental pore volume versus pore diameter plot for PAC

The change in the total pore volumes of the adsorbents is given in Table 5.2. The total pore volume which was 0.0184 mL/g for “basaltic tephra” has been decreased to 0.0043 mL/g after surface modification. This is about 4 times decrease in the original value. Similarly, 25 % decrease in total pore volume has been observed in total pore volume has been observed in “clinoptilolite” after surface modification.

**Table 5.2.** Average pore diameter and total pore volumes of the natural and modified adsorbents

<b>Material</b>	<b>Average pore diameter, A</b>	<b>Total pore volume, mL/g</b>
Basaltic Tephra, 0-0.60 mm	92.6	0.0184
Modified Basaltic Tephra	62.6	0.0043
Clinoptilolite, Powdered Form	96.5	0.0884
Modified Clinoptilolite	132.4	0.0633

## 5.5. Adsorption of Dyestuffs onto Basaltic Tephra

### 5.5.1. Effect of Particle Size on Adsorption

Two particle sizes of natural “basaltic tephra” were used in the adsorption of *basic blue* dyestuffs from aqueous solution in order to see the effect of particle size on the adsorption process. Adsorption isotherms for two particle sizes of “basaltic tephra” are presented in Figure 5.9. As seen from the figure, the smaller size particles ( $d_p < 0.60$  mm) have the higher adsorption capacity as expected due to higher surface area available for adsorption.

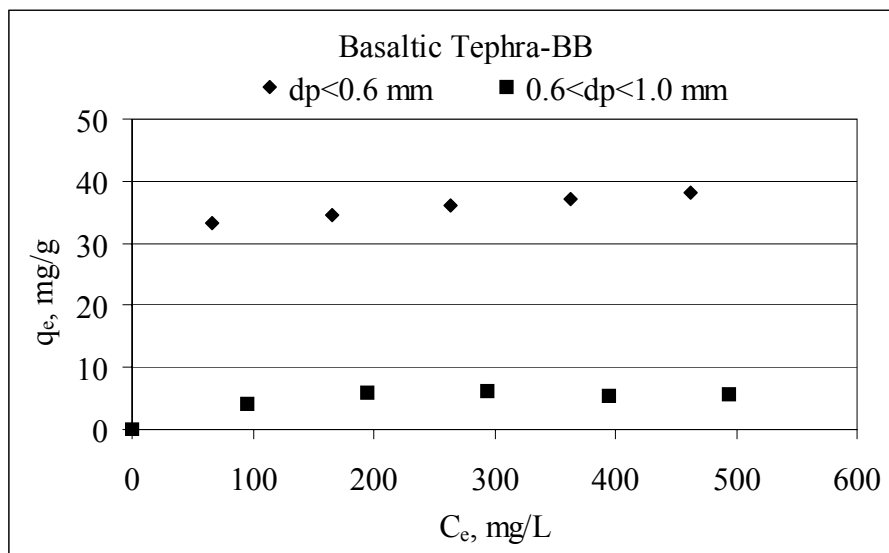


**Figure 5.9.** Adsorption isotherms for basic blue on two sizes of basaltic tephra

As can be seen from the figure higher adsorption capacity was obtained for the smaller particle size (lower than 0.6 mm) and the capacity is approximately 38 mg/g. Since the particle size  $d_p < 0.60$  mm gave better results than the other size, the smaller particle size of “basaltic tephra” was used in the other experiments.

### 5.5.2. Adsorption of “Basic Dyestuffs” onto Basaltic Tephra

Adsorption capacities of natural and modified “basaltic tephra” for *basic dyestuffs* were determined. Modification of the adsorbent was made as given in Chapter 4. Adsorption isotherms are given in Figure 5.10.

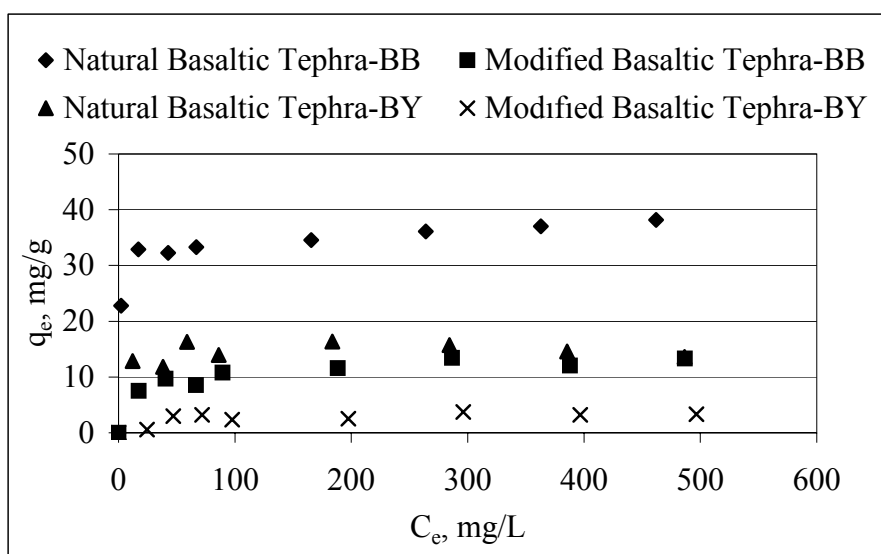


**Figure 5.10.** Adsorption isotherms for basic blue on natural and modified basaltic tephra

As can be seen from Figure 5.10, natural “basaltic tephra” has an adsorption capacity of about 38 mg/g for *basic blue (BB)* dye. However, the adsorption capacity of the “modified basaltic tephra” is about 10 mg/g. Therefore, it is seen from the result that “natural basaltic tephra” has higher adsorption capacity than that of “modified basaltic tephra” for *basic blue* dye.



A similar result was obtained for *basic yellow (BY)* dye. The adsorption capacity of the “natural basaltic tephra” was 16 mg/g. However, the adsorption capacity became about 3 mg/g for the “modified basaltic tephra”.

In adsorption processes, the rate limiting step may be surface layer resistance or diffusion through pores in the adsorbents. In batch reactors, the surface layer resistance can be eliminated due to agitation. Therefore, pore diffusion is the main rate limiting step in adsorption process in batch experiments.

Also, there are two main forces in adsorption. The first one is the electrostatic interactions between the surface of adsorbents and adsorbates. For this study, the experiments were performed at the neutral pH range (6.5-8.5) and the zeta potential of “basaltic tephra” measured at pH=7 was approximately  $-20$  mV. As a result of this, electrostatic interaction between the “basaltic tephra” and *basic dyes* that are cationic dyes resulted in attraction forces. The second force in the adsorption process is the diffusion of adsorbate molecules through pores of the adsorbent. Therefore, the net adsorption force is the sum of these two forces. As a result, the sum of these forces resulted in higher adsorption capacity for “natural basaltic tephra” than “modified basaltic tephra”.

On the contrary, with the modification, the electrokinetic properties of the adsorbent were changed, i.e. zeta potential of the adsorbent became  $-5.8$  mV as compared to  $-20$  mV previously. Therefore, the magnitude of the attraction forces decreased. Also, the surface area of the “basaltic tephra” was decreased after modification with HTAB because some of the pore area of the adsorbent was closed with HTAB molecules. That difference can be seen in Figure C.1. As a result, the effect of diffusion forces also reduced due to modification with HTAB. Consequently, the decreased net adsorption forces resulted in lower adsorption capacity of “modified basaltic tephra” for *basic dyes*.

After determining the capacities of the natural and modified adsorbent Langmuir and Freundlich Isotherm Equations were applied in order to find out which equation represents the results of this study better. Langmuir and Freundlich Isotherm plots are given in Figure 5.11 and Figure 5.12, respectively.

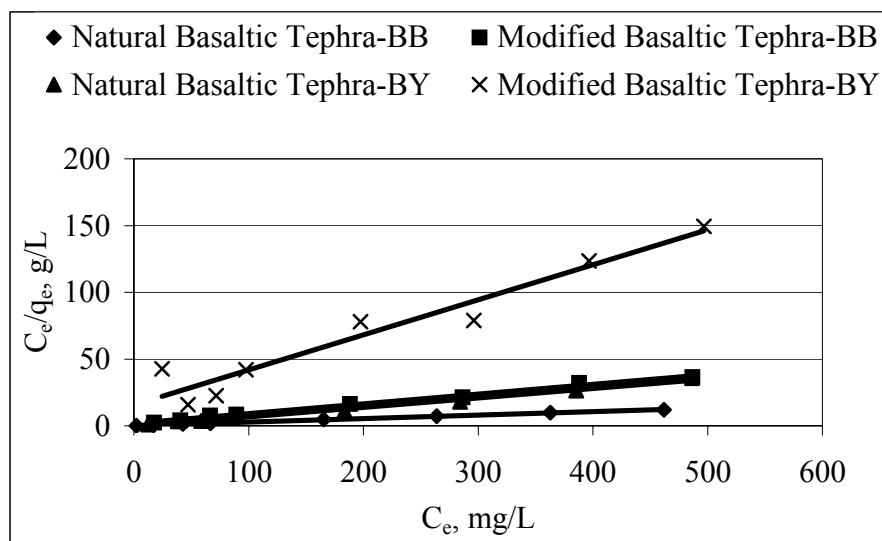


**Figure 5.11.** Langmuir plots for the adsorption of basic blue on natural and modified basaltic tephra

Langmuir Equation constants as explained in Chapter 3 were calculated from Figure 5.11 and are given in Table 5.3.

**Table 5.3.** Langmuir isotherm constants for natural and modified basaltic tephra

Adsorbent	Dye	$q_{mon}$ (mg/g)	$K_L$ (L/g)	$R_L$ (-)	$R^2$ (-)
Natural	BB	38.1	0.13	0.015	0.998
Modified	BB	13.6	0.04	0.045	0.992
Natural	BY	14.1	0.17	0.012	0.992
Modified	BY	3.8	0.02	0.106	0.934

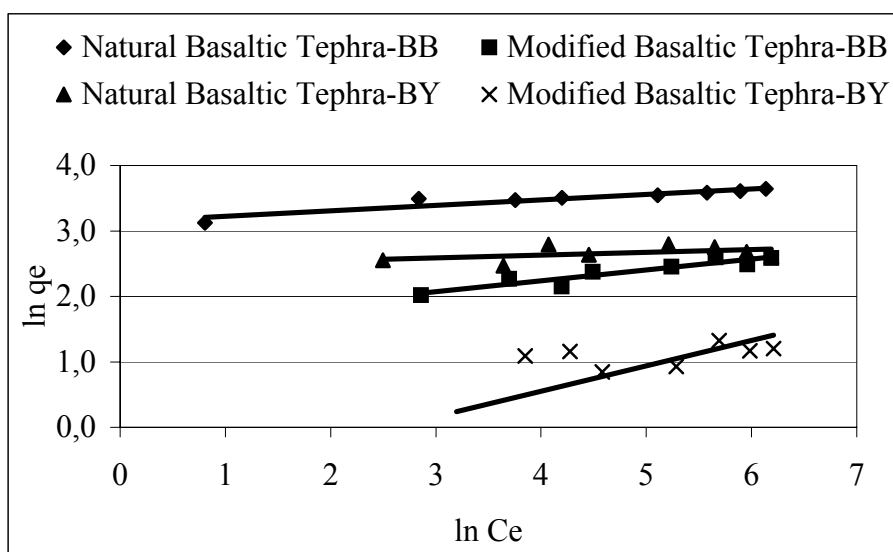


**Figure 5.12.** Freundlich plots for the adsorption of basic blue on natural and modified basaltic tephra

Freundlich Equation constants calculated from Figure 5.12 are given in Table 5.4.

**Table 5.4.** Freundlich isotherm constants for natural and modified basaltic tephra

Adsorbent	Dye	$K_F (-)$	$b_F (-)$	$R^2 (-)$
Natural	BB	23.06	0.083	0.877
Modified	BB	4.84	0.165	0.873
Natural	BY	11.78	0.041	0.202
Modified	BY	0.37	0.388	0.478

As can be seen from Table 5.4 the correlation coefficients are smaller than those calculated from Langmuir Equation for both natural and modified “basaltic tephra”. Therefore, it can be said that adsorption of *basic blue* and *basic yellow* dyestuffs can fit better to Langmuir Isotherm Equation than Freundlich Isotherm Equation. It means that the adsorption occurs as a monolayer at specific sites.

### 5.5.3. Adsorption of “Acid Dyestuffs” onto Basaltic Tephra

Figure 5.13 shows the adsorption isotherms of *acid dyestuffs* on natural and modified “basaltic tephra”.

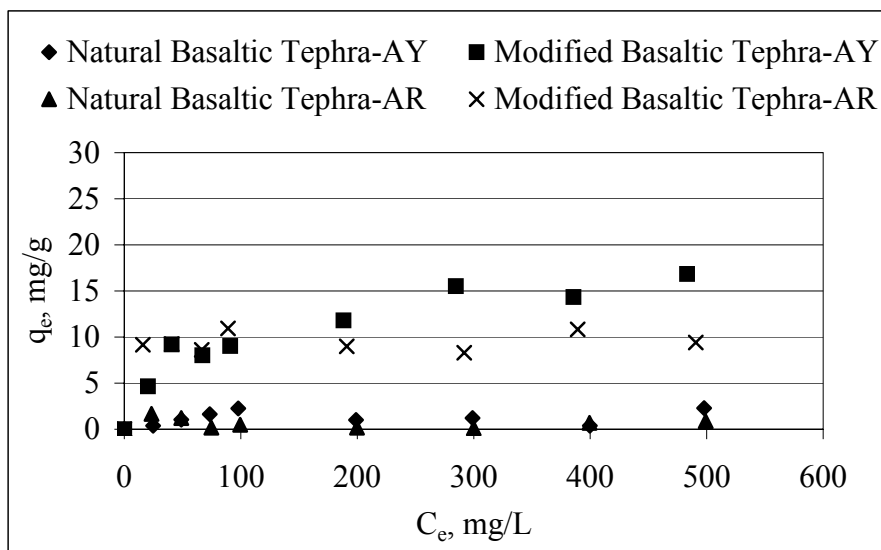


**Figure 5.13.** Adsorption isotherms for acid dyes on natural and modified basaltic tephra

It is interesting to note that the adsorption capacity of “modified basaltic tephra” for *acid dyes* are higher than those of “natural basaltic tephra”. The adsorption capacity of “natural basaltic tephra” for *acid yellow (AY)* and *acid red (AR)* dyestuffs was between 0-2 mg/g. After the surface was modified with HTAB, the adsorption capacity increased and became about 15 mg/g for *acid yellow (AY)* and 10 mg/g for *acid red (AR)*. This is a very good indication that adsorption capacity can be modified (increased) several times by changing the surface properties.

Prior to modification, repulsive forces between *acid dyes*, which are anionic dyes, and natural adsorbent, of which surface charges are negative, caused little adsorption of *acid dyes* on natural material. The zeta potential of the “basaltic tephra” is about -20 mV at pH=7. Since the *acid dyes* have negative groups, the repulsive forces between the surface of “basaltic tephra” and dyestuffs are effective. However, there are also dispersion forces between the adsorbents and adsorbates in the adsorption process. Therefore, the adsorption forces are the sum of dispersion and electrostatic forces (Dai, 1998). As a result of this, little adsorption may be explained by small positive adsorption forces between dyestuffs and the adsorbent.

However, with the modification with HTAB, the surface charges of the “natural basaltic tephra” were changed from stronger anionic state to weaker anionic state. Consequently, the effect of repulsion forces was decreased. Therefore the total adsorption forces between the surface of adsorbent and dyestuffs increased.

Langmuir and Freundlich Equations were applied to the adsorption of *acid dyes* on “modified adsorbents”. These two equations were not applied to the adsorption of *acid dyes* on “natural basaltic tephra” due to very small capacity of “natural basaltic tephra”. Langmuir and Freundlich Isotherm plots are given in Figure 5.14 and Figure 5.15, respectively.

Langmuir Equation constants calculated from Figure 5.14 are given in Table 5.5.

**Table 5.5.** Langmuir isotherm constants for modified basaltic tephra

Adsorbent	Dye	$q_{mon}$ (mg/g)	$K_L$ (L/g)	$R_L$ (-)	$R^2$ (-)
Modified	AY	18.4	0.01	0.129	0.975
Modified	AR	9.7	0.23	0.009	0.980

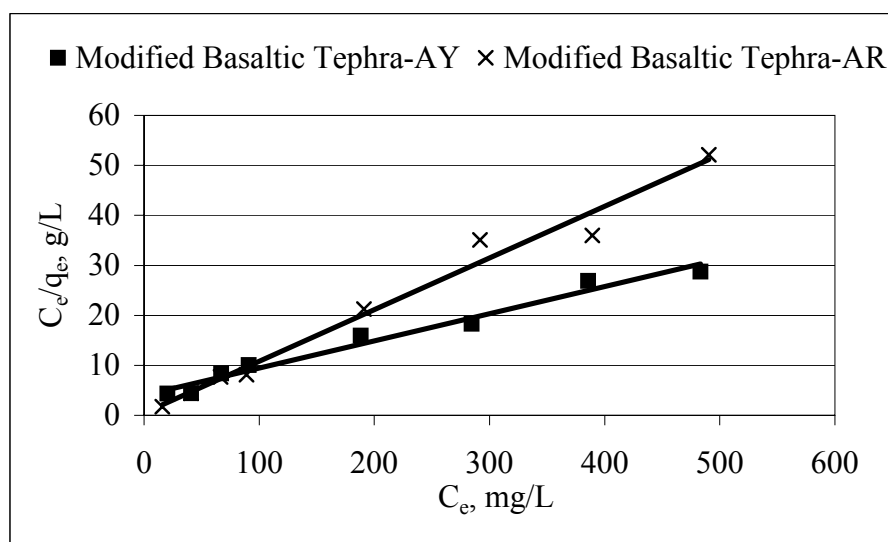


**Figure 5.14.** Langmuir plots for the adsorption of acid dyes on modified basaltic tephra

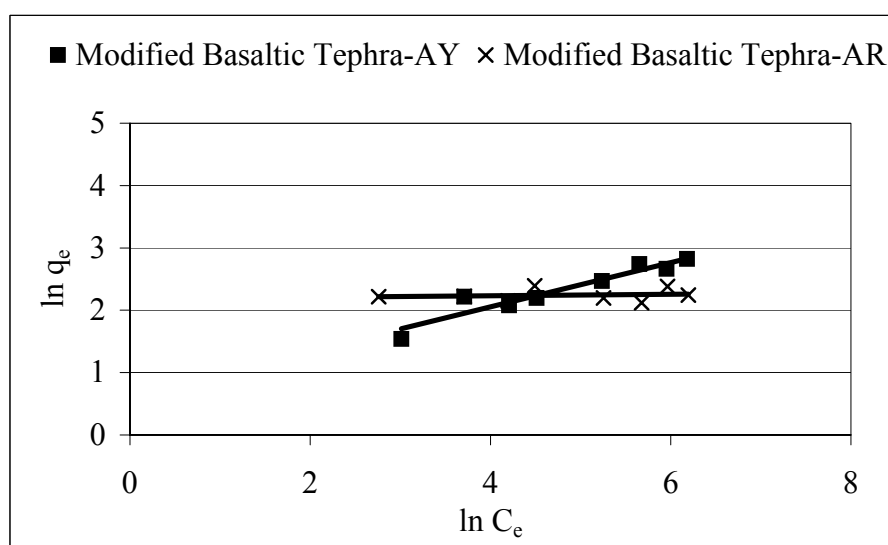


**Figure 5.15.** Freundlich plots for the adsorption of acid dyes on modified basaltic tephra

Freundlich equation constants were calculated by using Figure 5.15 and they are presented in Table 5.6.

**Table 5.6.** Freundlich isotherm constants for modified basaltic tephra

Adsorbent	Dye	$K_F (-)$	$b_F (-)$	$R^2 (-)$
Modified	AY	1.88	0.356	0.904
Modified	AR	8.91	0.011	0.018

As seen from Table 5.6, the correlation coefficients calculated from Freundlich Equation for both natural and modified “basaltic tephra” are smaller than those calculated from Langmuir Equation. Therefore, adsorption isotherms of *acid dyestuffs* fit better to Langmuir Isotherm Equation than Freundlich Equation.

#### 5.5.4. Adsorption of “Reactive Dyestuffs” onto Basaltic Tephra

Figure 5.16 presents the adsorption isotherms of *reactive dyestuffs* on natural and modified “basaltic tephra”.

As can be seen from Figure 5.16, adsorption capacities of “modified basaltic tephra” for *reactive dyes* are again higher than those of “natural tephra” as in the case of *acid dyes*. The adsorption capacity of “natural tephra” for *reactive red (RR)* was between 0-1 mg/g. After the surface modification with HTAB, the adsorption capacity became about 12 mg/g.

Prior to modification, repulsive forces between *reactive dyes*, which are anionic dyes due to negative sulfonate groups, and natural adsorbent, of which surface charges are negative, caused little or no adsorption of reactive dyes on natural material.

Negative capacity was observed with the adsorption of *reactive yellow (RY)* dyestuff onto “natural basaltic tephra” because pores of the “basaltic tephra” are

not big enough for the penetration of bigger dye molecules. Therefore, smaller molecules like water molecules penetrated through those pores and consequently water amount decreased in the solution so apparent dye concentration increased. This caused negative values in the adsorption of *reactive yellow* dyes on “natural basaltic tephra”. Similar result was obtained in a study performed by Armagan et al (2003a).

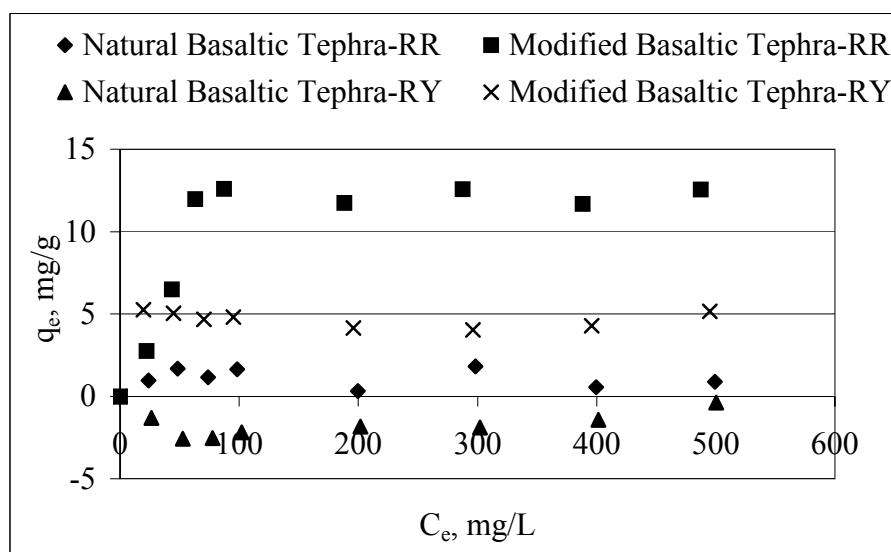


**Figure 5.16.** Adsorption isotherms for reactive dyes on natural and modified basaltic tephra

For *reactive red* dyestuff, little adsorption was achieved similar to adsorption of *acid dyes* on “natural basaltic tephra” which is explained in the previous section. With the modification, the surface charges of the “natural basaltic tephra” were changed from stronger anionic state to weaker anionic state. Therefore, the total adsorption forces between the surface of adsorbent and dyestuffs increased. The adsorption capacity of *reactive yellow* dye was increased from about  $-2$  mg/g to  $+5$  mg/g with modification.



Langmuir and Freundlich equations were applied to adsorption of *reactive dyes* on modified adsorbents. These two equations were not applied to the adsorption of *reactive dyes* on “natural basaltic tephra” due to very small capacity of “natural basaltic tephra”. Langmuir and Freundlich Isotherm plots are given in Figure 5.17 and Figure 5.18, respectively. Langmuir Equation constants calculated from Figure 5.17 are given in Table 5.7.

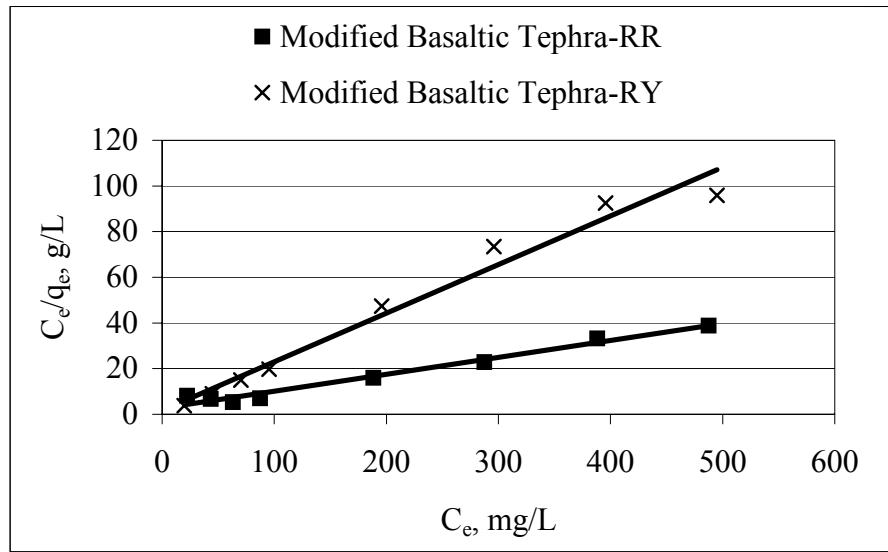


**Figure 5.17.** Langmuir plots for adsorption of reactive dyes on modified basaltic tephra

**Table 5.7.** Langmuir isotherm constants for modified basaltic tephra

Adsorbent	Dye	$q_{mon}$ (mg/g)	$K_L$ (L/g)	$R_L$ (-)	$R^2$ (-)
Modified	RY	4.7	0.13	0.016	0.973
Modified	RR	13.5	0.03	0.069	0.976

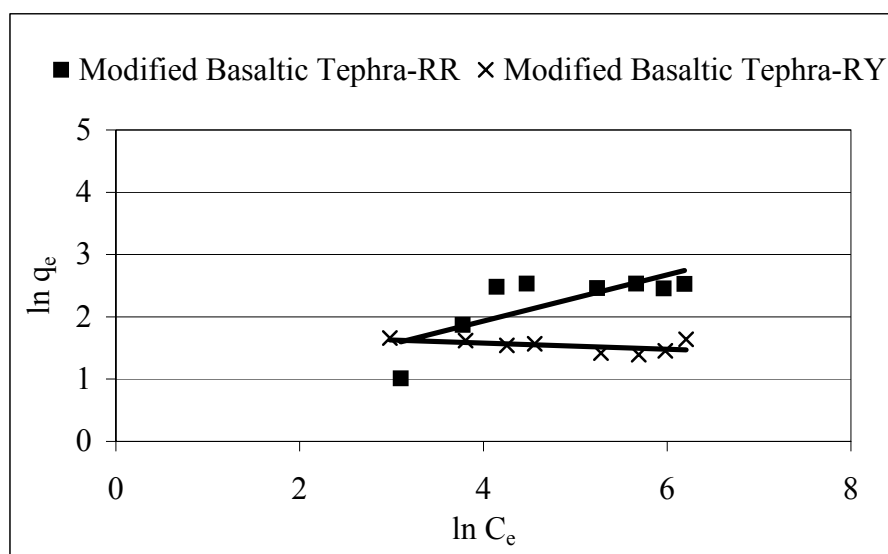


**Figure 5.18.** Freundlich plots for the adsorption of reactive dyes on modified basaltic tephra

Freundlich equation constants were calculated by using Figure 5.18 and they are presented in Table 5.8.

**Table 5.8.** Freundlich isotherm constants for modified basaltic tephra

Adsorbent	Dye	K <sub>F</sub> (-)	b <sub>F</sub> (-)	R <sup>2</sup> (-)
Modified	RY	5.92	0.050	0.300
Modified	RR	1.57	0.370	0.577

As seen from Table 5.8, the correlation coefficients calculated from Freundlich Equation for both natural and modified “basaltic tephra” are smaller than those calculated from Langmuir Equation. Therefore, adsorption of *reactive dyestuffs* can be interpreted better with Langmuir Isotherm Equation than Freundlich Isotherm Equation.

## 5.6. Adsorption of Dyestuffs onto Clinoptilolite

### 5.6.1. Effect of Particle Size on Adsorption

Two different sizes of “clinoptilolite” (0-0.5 mm and powdered form) were compared in their adsorption capacities for *basic blue* dyestuffs under the same experimental conditions. The adsorption isotherms are shown in Figure 5.19.

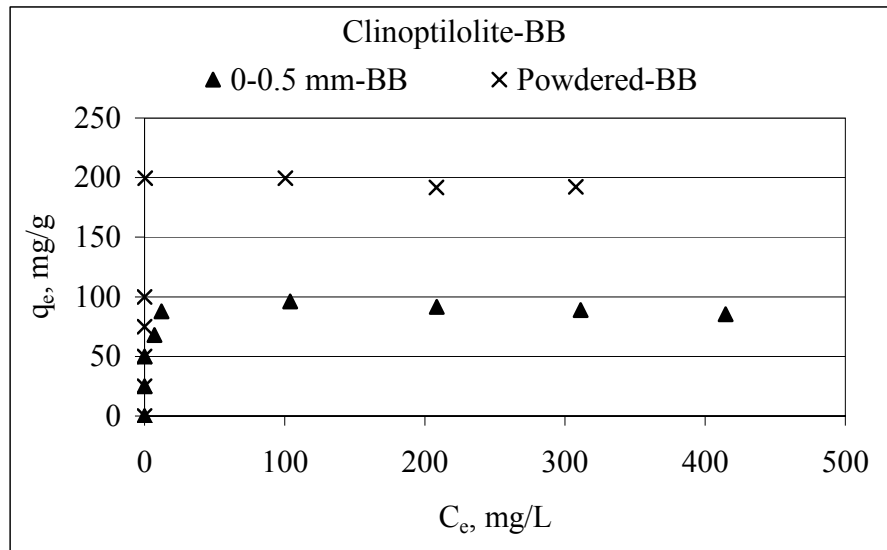


**Figure 5.19.** Adsorption of basic blue dyestuff onto natural clinoptilolite

From Figure 5.19 it is seen that smaller particles have much higher adsorption capacity than that of larger particles. Since the particle size  $d_p < 63 \mu\text{m}$  gave better results than the other size, powdered form of the “clinoptilolite” was used in other experiments.

### 5.6.2. Adsorption of “Basic Dyestuffs” onto Clinoptilolite

Adsorption capacities of natural “clinoptilolite” and its modified form were investigated to obtain the isotherms for the *basic dyestuff* by applying the same experimental procedure. Modification of the surface properties of “clinoptilolite” was made as described in Chapter 4. Adsorption isotherms are given in Figure 5.20.

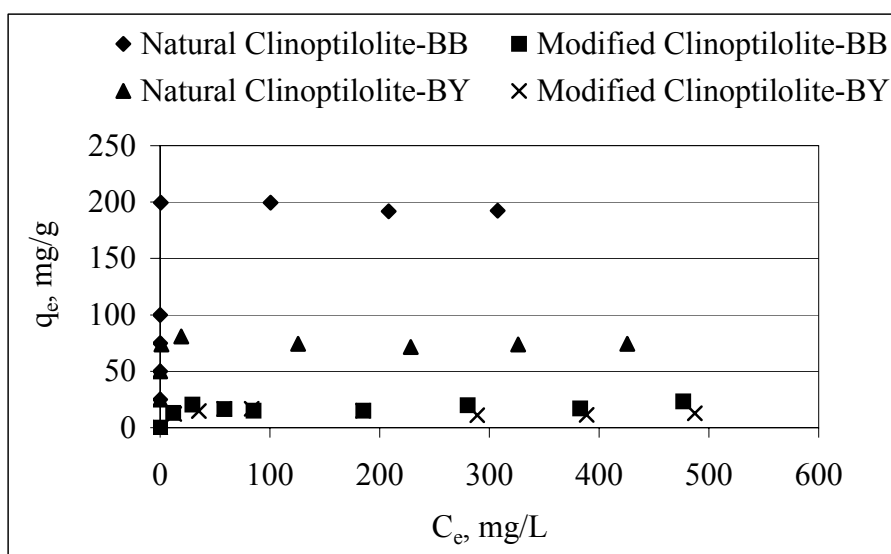


**Figure 5.20.** Adsorption isotherms for basic dyestuffs on natural and modified clinoptilolite

As can be seen from Figure 5.20, the adsorption capacity of “natural clinoptilolite” for *basic blue (BB)* is about 200 mg/g. On the other hand the adsorption capacity of “modified clinoptilolite” for *basic blue (BB)* is about 20 mg/g. Therefore, it was seen that “natural clinoptilolite” has higher adsorption capacity than that of “modified clinoptilolite”. Therefore, there is no need to make surface modification of “clinoptilolite” for these *basic* types of dyes.

A similar result was obtained for *basic yellow (BY)* dye. The adsorption capacity of the “clinoptilolite” was 16 mg/g. However, the adsorption capacity became about 3 mg/g for the “modified clinoptilolite”.

As it was mentioned before, there are two main forces in the adsorption process. The first one is the electrostatic interaction between the surface of adsorbents and adsorbates. For this study, the experiments were performed at the neutral pH (6.5-8.5). At that pH range the zeta potential of “clinoptilolite” is given as approximately  $-28$  mV. As a result of this, electrostatic interaction between the “clinoptilolite” and *basic dyes* that are cationic dyes resulted in attraction forces. The second force in the adsorption process is the diffusion of adsorbate molecules through pores of the adsorbent. This is a slow process. Therefore, the net adsorption force is the sum of these two forces. As a result, the sum of these forces resulted in higher adsorption capacity for “natural clinoptilolite” than “modified clinoptilolite”. This means, “clinoptilolite” attracts the dyestuff onto its surface.

On the contrary, with modification with HTAB, the surface charges of “natural clinoptilolite” were changed from negative to positive, i.e. zeta potential of “clinoptilolite” was changed from  $-28$  mV to  $+18$  mV. Therefore, electrostatic forces between *basic dyes* and “modified clinoptilolite” became repulsive forces. Also, the surface area of the “clinoptilolite” was decreased after modification with HTAB because some of the pore area of the adsorbent was closed with HTAB molecules. That difference can be seen in Figure 5.2. As a result, the effect of diffusion forces was also decreased due to modification with HTAB. As a result of those, adsorption capacity of “clinoptilolite” for *basic dyes* were decreased significantly with the modification.

Langmuir and Freundlich Equations were applied to adsorption isotherms of *basic dyes* on natural and modified adsorbents. Langmuir and Freundlich Isotherm plots

are given in Figure 5.21 and Figure 5.22, respectively. Langmuir Equation constants calculated from Figure 5.21 are given in Table 5.9.

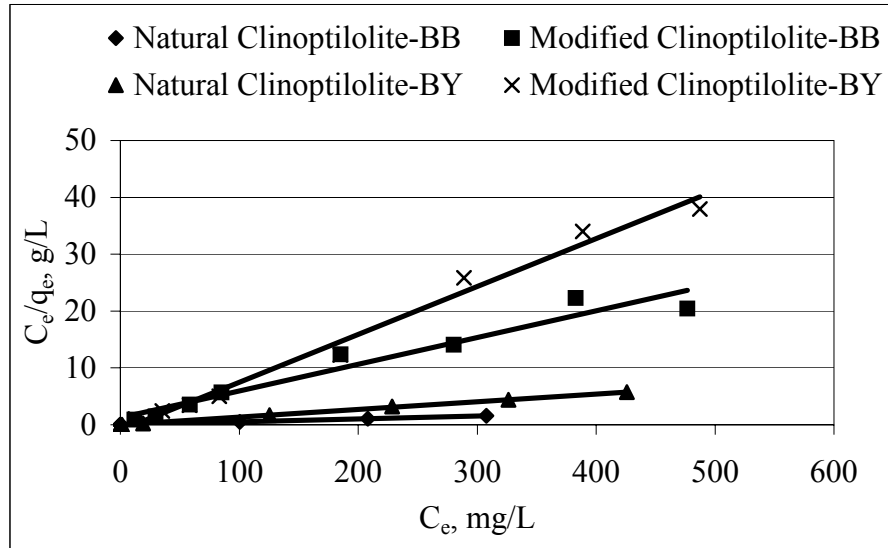


**Figure 5.21.** Langmuir plots for the adsorption of basic dyestuffs on natural and modified clinoptilolite

**Table 5.9.** Langmuir isotherm constants for natural and modified clinoptilolite

Adsorbent	Dye	$q_{mon}$ (mg/g)	$K_L$ (L/g)	$R_L$ (-)	$R^2$ (-)
Natural	BY	74.1	5.19	0.001	0.999
Modified	BY	11.9	0.09	0.023	0.985
Natural	BB	192.3	2.60	0.001	0.999
Modified	BB	21.3	0.04	0.050	0.943

Freundlich equation constants were calculated by using Figure 5.22 and they are presented in Table 5.10.

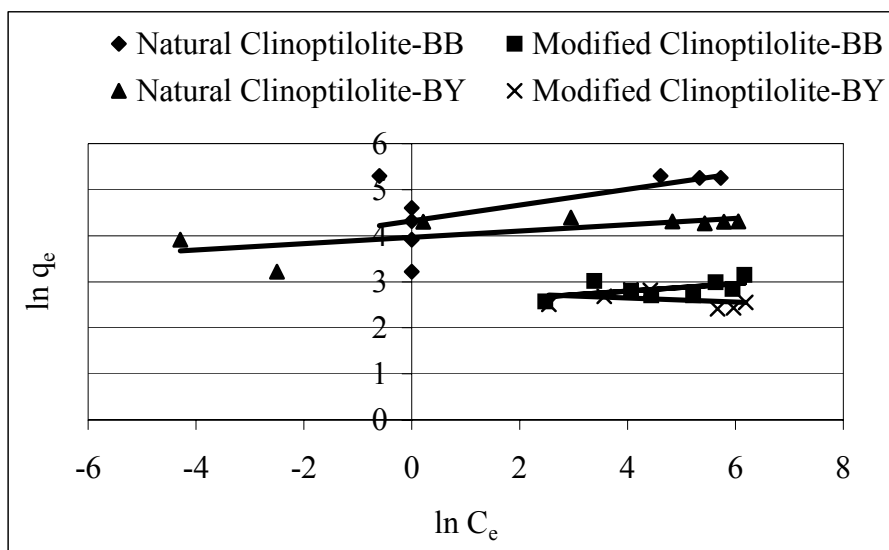


**Figure 5.22.** Freundlich plots for the adsorption of basic dyestuffs on natural and modified clinoptilolite

**Table 5.10.** Freundlich isotherm constants for natural and modified clinoptilolite

Adsorbent	Dye	K <sub>F</sub> (-)	b <sub>F</sub> (-)	R <sup>2</sup> (-)
Natural	BY	52.88	0.068	0.489
Modified	BY	16.85	0.043	0.118
Natural	BB	72.23	0.172	0.378
Modified	BB	11.93	0.078	0.288

As can be seen from Table 5.10 correlation coefficients calculated from Freundlich Equation for both natural and modified “clinoptilolite” are much smaller than those calculated from Langmuir equation. Therefore, the adsorption of *basic blue* and *basic yellow* dyestuffs onto “clinoptilolite” can fit better with Langmuir Isotherm Equation than Freundlich Isotherm Equation.

### 5.6.3. Adsorption of “Acid Dyestuffs” onto Clinoptilolite

Figure 5.26 presents the adsorption isotherms of *acid dyestuffs* on natural and modified “clinoptilolite”.

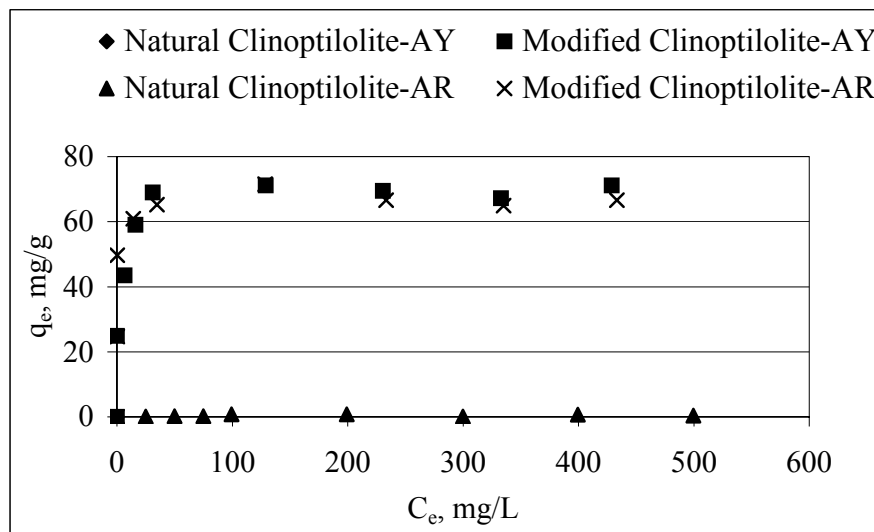


**Figure 5.23** Adsorption isotherms for acid dyes on natural and modified clinoptilolite

As can be seen from Figure 5.23, adsorption capacities of “modified clinoptilolite” for *acid dyes* are higher than those of “natural clinoptilolite”. The adsorption capacity of “natural clinoptilolite” for *acid yellow (AY)* and *acid red (AR)* was very close to 0. After the surface is modified with HTAB, the adsorption capacity increased significantly and became about 70 mg/g. This is an extraordinary increase in capacity.

Prior to modification, repulsive forces between *acid dyes*, which are anionic dyes, and natural adsorbent, of which surface charges are negative, caused little adsorption of acid dyes on natural material. The zeta potential of the



“clinoptilolite” is about -28 mV at pH=7. Since the *acid dyes* have negative groups, the repulsive forces between the surface of “clinoptilolite” and dyestuffs are effective. However, there are also dispersion forces between the adsorbents and adsorbates in the adsorption process. Therefore, the adsorption forces are the sum of dispersion and electrostatic forces (Dai, 1998).

With the modification, the surface charges of the “natural clinoptilolite” were changed from anionic to cationic state, i.e. zeta potential was changed from -28 mV to +18 mV. Therefore, attractive forces between the surface of adsorbent and dyestuffs became dominant. As result of this the adsorption capacities of the “clinoptilolite” for *acid dyes* were improved significantly after modification with HTAB.

Langmuir equation was applied to adsorption of *acid dyes* on “modified adsorbents”. Langmuir Isotherm plots are given in Figure 5.24. This equation was not applied to the adsorption of *acid dyes* on “natural clinoptilolite” due to very small capacity on “natural clinoptilolite”. Langmuir Equation constants calculated from Figure 5.24 are given in Table 5.11.

**Table 5.11.** Langmuir isotherm constants for natural and modified clinoptilolite

Adsorbent	Dye	$q_{mon}$ (mg/g)	$K_L$ (L/g)	$R_L$ (-)	$R^2$ (-)
Modified	AY	69.9	0.52	0.003	0.998
Modified	AR	66.2	1.31	0.001	0.999

Freundlich isotherm equation was also applied for the adsorption of *acid dyes* onto “modified clinoptilolite”. The adsorption of *acid dyes* onto “natural clinoptilolite” was very small adsorption (0-1 mg/g). Due to these very small values, calculated

$\ln q_e$  values were negative. Therefore, these are excluded from the plot. Freundlich isotherm plots are given in Figure 5.25.

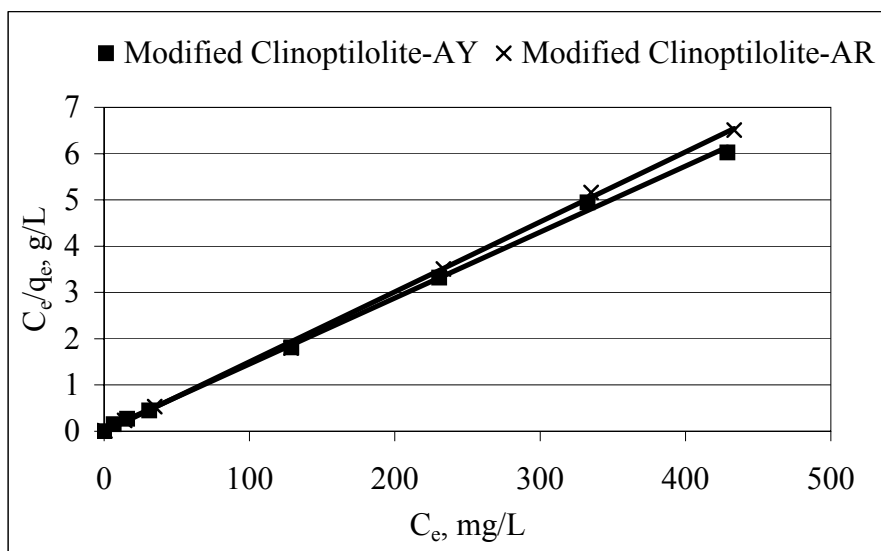


**Figure 5.24.** Langmuir plots for the adsorption of acid dyes on natural and modified clinoptilolite

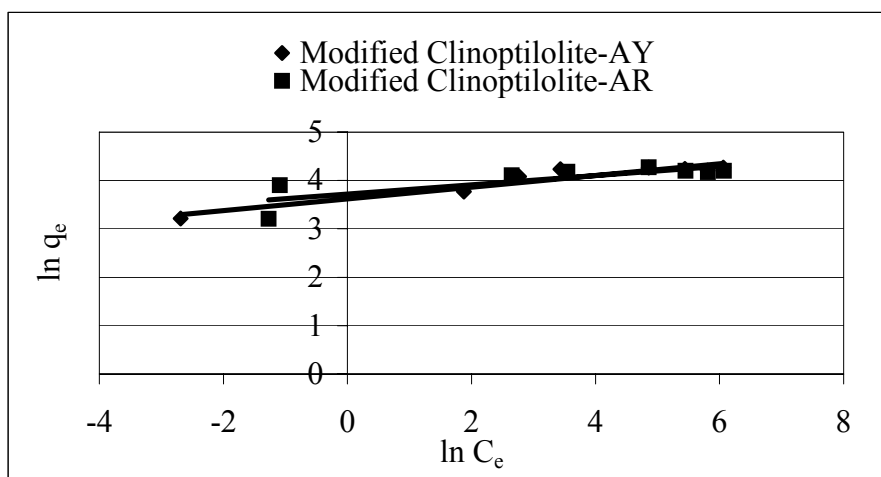


**Figure 5.25.** Freundlich plots for the adsorption of acid dyes on modified clinoptilolite

Freundlich equation constants calculated from Figure 5.25 and are presented in Table 5.12.

**Table 5.12.** Freundlich isotherm constants for modified clinoptilolite

Adsorbent	Dye	$K_F (-)$	$b_F (-)$	$R^2 (-)$
Modified	AY	37.22	0.121	0.904
Modified	AR	41.31	0.095	0.650

As can be seen from Table 5.12, the correlation coefficients calculated from Freundlich Equation for “modified clinoptilolite” are smaller than those calculated from Langmuir Equation. Therefore, adsorption of *acid dyestuffs* onto “modified clinoptilolite” can be interpreted better with Langmuir Isotherm Equation. Also, Freundlich Equation may be used to represent adsorption isotherms of *acid yellow* dyestuff onto “modified clinoptilolite”.

#### 5.6.4. Adsorption of “Reactive Dyestuffs” onto Clinoptilolite

Figure 5.26 shows the adsorption isotherms of *reactive dyestuffs* on natural and modified “clinoptilolite”.

As can be seen from Figure 5.26, adsorption capacities of “modified clinoptilolite” for *reactive dyes* are much higher than those of “natural clinoptilolite” as in the case of *acid dyes*. The adsorption capacity of “natural clinoptilolite” for *reactive yellow (RY)* and *reactive red (RR)* was very close to 0. After the surface is modified with HTAB, the adsorption capacity increased significantly and became about 30 mg/g for *reactive yellow* and 40 mg/g for *reactive red*.

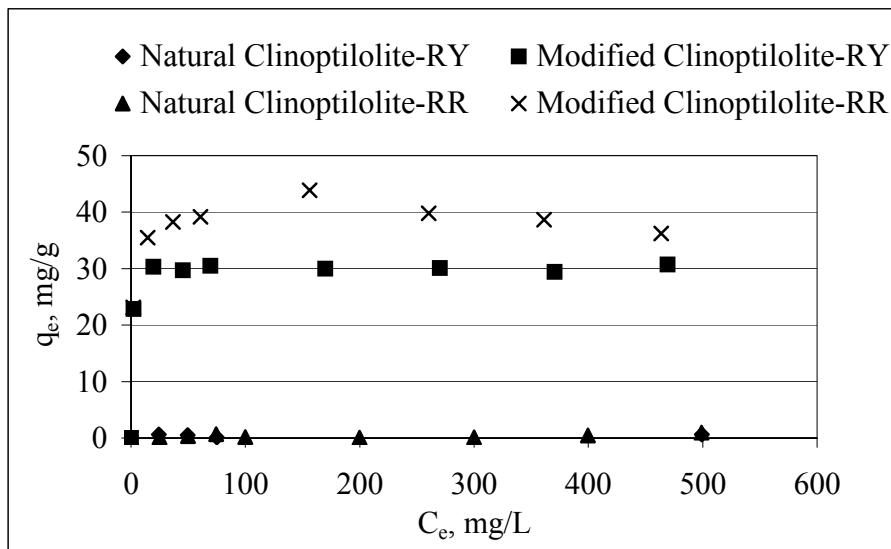


**Figure 5.26.** Adsorption isotherms for reactive dyes on natural and modified clinoptilolite

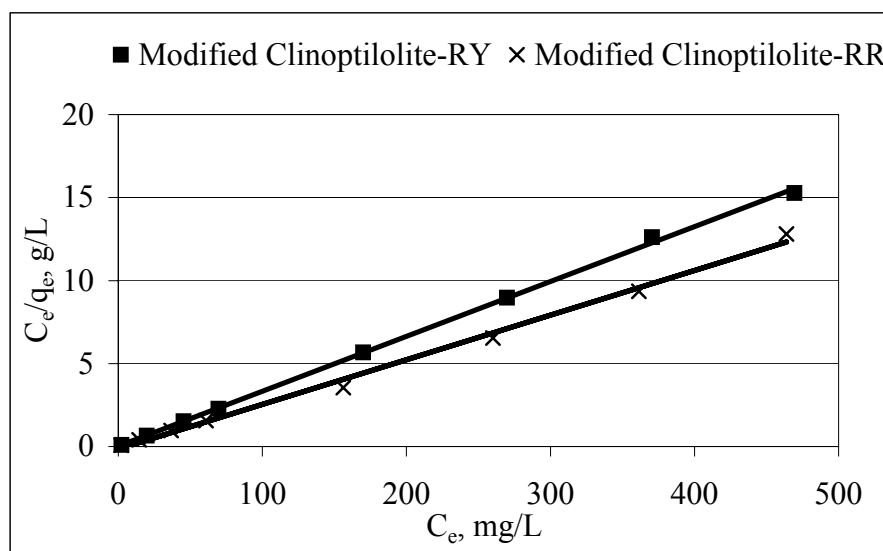
Prior to modification, repulsive forces between *reactive dyes*, which are anionic dyes, and natural adsorbent, of which surface charges are negative, caused little adsorption of *reactive dyes* on natural material.

With the modification, the surface charges of the “natural clinoptilolite” were changed from anionic to cationic state, i.e. zeta potential was changed from  $-28$  mV to  $+18$  mV. Therefore, attractive forces between the surface of adsorbent and dyestuffs became dominant and adsorption capacity of “modified clinoptilolite” on *reactive dyestuffs* was significantly increased.

Langmuir and Freundlich equations were applied to adsorption of *reactive dyes* on natural and modified adsorbents. These equations were not applied to the adsorption of *reactive dyes* on “natural clinoptilolite” due to very small capacity of “natural clinoptilolite”. Langmuir and Freundlich Isotherm plots are given in Figure 5.27 and Figure 5.28, respectively. Langmuir Equation constants calculated from Figure 5.27 are given in Table 5.13.

**Table 5.13.** Langmuir isotherm constants for modified clinoptilolite

Adsorbent	Dye	$q_{\text{mon}}$ (mg/g)	$K_L$ (L/g)	$R_L$ (-)	$R^2$ (-)
Modified	RY	30.2	1.02	0.002	0.999
Modified	RR	37.2	0.18	0.011	0.995

**Figure 5.27.** Langmuir plots for the adsorption of reactive dyes on modified clinoptilolite

Freundlich equation constants were calculated from Figure 5.28 and are presented in Table 5.14.

**Table 5.14.** Freundlich isotherm constants for modified clinoptilolite

Adsorbent	Dye	$K_F$ (-)	$b_F$ (-)	$R^2$ (-)
Modified	RY	24.20	0.042	0.610
Modified	RR	25.80	0.081	0.618

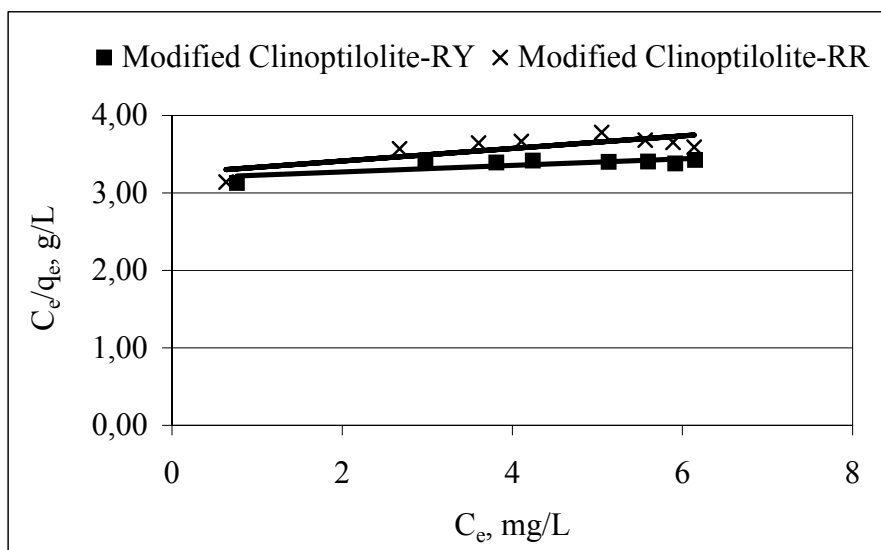


**Figure 5.28.** Freundlich plots for the adsorption of reactive dyes on modified clinoptilolite

As can be seen from Table 5.14, the correlation coefficients calculated from Freundlich Equation for both natural and modified “clinoptilolite” are smaller than those calculated from Langmuir Equation. Therefore, adsorption of *reactive dyestuffs* can be interpreted better with Langmuir Isotherm Equation..

## 5.7. Adsorption of Dyestuffs onto Powdered Activated Carbon

### 5.7.1. Adsorption of “Basic Dyestuffs” onto Powdered Activated Carbon

“Powdered activated carbon (PAC)” was used as a reference material in order to compare the adsorption capacities of natural and modified adsorbents. The adsorption capacity of “PAC” for *basic dyestuffs* was determined and the adsorption isotherms obtained for *basic dyes* are shown in Figure 5.29.

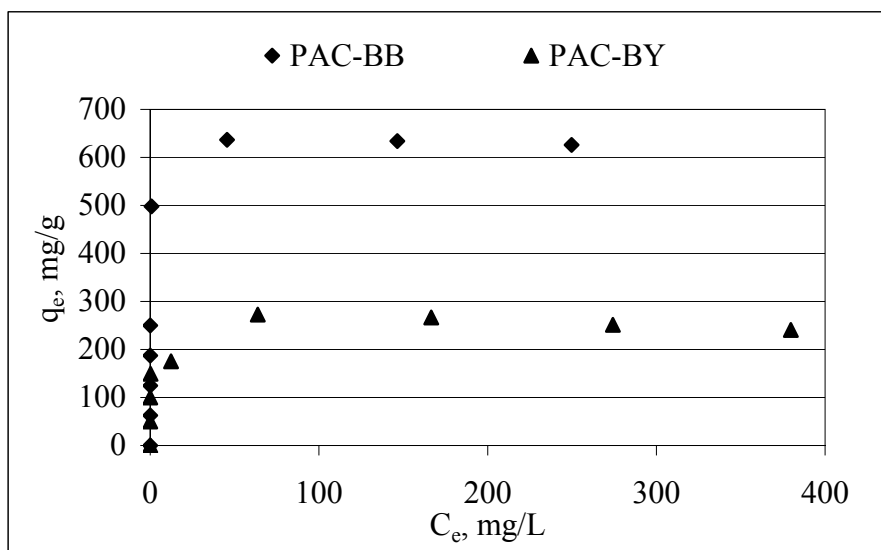


**Figure 5.29.** Adsorption isotherms for basic dyestuffs on PAC

As seen from Figure 5.29, the adsorption capacities of “powdered activated carbon” for *basic blue* and *basic yellow* dyestuffs are approximately 630 and 280 mg/g, respectively. This is a very high capacity, simply because of very fine porous structure of “PAC”.

Dai (1998) has reported that in the neutral potential state the zeta potential is nearly zero and therefore, the electrostatic interactions between the carbon surface and the dyes are negligible. Therefore, the adsorption of *basic dyes* on “powdered activated carbon” is mainly due to dispersion forces. Because “powdered activated carbon” has much higher surface area than other adsorbents used in this study its adsorption capacity for *basic dyes* is much higher than that of other adsorbents.

Langmuir and Freundlich Isotherm Equations were applied to adsorption of *basic dyes* on “powdered activated carbon”. Langmuir and Freundlich Isotherm plots are given in Figure 5.30 and Figure 5.31, respectively. Langmuir Equation constants calculated from Figure 5.30 are given in Table 5.15.

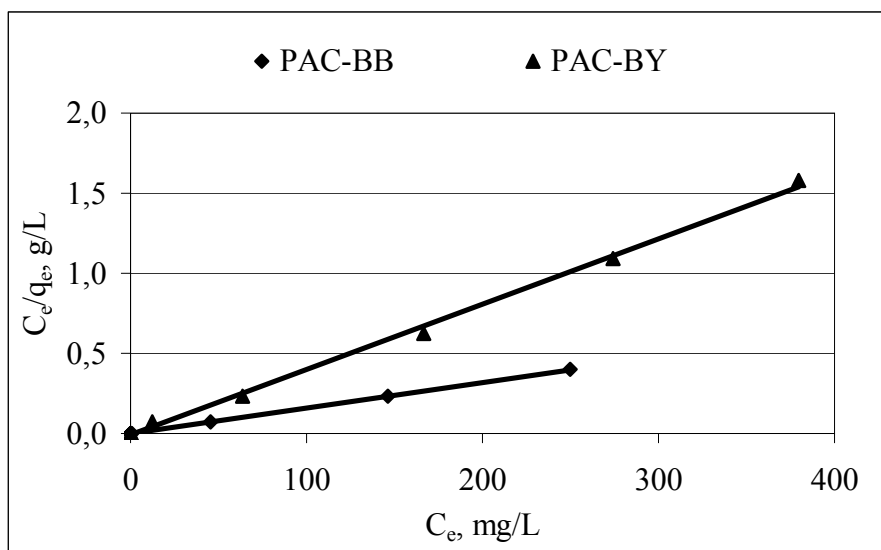


**Figure 5.30.** Langmuir plots for the adsorption of basic dyestuffs on PAC

**Table 5.15.** Langmuir isotherm constants for PAC

Adsorbent	Dye	$q_{mon}$ (mg/g)	$K_L$ (L/g)	$R_L$ (-)	$R^2$ (-)
Natural	BB	625.0	8.00	0.000	0.999
Natural	BY	243.9	0.58	0.004	0.998

Freundlich equation constants for the adsorption of *basic dyes* on “powdered activated carbon” were calculated from Figure 5.31 and the results are presented in Table 5.16.

**Table 5.16.** Freundlich isotherm constants for PAC

Adsorbent	Dye	$K_F$ (-)	$b_F$ (-)	$R^2$ (-)
Natural	BB	220.68	0.187	0.397
Natural	BY	89.21	0.154	0.577



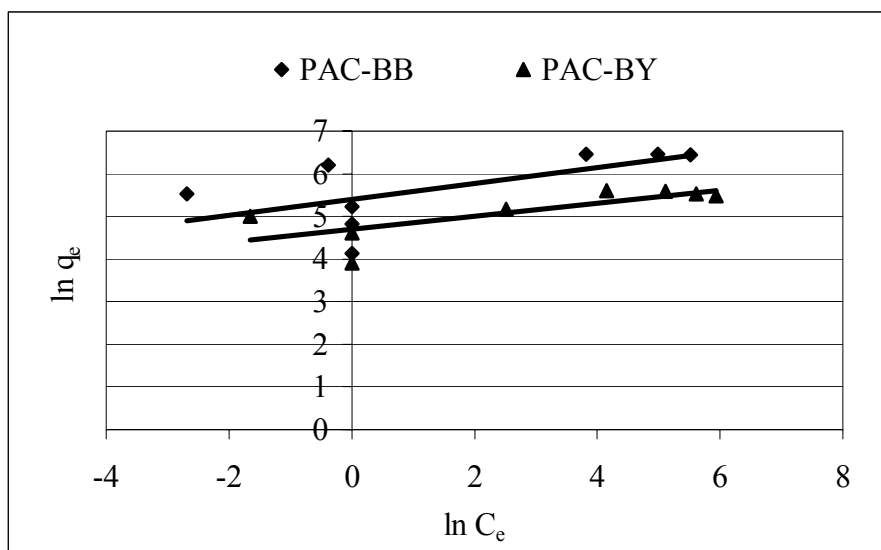


**Figure 5.31.** Freundlich plots for the adsorption of basic dyestuffs on PAC

As seen from Table 5.16 the correlation coefficients calculated from Freundlich Equation for “powdered activated carbon” are much smaller than those calculated from Langmuir equation. Therefore, adsorption of *basic dyestuffs* onto “powdered activated carbon” can be represented better with Langmuir Isotherm Equation than Freundlich Isotherm Equation.

#### 5.7.2. Adsorption of “Acid Dyestuffs” onto Powdered Activated Carbon

Figure 5.32 shows the adsorption isotherms of *acid dyestuffs* onto “powdered activated carbon (PAC)”.

As can be seen from Figure 5.32, the adsorption capacities of “powdered activated carbon” for *acid red* and *acid yellow* dyestuffs are about 310 and 290 mg/g, respectively. The adsorption of *acid dyes* on “powdered activated carbon” is resulted from mainly dispersion forces as in the case *basic dyes*. Due to higher

surface area of “powdered activated carbon” its adsorption capacity for *acid dyes* is higher than that of other adsorbents used in this study.

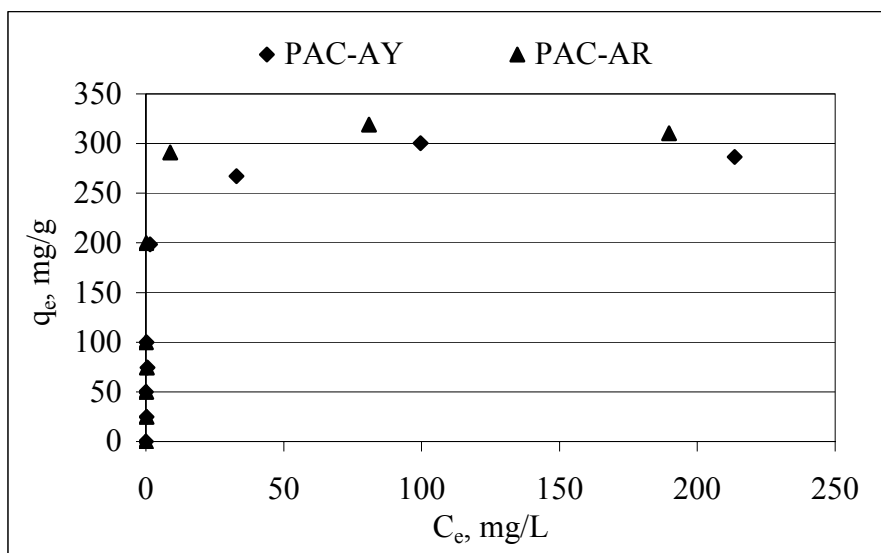


**Figure 5.32.** Adsorption isotherms for acid dyes on PAC

Langmuir equation was applied to adsorption of *acid dyes* on “powdered activated carbon” Langmuir Isotherm plots are given in Figure 5.33. Langmuir Equation constants calculated from Figure 5.33 are given in Table 5.17.

**Table 5.17.** Langmuir isotherm constants for PAC

Dye	$q_{\text{mon}}$ (mg/g)	$K_L$ (L/g)	$R_L$ (-)	$R^2$ (-)
AY	294.1	1.00	0.002	0.999
AR	312.5	1.52	0.001	0.999

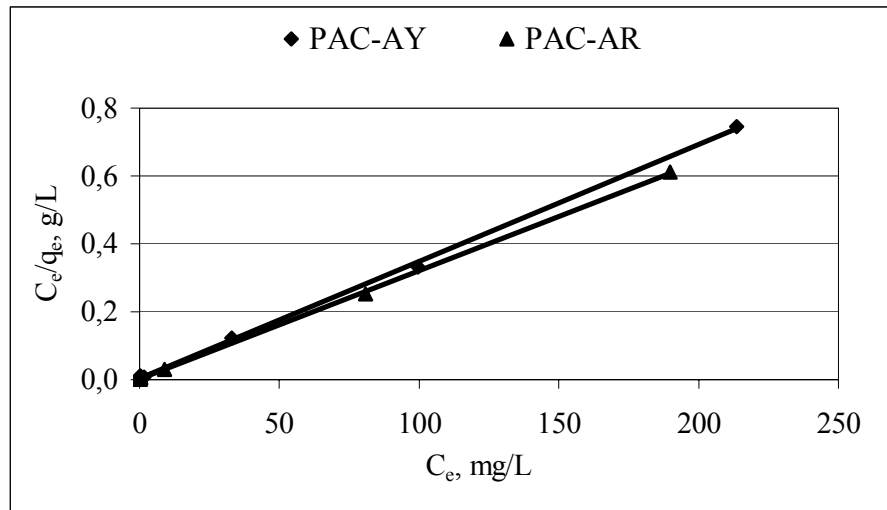


**Figure 5.33.** Langmuir plots for the adsorption of acid dyes on PAC

Freundlich isotherm equation was also applied for the adsorption of *acid dyes* onto “powdered activated carbon”. Freundlich isotherm plots are given in Figure 5.34.

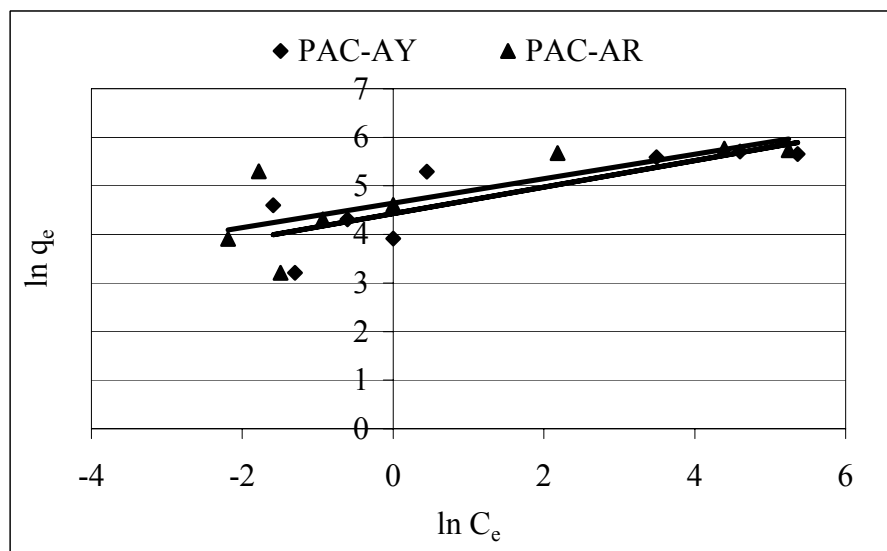


**Figure 5.34.** Freundlich plots for the adsorption of acid dyes on PAC

Freundlich equation constants were calculated from Figure 5.34 and the results are presented in Table 5.18.

**Table 5.18.** Freundlich isotherm constants for PAC

<b>Dye</b>	<b>K<sub>F</sub> (-)</b>	<b>b<sub>F</sub> (-)</b>	<b>R<sup>2</sup> (-)</b>
AY	83.83	0.273	0.662
AR	103.82	0.252	0.585

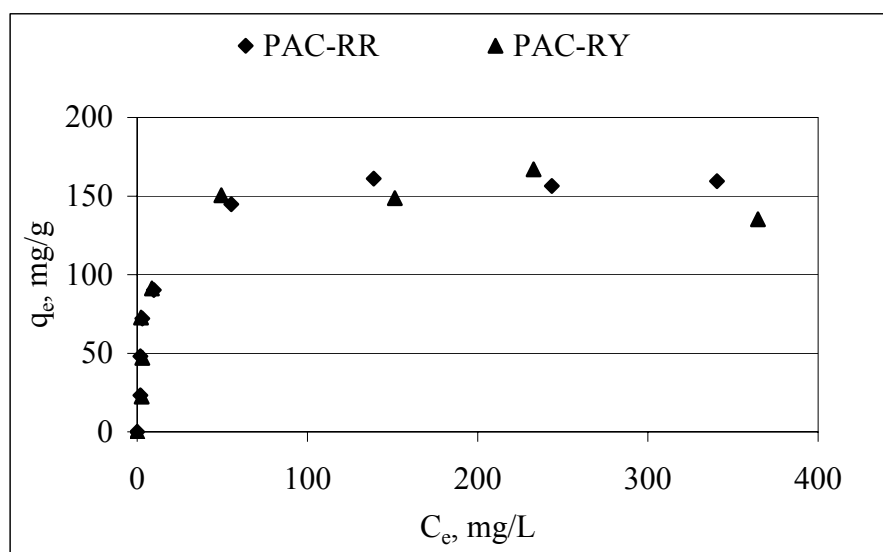
As seen from Table 5.18 the correlation coefficients calculated from Freundlich Equation for “powdered activated carbon” are much smaller than those calculated from Langmuir equation. Therefore, adsorption of *acid dyestuffs* onto “powdered activated carbon” can be interpreted better with Langmuir Isotherm Equation.

#### 5.7.3. Adsorption of “Reactive Dyestuffs” onto Powdered Activated Carbon

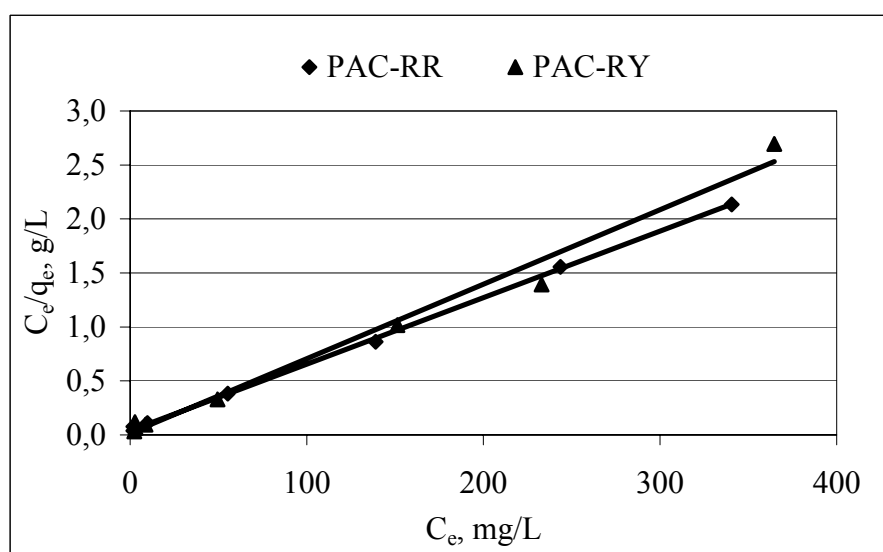
Figure 5.35 shows the adsorption isotherms of *reactive dyestuffs* on “powdered activated carbon”.

As can be seen from Figure 5.35, the adsorption capacities of the “powdered activated carbon” for *reactive red* and *reactive yellow* dyestuffs are about 170 and 150 mg/g, respectively.

Langmuir and Freundlich equations were applied to adsorption of *reactive dyes* on “powdered activated carbon”. Langmuir and Freundlich Isotherm plots are given in Figure 5.36 and Figure 5.37, respectively. Langmuir Equation constants calculated from Figure 5.36 are given in Table 5.19.



**Figure 5.35.** Adsorption isotherms for reactive dyes on PAC

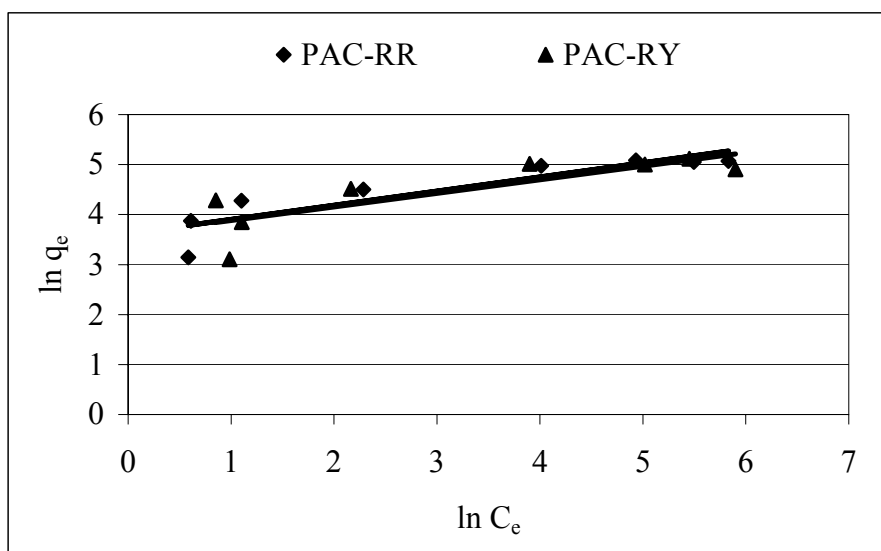


**Figure 5.36.** Langmuir plots for the adsorption of reactive dyes on PAC

Freundlich equation constants were calculated from Figure 5.37 and the results are presented in Table 5.20.

**Table 5.19.** Langmuir isotherm constants for PAC

Dye	$q_{\text{mon}}$ (mg/g)	$K_L$ (L/g)	$R_L$ (-)	$R^2$ (-)
RY	145.9	0.43	0.004	0.999
RR	161.3	0.16	0.012	0.985

**Figure 5.37.** Freundlich plots for the adsorption of reactive dyes on PAC**Table 5.20.** Freundlich isotherm constants for PAC

Dye	$K_F$ (-)	$b_F$ (-)	$R^2$ (-)
RY	37.09	0.271	0.680
RR	37.24	0.283	0.799

As can be seen from Table 5.20 the correlation coefficients calculated from Freundlich Equation for “powdered activated carbon” are smaller than those

calculated from Langmuir Equation. Therefore, it is possible to say that Langmuir Isotherm Equation represents the adsorption of *reactive dyestuffs* very well.

### 5.8. Comparison of the Adsorption Capacities of the Adsorbents

The adsorption capacities of the “basaltic tephra” and “clinoptilolite” in their natural and modified forms and “powdered activated carbon (PAC)” for the dyestuffs used in this study are summarized in Table 5.21.

**Table 5.21.** Adsorption capacities of the adsorbents used in this study

Dyestuff	Basaltic Tephra, mg/g		Clinoptilolite, mg/g		PAC, mg/g
	Natural	Modified	Natural	Modified	
Basic Blue	38.1	13.6	192.3	21.3	625.0
Basic Yellow	14.1	3.8	74.1	11.9	243.9
Acid Yellow	0-1	18.4	0-1	69.9	294.1
Acid Red	0-1	9.7	0-1	66.2	312.5
Reactive Yellow	-3.0	4.7	0-1	30.2	145.9
Reactive Red	0-1	13.5	0-1	37.2	164.3

As can be seen from the table, adsorption capacities of “natural basaltic tephra” and “natural clinoptilolite” for *cationic dyes* that are *basic blue* and *basic yellow* are much higher than that of *anionic dyes* because electrostatic interactions between the negatively charged surface of the natural adsorbents and positively charged dye molecules result in “attractive forces”. Also, adsorption capacity of “clinoptilolite” for *basic dyes* is approximately 5 times more of “basaltic tephra”.

For *anionic dyes*, “natural basaltic tephra” and “clinoptilolite” has limited adsorption capacities. The negatively charged adsorbent surface repels the dye molecules that have also negative ions. The dispersion force is small as compared to repulsive forces. As a net result of repulsion and dispersion forces, very small adsorption of *anionic dyes* was obtained for the natural adsorbents.

Also, a negative capacity was observed in the case of the adsorption of *reactive yellow* dyestuff on “basaltic tephra” because pores of “basaltic tephra” are not big enough for the penetration of bigger dye molecules. Therefore, smaller molecules like water molecules penetrated through those pores and therefore water amount decreased in the solution so apparent dye concentration increased. This caused a negative capacity value.

With the modification of surface properties of “basaltic tephra” and “clinoptilolite”, their surface charges and surface areas were changed. Surface charge of “basaltic tephra” was still in anionic state but it was not strong as in the case before modification. Therefore, the magnitude of attraction forces between *cationic dyes* and the “basaltic tephra” was decreased. Also, magnitude of dispersion forces were decreased due to smaller surface area of “modified basaltic tephra”.

Similar results were obtained for “clinoptilolite”. Surface charge of “clinoptilolite” was changed from anionic state to cationic state with HTAB modification. Also, surface area of “clinoptilolite” was decreased. Therefore, electrostatic forces between *basic dyes* and “clinoptilolite” became repulsion forces and dispersion forces were decreased due to smaller surface area. As a result, adsorption capacities of two adsorbents for *basic dyes* decreased significantly with the modification. On the contrary, adsorption of *anionic dyes* onto “basaltic tephra” and “clinoptilolite” were improved significantly after the surface modification with HTAB. Because the effect of repulsion forces between the *anionic dyes* and



“basaltic tephra” was decreased with modification, adsorption of those dyes onto “basaltic tephra” increased significantly.

For “clinoptilolite”, repulsive forces were changed to attractive forces with surface modification and consequently, important adsorption of *anionic dyes* onto “clinoptilolite” surface was achieved. This is a very important achievement in this study

“Powdered activated carbon” has highest capacity for all dyestuffs used because its surface area is much higher than that of other adsorbents. In the neutral potential state the zeta potential is nearly zero and therefore, the electrostatic interactions between the carbon surface and the dyes are negligible. The adsorption forces are mainly dispersion forces. Adsorption capacity of “powdered activated carbon” for *basic dyes* is approximately 3 times higher than that of “clinoptilolite” and 15 times greater than that of “basaltic tephra”.

In order to compare results of this study with results obtained from the literature, results of some studies taken from the literature are summarized in Table 5.22.

As can be seen from the table various type of adsorbents were used to adsorb various dyestuffs from aqueous solutions. The best adsorption capacities of the adsorbents were obtained for *basic dyes* similar to this study.

“Basaltic tephra” used in this study has much smaller capacity for *basic dyes* than adsorbents used in the literature. However, the adsorption capacity of “clinoptilolite” compared very well with the other adsorbents. Considering the low cost factor for natural materials, they can be very attractive for color removal for *cationic dyes*.

Also, “modified basaltic tephra” used in this study has much less capacity for *acid* and *reactive dyes* than the adsorbents used in the literature. However, the adsorption capacity of “modified clinoptilolite” is comparable, especially for *acid dyes*, with the other adsorbents.

**Table 5.22.** Summary of some studies from literature

Reference	Adsorbent	Adsorbent Form	Dye used		q <sub>mon</sub> , mg/g
			Type	Name	
Armağan et al. (2003)	Sepiolite	Natural	Reactive	Black 5  Red 239  Yellow 176	0.5-1
	Zeolite				Neg. values
	Sepiolite	Modified with HTAB			120 108 169
	Zeolite				111 61 89
Turabik and Kumbur (2003)	Bentonite	Natural	Basic	Red 46	312 476
		Acid activated		Blue 41	263 270
Turabik (2003)	Bentonite	Natural	Basic	Blue 3	75
Allen et al. (2003)	Kudzu	Natural	Basic	Yellow 21 Red 22	160 210
Choy et al. (1999)	Granular Activated Carbon	Natural	Acid	Red 114 Polar Yellow Polar Blue	101 129 101
Juang et al. (1997)	Chitosan	Natural	Reactive	Red 222 Yellow 145 Blue 222	379 179 87
Juang et al. (1997)	Clay	Acid activated	Basic	Blue 69 Red 62	394 406
			Acid	Blue 25	256
			Direct	Blue 183 Red 227	49 37
			Reactive	Red 123	36

## CHAPTER 6

### CONCLUSION

In this study, the adsorption of various dyestuffs (basic, acidic and reactive) onto natural “basaltic tephra” and “clinoptilolite” were investigated. In order to increase the adsorption capacities of “basaltic tephra” and “clinoptilolite” for *anionic dyestuffs*, surface modification with hexadecyltrimethylammonium bromide (HTAB) was applied to the adsorbents. With the surface modification the change in the surface charges of adsorbent materials was aimed. Finally, the adsorptive capacities of “basaltic tephra” and “clinoptilolite” were compared with that of “powdered activated carbon” for the same dyes and under the same experimental conditions.

The conclusions drawn from the results of this study are listed as follows:

1. “Basaltic tephra” and “clinoptilolite” in their natural forms can be used for the adsorption of *basic dyes* (cationic dyes). “Clinoptilolite” gives about 5 times better adsorption capacity than “basaltic tephra”. However, this capacity is about 1/3 of the capacity of “powdered activated carbon”. It is important to note that the cost of “clinoptilolite” is much much lower than that of “powdered activated carbon”.
2. The adsorption capacities of “basaltic tephra” and “clinoptilolite” in their natural form for the adsorption of *acidic* and *reactive dyes* (anionic dyes) are not high enough. Surface modifications of these adsorbents need to be done with a surfactant, like HTAB. The adsorption capacities of “basaltic tephra” and “clinoptilolite” for *anionic dyes* were increased several times based on the type of the dye. “Modified clinoptilolite” 3-7 times has higher

adsorption capacity for *acid* and *reactive dyes* than “modified basaltic tephra”. The adsorption capacity of “modified clinoptilolite” is comparable with that of “powdered activated carbon” for *acidic* and *reactive dyes* (approximately 1/4-1/5 of the capacity of “powdered activated carbon”)

3. For the adsorption of all dyestuffs, “powdered activated carbon” gave the best results among the adsorbents used in this study. *Basic blue* dye was also adsorbed on this adsorbent better than the other dyes used in this study.
4. Langmuir Isotherm Equation represents the adsorption of all dyestuffs on the adsorbents used in this study better than Freundlich Isotherm Equation.

## REFERENCES

- Al-Degs, Y., Khraisheh, M. A. M., Allen, S. J., Ahmad, M. N. (2000), Effect of Carbon Surface Chemistry on the Removal Of Reactive Dyes from Textile Effluents, *Water Research*, **34** (3), 927-935.
- Allen, S. J., Gan, Q., Matthews, R., Johnson, P. A. (2003), Comparison of Optimised Isotherm Models for Basic Dye Adsorption by Kudzu, *Bioresource Technology*, **88**, 143-152.
- Annadurai, G., Juang, R. S., Lee, D. J. (2001), Adsorption of Rhodamine 6G from Aqueous Solutions on Activated Carbon, *Journal of Environmental Science Health*, **36** (5), 715-725.
- Arbeloa, F. L., Arbeloa, T. L., Arbeloa, I. L. (1997), Spectroscopy of Rhodamine 6G Adsorbed on Sepiolite Aqueous Suspensions, *Journal of Colloidal and Interface Science*, **187**, 105-112.
- Armagan, B., Turan, M., Çelik, M. S. (2003a), The Removal of Reactive Azo Dyes by Natural and Modified Zeolites, *Journal of Chemical Technology and Biotechnology*, **78**, 725-732.
- Armagan, B., Turan, M., Çelik, M. S. (2003b), Adsorption of Dyestuffs onto Natural Clay Minerals: Effects of Solids Concentration and Mixing Time, V. *National Environmental Engineering Congress of UCTEA The Chamber of Environmental Engineers*, 179-186, Ankara.

Armagan, B., Turan, M., Çelik, M. S. (2003c), Application of Modified Sepiolite and Zeolite as an Adsorbent for Textile Wastewaters: A Comparative Evaluation, *V. National Environmental Engineering Congress of UCTEA The Chamber of Environmental Engineers*, 187-195, Ankara.

Asfour, H. M., Nassar, M. M., Fadali, O. A., El-Geundi, M. S., (1985), Colour Removal from Textile Effluents Using Hardwood Sawdust as an Absorbent, *Journal of Chemical Technology Biotechnology*, **35A**, 28-35.

Atun, G., Hisarli, G., Sheldrick, W. S., Muhler, M. (2003), Adsorptive Removal of Methylene Blue from Colored Effluents on Fuller's Earth, *Journal of Colloidal and Interface Science*, **261**, 32-39.

Bayraktar, C. T., 1984, *Kurmeller Mining Analyse Report*, Mining Engineering Department, ITU, Istanbul.

Choy, K. K. H., McKay, G., Porter, J. F. (1999), Sorption of Acid Dyes from Effluents using Activated Carbon, *Resources, Conservation and Recycling*, **27**, 57-71.

Dai, M. (1998), Mechanism of Adsorption for Dyes on Activated Carbon, *Journal of Colloidal and Interface Science*, **198**, 6-10.

Juang, R. S., Wu, F. C., Tseng, R. L. (1997a), The Ability of Activated Clay for the Adsorption of Dyes from Aqueous Solutions, *Environmental Technology*, **18**, 525-531.

Juang, R. S., Tseng, R. L., Wu, F. C., Lee, S. H. (1997b), Adsorption Behavior of Reactive Dyes from Aqueous Solutions on Chitosan, *Journal of Chemical Technology Biotechnology*, **70**, 391-399.

Kilavuz, M., 1994, *Adsorption of Methylene Blue and Cr<sup>+6</sup> Ions on Basaltic Tephra*, Master Thesis, Adana.

Lin C. C., Liu, H. S. (2000), Adsorption in a Centrifugal Field: Basic Dye Adsorption by Activated Carbon, *Resources, Conservation and Recycling*, **27**, 57-71.

Marzinkowski J.M. (1998) Schließung von Wasserkreisläufen bei der Textilveredlung, 4. Internationale Sommerakademie der Deutschen Bundesstiftung Umwelt.

McKay, G., Geundi, M. E, Nassar, M. M., (1987), Equilibrium Studies During the Removal of Dyestuffs from Aqueous Solutions Using Bagasse Pith, *Water Research*, **21** (12), 1513-1520.

McKay, G., (1986), Equilibrium Studies for the Adsorption of Dyestuffs from Aqueous Solutions by Low-Cost Materials, *Water, Air and Soil Pollution*, **29**, 273-283.

Meshko, V., Markovska, L., Mincheva, M., Rodrigues, A. E., (2001), Adsorption of Basic Dyes on Granular Activated Carbon and Natural Zeolite, *Water Research*, **35** (14), 3357-3366.

Morais, L. C., Freitas, O. M., Goncalves, E. P., Vasconcelos, I. T., Gonzalez Beca, C. G., (1999), Reactive Dyes Removal from Wastewaters by Adsorption on Eucalyptus Bark: Variables That Define the Process, *Water Research*, **33** (4), 979-988.

Nassar, M. M., Magdy, Y. H. (1997), Removal of Different Basic Dyes from Aqueous Solutions by Adsorption on Palm-Fruit Bunch Particles, *Chemical Engineering Journal*, **66**, 223-226.

Nassar, M. M., El-Geundi, M. S. (1991), Comparative Cost of Colour Removal from Textile Effluents Using Natural Adsorbents, *Journal of Chemical Technology Biotechnology*, **50**, 257-264.

Öztürk, N., Bektaş, T. E., Özdemir, M., Kıpçak, I. (2000), Investigation of Effectiveness of Sepiolite and Other Adsorbents in Removal of Dyestuffs, IV. *National Chemical Engineering Congress*, 158-163, Istanbul.

Poots, V. J. P., McKay, G., Healy, J. J., (1976), The Removal of Acid Dye from Effluent Using Natural Adsorbents-II Wood, *Water Research*, **10**, 1067-1070.

Robinson, T., Chandran, B., Naidu, G. S., Nigam, P. (2002a), Studies on the Removal of Dyes from a Synthetic Textile Effluent Using Barley Husk in Static-Batch Mode and in a Continuous Flow, Packed-Bed, Reactor, *Bioresource Technology*, **85**, 43-49.

Robinson, T., Chandran, B., Nigam, P. (2002b), Effect of Pretreatments of Three Waste Residues, Wheat Straw, Corncobs and Barley Husks on Dye Adsorption, *Bioresource Technology*, **85**, 119-124.

Slokar, Y., M., Marechal, A. M. L. (1998), Methods of Decoloration of Textile Wastewaters, *Dyes and Pigments*, **37** (4), 335-356.s

State Institute of Statistics Prime Ministry Republic of Turkey (SIS), 2003, *Statistical Yearbook of Turkey 2002*, pp 360.



Sun G., Xu X. (1997), Sunflower Stalks as Adsorbents for Color Removal from Textile Wastewater, *Industrial Engineering Chemical Research*, **36**, 808-812.

Turabik, M. (2003), The Investigation of Adsorption Mechanism of Basic Blue 3 Dyestuff on Bentonite, *V. National Environmental Engineering Congress of UCTEA The Chamber of Environmental Engineers*, 592-600, Ankara.

Turabik, M., Kumbur, H. (2003), Removal of Some Basic dyes with Adsorption onto Natural and Activated Clay, *V. National Environmental Engineering Congress of UCTEA The Chamber of Environmental Engineers*, 208-215, Ankara.

Ulasoglu, D., 1995, *Removal of Phosphorus from Domestic Wastewater by Basaltic Tephra*, Master Thesis, Adana.

Yasyerli, S., Ar, I., Dogu, G., Dogu, T. (2002), Removal of Hydrogen Sulfide by Clinoptilolite in a Fixed Bed Adsorber, *Chemical Engineering and Processing*, **41**, 785-792.

Weber, W. J., 1972, *Physicochemical Processes for Water Quality Control*, pp 199-259, John Wiley & Sons, Inc., USA.

Wu, F. C., Tseng, R. L., Juang, R. S. (2001), Kinetics of Color Removal by Adsorption from Water Using Activated Clay, *Environmental Technology*, **22**, 721-729.

Wu, G., Koliadima, A., Her, Y. S., Matijevic, E. (1997), Adsorption of Dyes on Nanosize Modified Silica Particles, *Journal of Colloidal and Interface Science*, **195**, 222-228.

## APPENDIX A

### CALIBRATION CURVES

Absorbance values for the *basic blue* dyestuff were determined at the wavelength of 600 nm for calibration curve.

**Table A.1.** Data for calibration curve of basic blue dye (BB)

Concentration (mg/L)	Absorbance
2	0,081
4	0,180
6	0,289
8	0,383
10	0,490

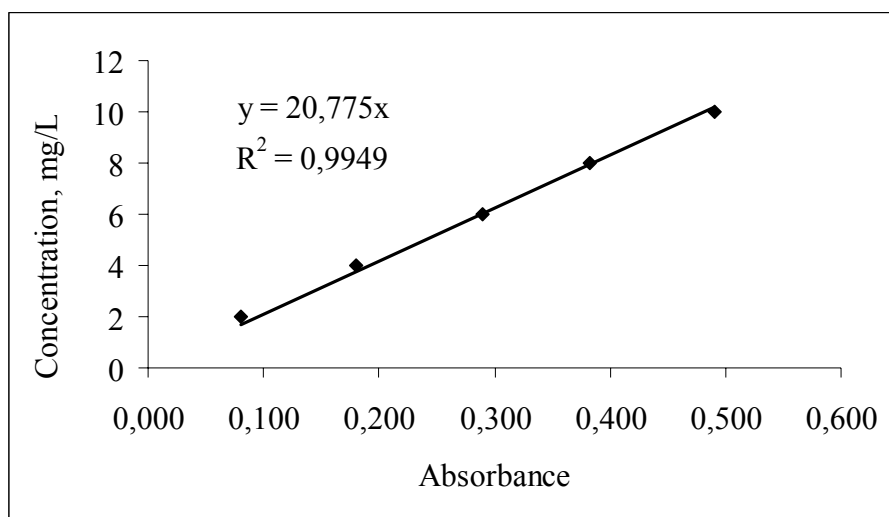


**Figure A.1.** Calibration curve for basic blue dye

Absorbance values for the *basic yellow* dyestuff were determined at the wavelength of 440 nm for calibration curve.

**Table A.2.** Data for calibration curve of basic yellow dye (BY)

Concentration (mg/L)	Absorbance
2	0,152
4	0,318
6	0,482
8	0,625

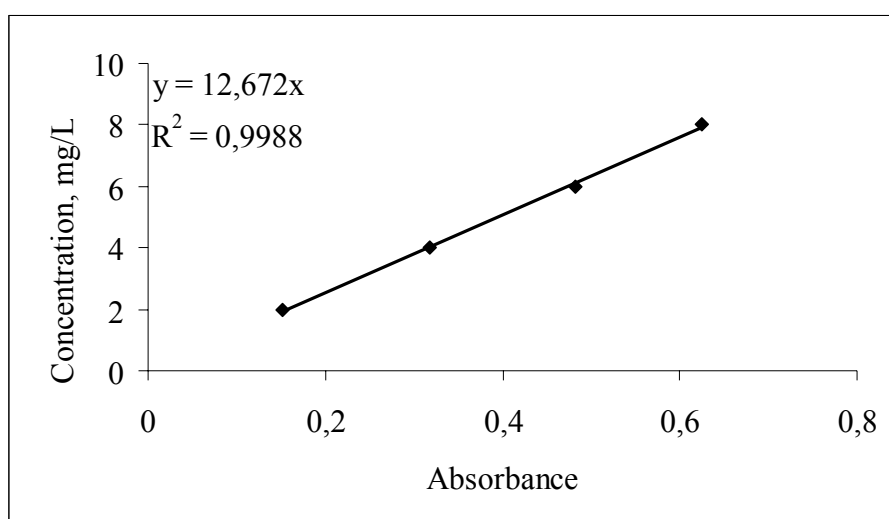


**Figure A.2.** Calibration curve for basic yellow dye

Absorbance values for the *acid yellow* dyestuff were determined at the wavelength of 420 nm for calibration curve.

**Table A.3.** Data for calibration curve of acid yellow (AY)

Concentration (mg/L)	Absorbance
2	0,034
4	0,062
6	0,104
8	0,132
10	0,154
20	0,302
30	0,437

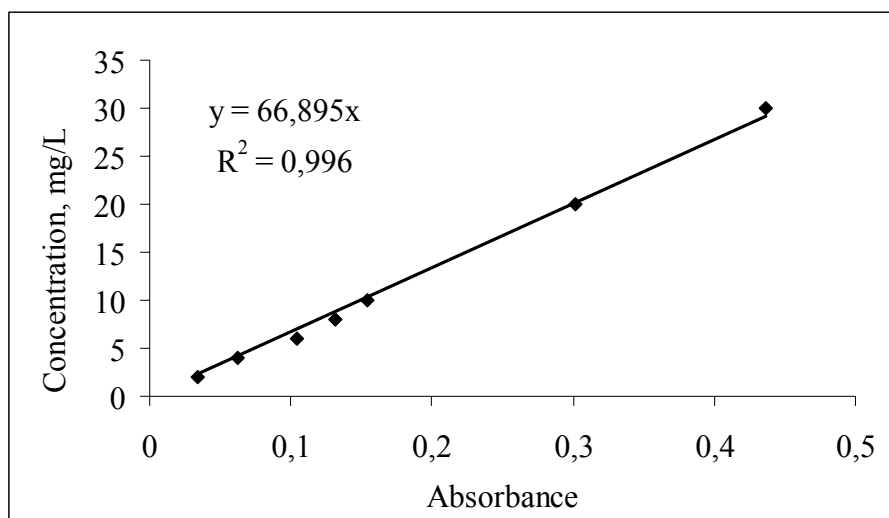


**Figure A.3.** Calibration curve for acid yellow dye

Absorbance values for the *acid red* dyestuff were determined at the wavelength of 515 nm for calibration curve.

**Table A.4.** Data for calibration curve of acid red dye (AR)

Concentration (mg/L)	Absorbance
2	0,053
4	0,090
6	0,135
8	0,155
10	0,205
20	0,372
30	0,556

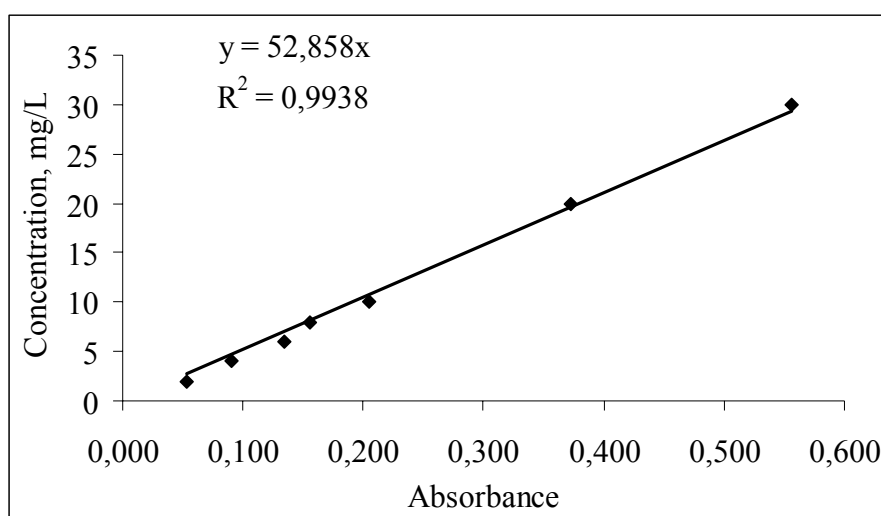


**Figure A.4.** Calibration curve for acid red dye

Absorbance values for the *reactive yellow* dyestuff were determined at the wavelength of 420 nm for calibration curve.

**Table A.5.** Data for calibration curve of reactive yellow (RY)

Concentration (mg/L)	Absorbance
2	0,023
4	0,051
6	0,081
8	0,110
10	0,148
20	0,290
30	0,460
40	0,615

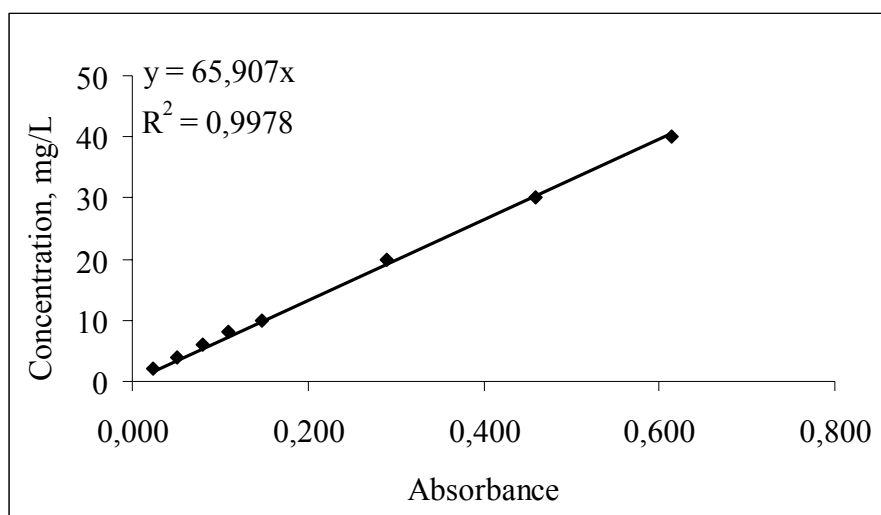


**Figure A.5.** Calibration curve for reactive yellow dye

Absorbance values for the *reactive red* dyestuff were determined at the wavelength of 540 nm for calibration curve.

**Table A.6.** Data for calibration curve of reactive red (RR)

Concentration (mg/L)	Absorbance
2	0,050
4	0,089
6	0,133
8	0,170
10	0,214
20	0,443

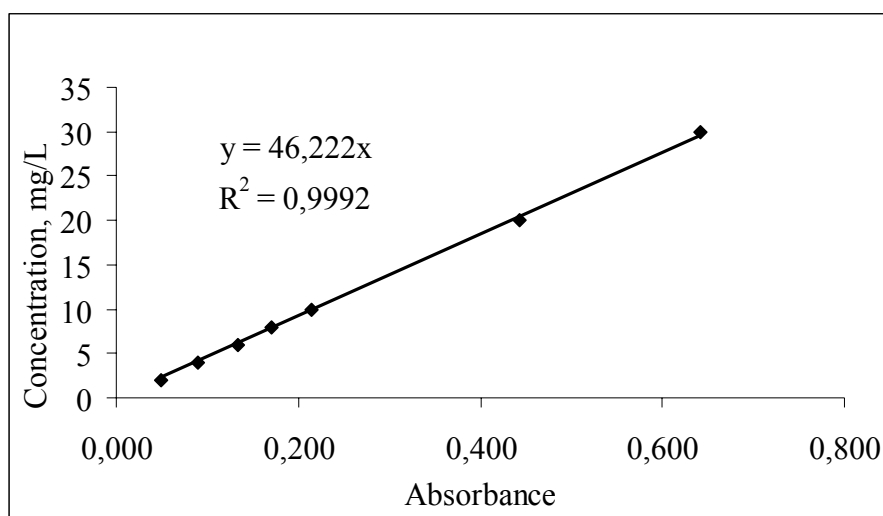


**Figure A.6.** Calibration curve for reactive red dye

## APPENDIX B

### RATE CURVES

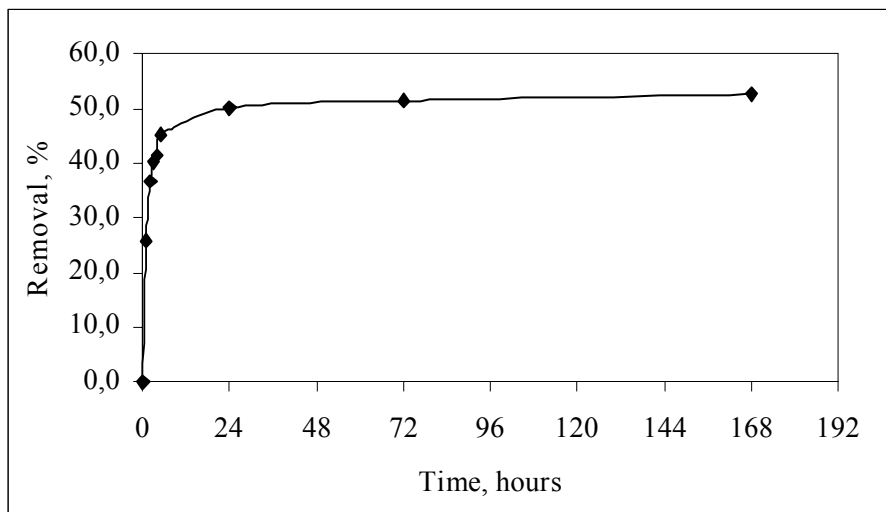


**Figure B.1.** Rate curve of basaltic tephra for basic blue

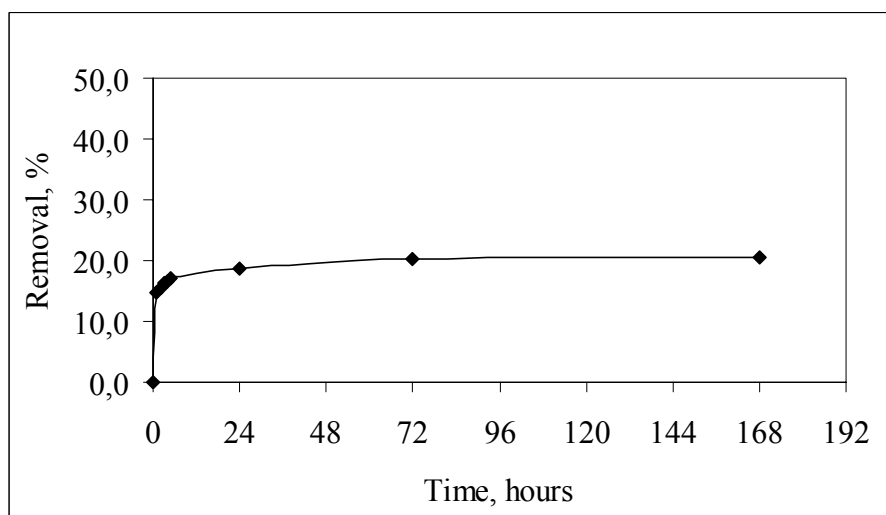


**Figure B.2.** Rate curve of basaltic tephra for basic yellow



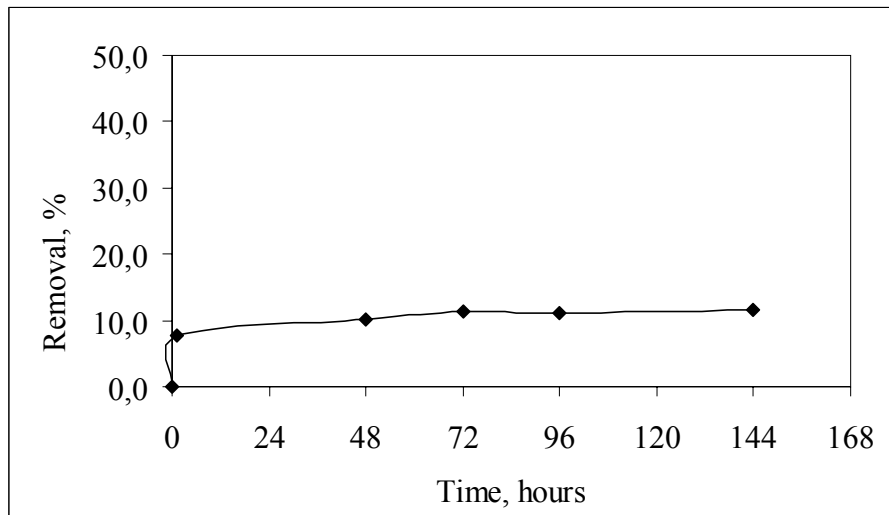


**Figure B.3.** Rate curve of basaltic tephra for acid yellow

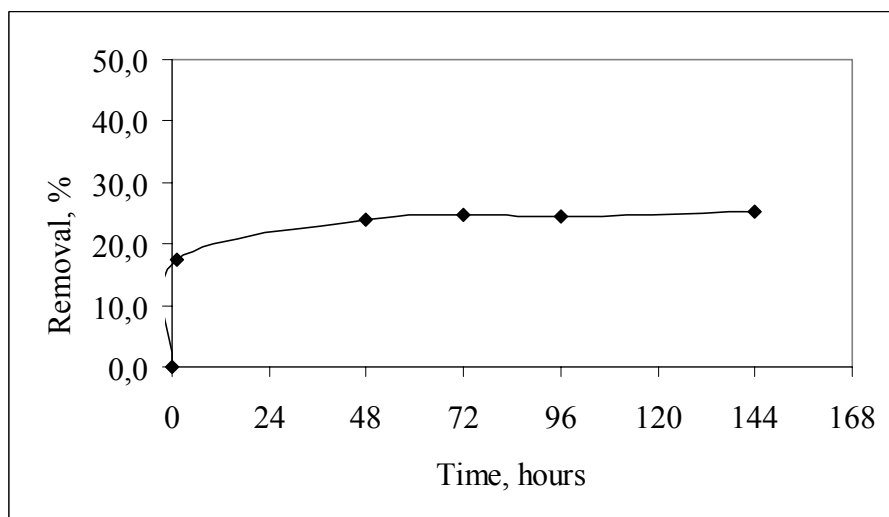


**Figure B.4.** Rate curve of basaltic tephra for acid red

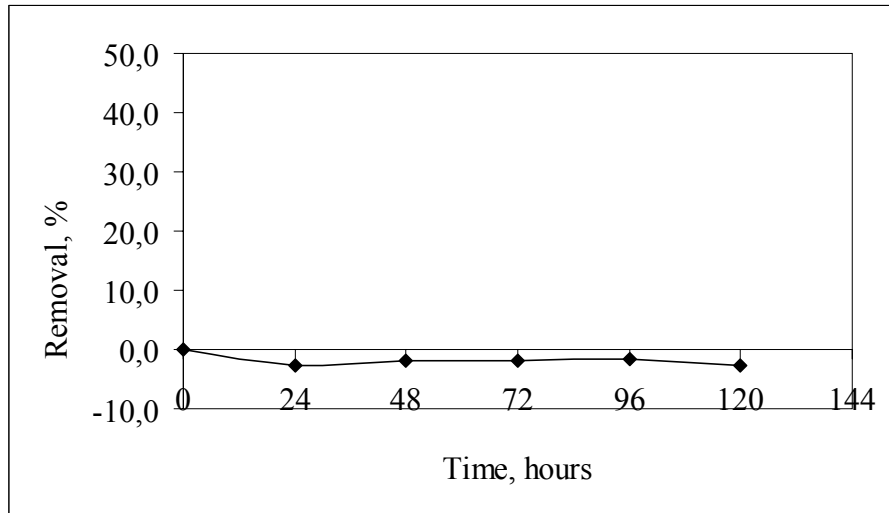


**Figure B.5.** Rate curve of basaltic tephra for reactive yellow

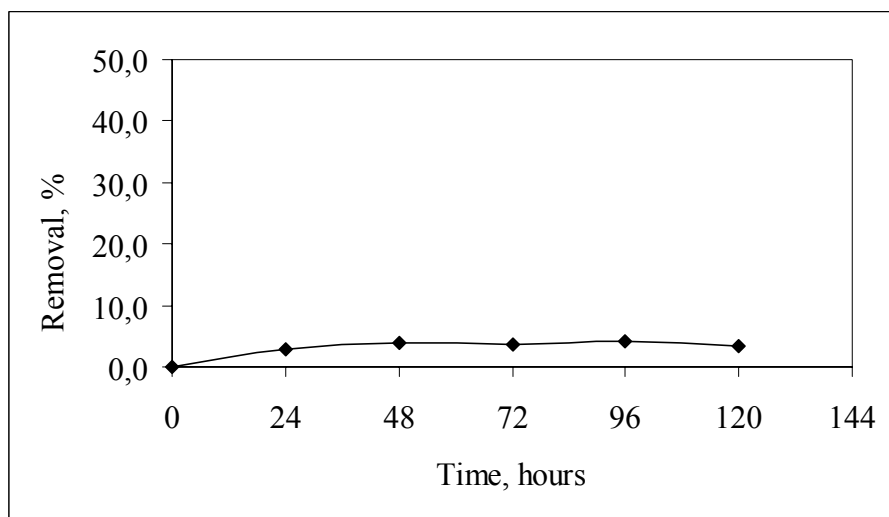


**Figure B.6.** Rate curve of basaltic tephra for reactive red

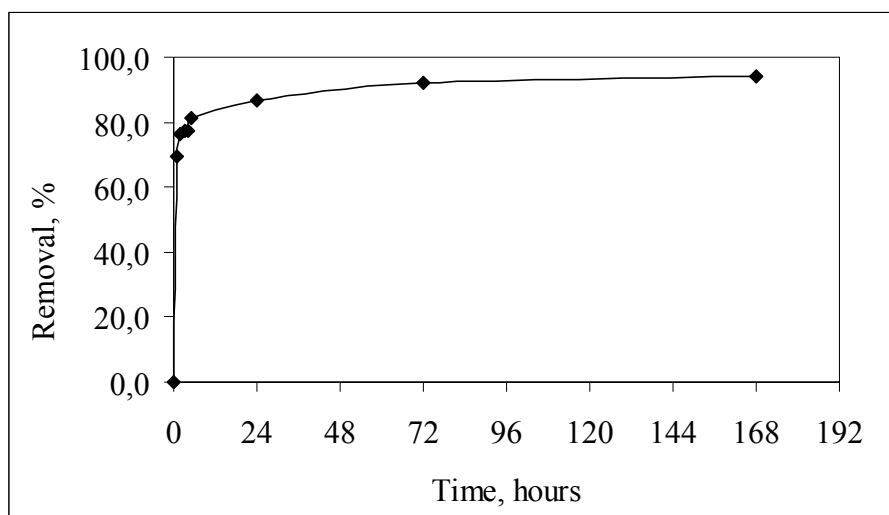


**Figure B.7.** Rate curve of clinoptilolite for basic blue

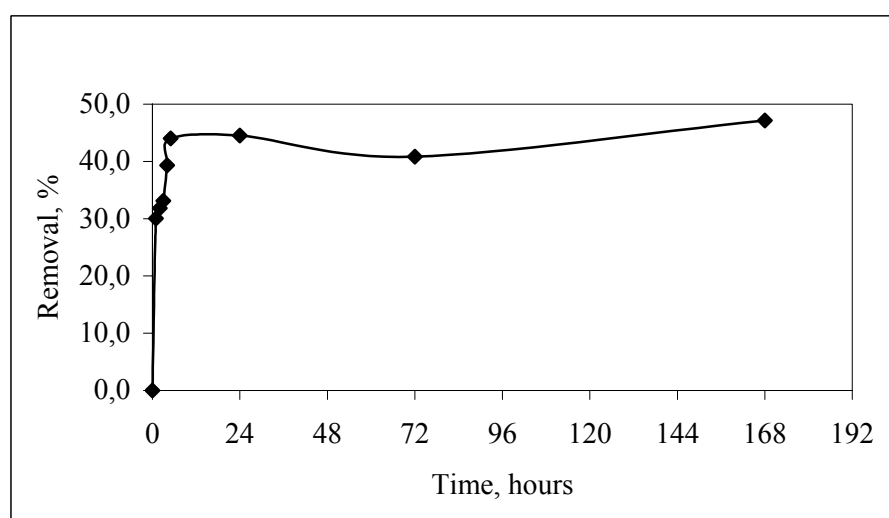


**Figure B.8.** Rate curve of clinoptilolite for basic yellow

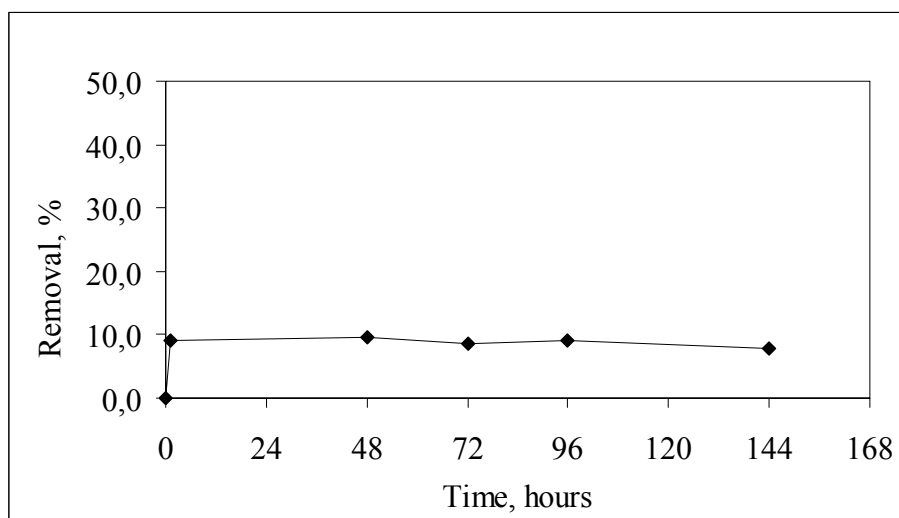


**Figure B.9.** Rate curve of clinoptilolite for acid yellow

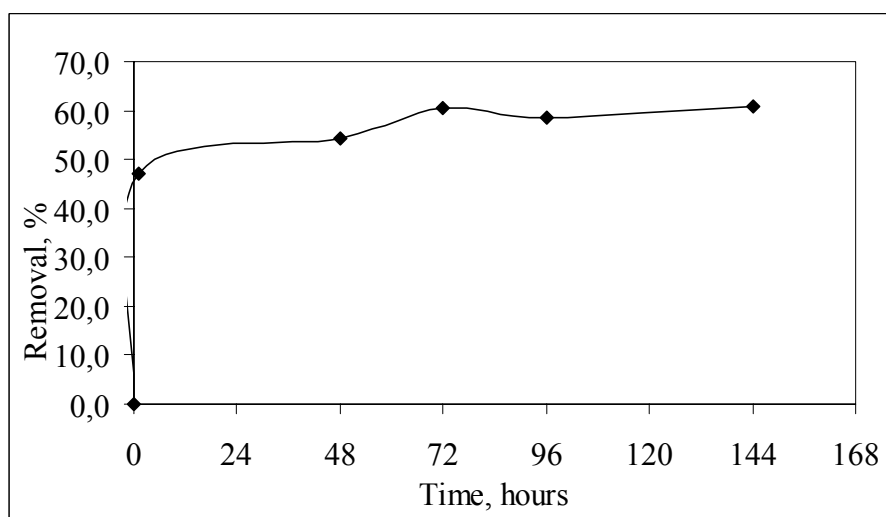


**Figure B.10.** Rate curve of clinoptilolite for acid red

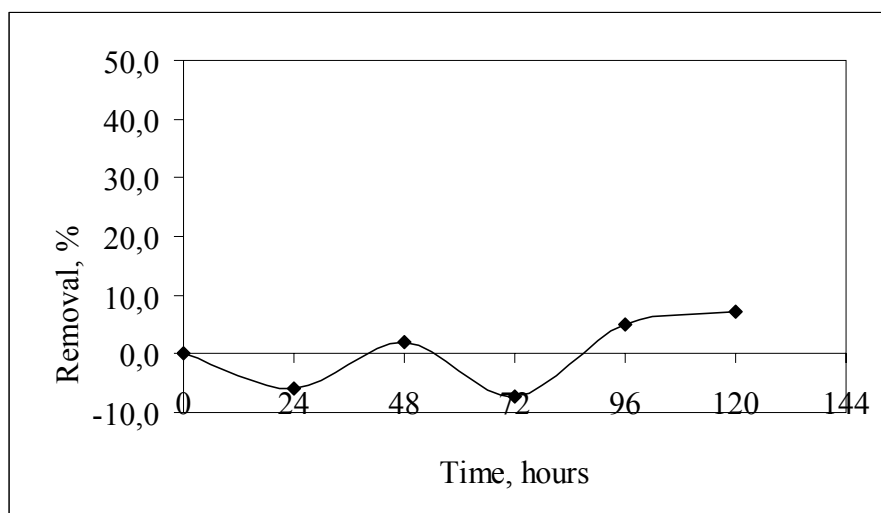


**Figure B.11.** Rate curve of clinoptilolite for reactive yellow

For the removal of reactive yellow dyestuff it is difficult to obtain an equilibrium point because interaction between dyestuff and adsorbent is changing with time probably due to experimental errors resulting from dilutions. Actually adsorption of that dye onto adsorbent is very small or none.

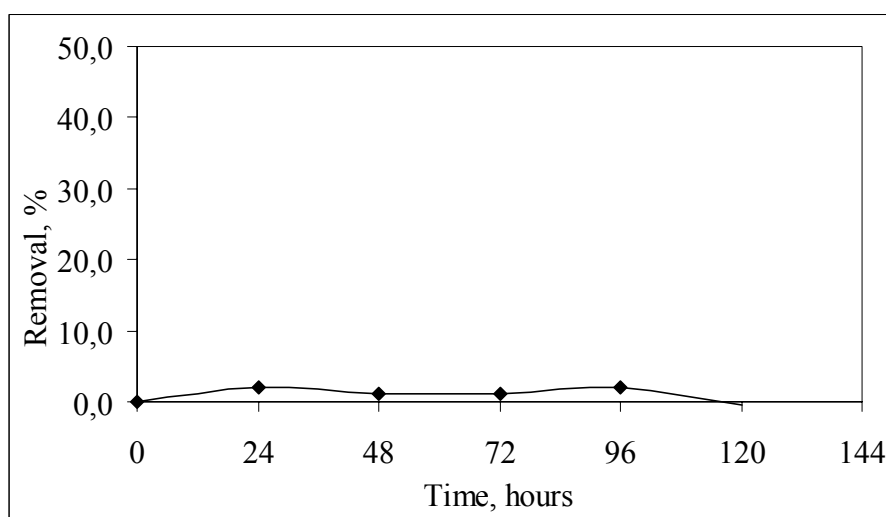


**Figure B.12.** Rate curve of clinoptilolite for reactive red

## APPENDIX C

### EFFECT OF FILTER PAPER IN DYE REMOVAL

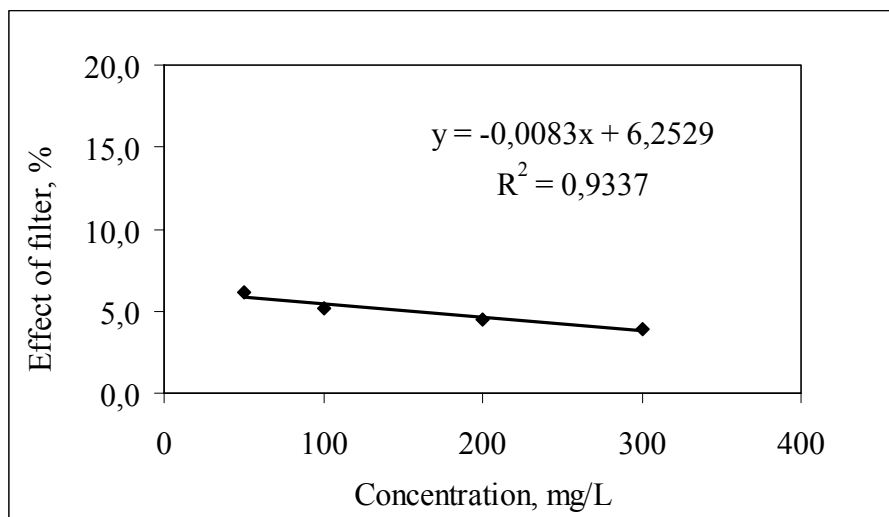


**Figure C.1.** Amount of acid red dyestuff adsorbed by the filter paper

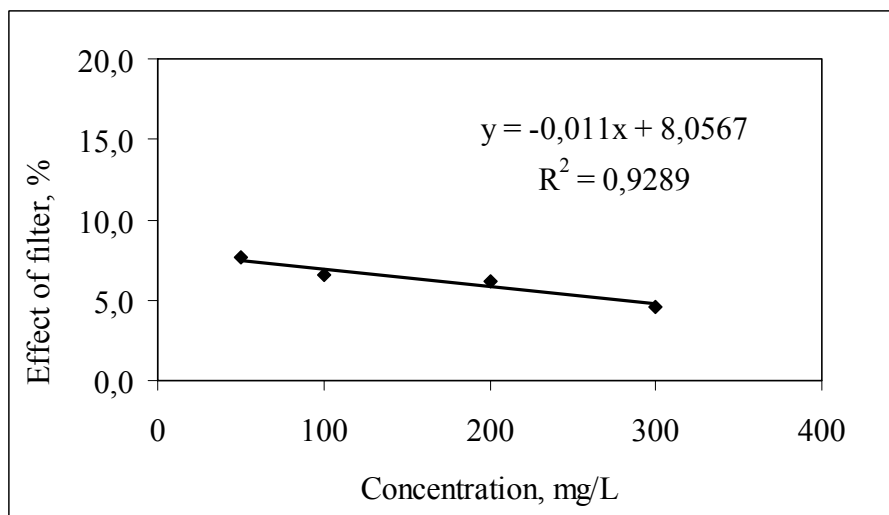


**Figure C.2.** Amount of basic yellow dyestuff adsorbed by the filter paper

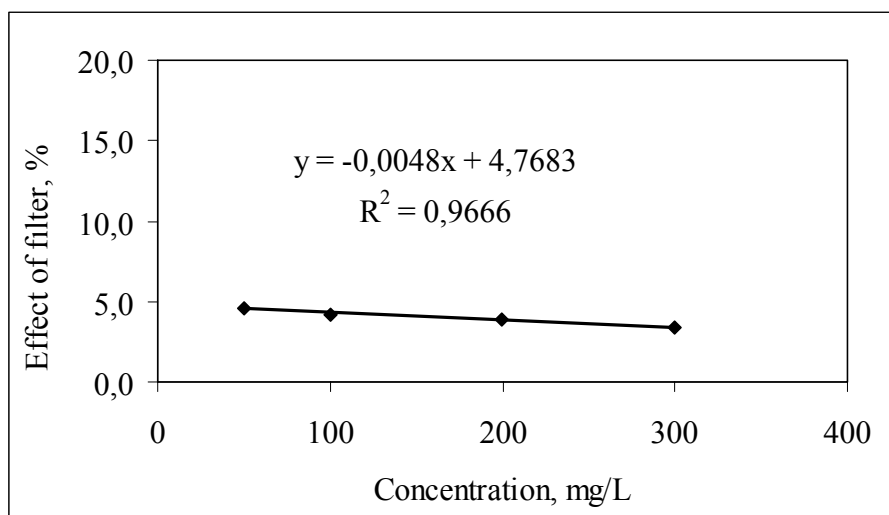


**Figure C.3.** Amount of reactive red dyestuff adsorbed by the filter paper

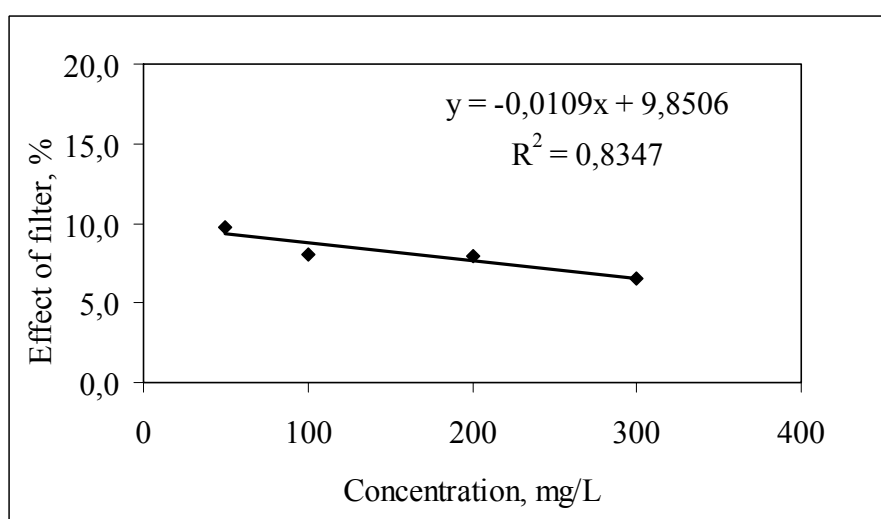


**Figure C.4.** Amount of basic blue dyestuff adsorbed by the filter paper

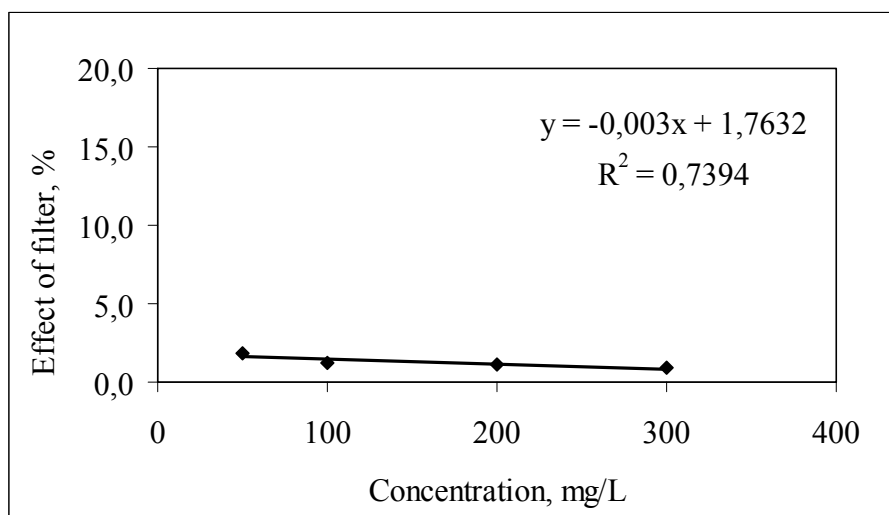


**Figure C.5.** Amount of acid yellow dyestuff adsorbed by the filter paper

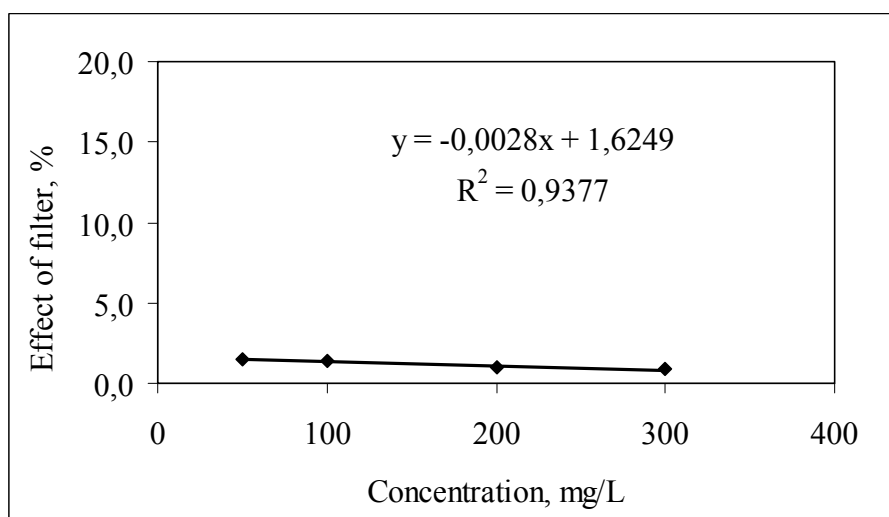


**Figure C.6.** Amount of reactive yellow dyestuff adsorbed by the filter paper